Republic of Iraq
Ministry of Higher Education & Scientific Research
Mustansiriyah University
College of Engineering
Mechanical Engineering Department

Low Speed Impact Response of Polymer Based Material under Different Thickness of Samples

A Thesis
Submitted to the Mechanical Engineering Department,
College of Engineering, Mustansiriyah University, in Partial
the Fulfillment of the Requirements for the Degree of Master of Science in
Mechanical Engineering / Applied

By:
Ali Jasim Mohammed
(B.Sc. Mechanical Engineering, 2015)

Supervised By
Prof. Dr. Bashar Owaid Bedaiwi

Rajab1442 February 2021

جمهورية العراق
وزارة التعليم العالي والبحث العلمي
الجامعة المستنصرية
كلية الهندسة
قسم الهندسة الميكانيكية

استجابة المادة ذات الاساس البوليمري عند تأثير سرعة الصدمة المنخفضة لاسماك مختلفه من النماذج

رسالة مقدمة الى
كلية الهندسة الجامعة المستنصرية
كجزء من متطلبات نيل شهادة الماجستير
في الهندسة الميكانيكية/ تطبيقي

من قبل:
علي جاسم محمد
(بكالوريوس هندسة ميكانيكية - 2015)

بأشراف
أ.د. بشار عويد بديوي

رجب 1442

شباط 2021

بسم الله الرحمن الرحيم

(قَالُوا سُبْحَانَكَ لا عِلْمَ لَنَا إِلَّا مَا عَلَّمْتَنَا إِنَّكَ

أَنْتَ الْعَلِيمُ الْحَكِيمُ)

صدق الله العلي العظيم

(البقرة: ٣٢)

dedication

To my father and my venerable mother ... May God have mercy on them

To my dear brother, who had two assistants in Shaddad

For my wife ... a struggling companion who spared no time or effort to help me

To a crowd of friends and family

I dedicate my scientific thesis to you in .....

Ali

Supervisor Certification

I certify that this thesis entitled *" **low Speed Impact Response of Polymer Based Material under different thickness of samples** "* was prepared under our supervision at the Department of Mechanical Engineering, College of Engineering, Mustansiriyah University, in partial fulfillment of the requirements for the degree of master in Mechanical Engineering /Applied.

Prof. Dr. Bashar Owaid Bedaiwi

Supervisor

/ / 2021

In view of the available recommendation, I forward this thesis for debate by the examining committee.

Prof. Dr. Bashar Owaid Bedaiwi

Head of the Department

/ / 2021

Linguistic Certification

This is to certify that the thesis entitled *" **low Speed Impact Response of Polymer Based Material under different thickness of samples** "*was prepared under my linguistic supervision. Its language was amended to meet the style of the English language.

Signature:

Name: Dr. Samir Ali Amin Al-Rabii

Department of Mechanical Engineering

University of Technology

Data: / / 2021

Examining Committee Certification

We certify that we have read the thesis entitled *" **low Speed Impact Response of Polymer Based Material under different thickness of samples** "* and as Examining Committee examined the student *" **Ali Jasim Mohammed**"* in its contents and in what it concerned, that in our opinion it is adequate as a thesis for the degree of Master of Science in Mechanical Engineering.

Prof. Dr. Hussain .J. M.AL-alkawi
Chairman
/ / 2021

Asst. Prof. Dr.Suhad Dawood Salman
Member
/ / 2021

Asst. Prof. Dr. Basim Ajel Sadkhan
Member
/ / 2021

Prof. Dr. Bashar Owaid Bedaiwi
Supervisor
/ / 2021

Approved by the Dean of the College of Engineering Mustansiriyah University.

Asst. Prof. Dr. Malik Jasim Farhan Al-Khalidi
The Dean of The College of Engineering
/ / 2021

ACKNOWLEDGEMENTS

Praise to our almighty **Allah**, the most merciful and most gracious for enabling me to complete this thesis. The thankful permanent to the **Merciful Prophet Mohammad** and his viticulturist **Ahl-Albait** (peace be upon them).

I would like to express my deepest thanks and sincere gratitude to my supervisors **" Prof. Dr. Bashar Owaid Bedaiwi"** for his assistance, guidance, encouragement and help throughout the steps of this work. My gratitude also goes to the staff members of the Mechanical Engineering Department/ Mustansiriyah University

I would like to thank all my beloved friends for their unparallel help, kindness and supports.

Finally, I wish to extend my gratitude to my family; my mother, father, brothers, sisters, and my wife and boys (Abdullah and Abbas) for all the patience and support given during the time I spent doing all this work.

Ali Jasim Mohammed

2021

Abstract

An investigational study was used on 18 low-speed effect samples. When three types of thicknesses were used, sample dimensions were fixed. The dynamic behavior of the material due to the blow was observed. This study aims to verify the mechanical shock by measuring shock force, acceleration and its effect on the manufactured materials. Poly-lactic acid was used to measure the impact energy through three levels and three different energies were obtained which are 2.4 Joule, 4.9 Joule and 7.3 J. Samples were first modeled in Solid works program and then transferred in G-Code format and samples using a 3D printer The print density was 100%. Samples of various thicknesses were used in accordance with ASTMD7136 standards. Tensile test was carried out according to ASTMD638 standard. The test device was manufactured according to AISTMD7136 standard. The device was designed in the AutoCAD program, and FSR force sensors and MPU6050 acceleration were used. The diameter of ball was 16 mm, and the height of the falling tube was 200 cm. The absorbed energy of substance was calculated, and the results showed that the lactic acid has the ability to absorb energy from a low velocity blow. Use of finite element technique (ABAQUS / Explicit Dynamic 16) for analysis by observing the maximum total stress and deformation. Also, the results manifested that the elastic modulus, the maximum tensile strength, and the yield pressure were compared to the group. The results of the total energy and damage from the impact hit were compared and there was a convergence between them.

Table of Contents

Chapter Three Theoretical and Numerical Analysis

Chapter four Experimental Work

List of Figures

List of Tables

List of Acronyms

Acronym	Description
3D	Three-dimensional
ABS	Acrylonitrile Butadiene Styrene
PLA	poly lactic acid
HIPS	High Impact Polystyrene
LOW	Low Velocity Impact
FDM	Fused deposition modeling
STL	Stereolithographic
FEM	Finite Element Molding
Imp Lab	Impact program Laboratory
F S R	Force Sensitive Resistor
ASTM	American Society for Testing and Materials
ABAQUS/EXPLIT	Commercial software engineering
VUMAT	User Material

Nomenclatures

Symbol	Title	Unite
a	Width of beam	$\boldsymbol{m}$
b	Length of beam	$\boldsymbol{m}$
Di	Diameter of impactor	$\boldsymbol{m}$
Ei	Young's modulus of the impactor	$\boldsymbol{N/m2}$
Et	Total impact energy	$\boldsymbol{J}$
F	Impact force	$\boldsymbol{N}$
H	Height	$\boldsymbol{m}$
KE	Kinetic Energy	J
m	Mass	kg
PE	Potential Energy	J
t	time	s
vi	initial Velocity	$\boldsymbol{m/s}$
v2	Final Velocity	$\boldsymbol{m/s}$
Ea	Energy/Absorption Energy	J

Chapter one

Introduction

Chapter One

Introduction

1.1 General

The impact is a collision between two objects that causes damage to one or both of them. The effect is very important to know the mechanical properties and impact energy. The damage is a break, a crack or a scratch. Scientists need to study and know how the materials behave under the influence of shocks and the forces that can be resisted. The test can provide information about the samples and their response to see which pressure is applied to them suddenly such as in an impact. This is in hard and brittle materials.

1.2 Polymer Material

Natural polymers are one of the resources that can be obtained from some renewable energy sources. They are classified among the environmentally friendly materials and can be analyzed into other materials, such as small particles, carbon dioxide and water. There are different groups and physical and chemical methods through which natural polymers can be manufactured, or, through modifications, a new material using the latest technologies. Nowadays, the commonly used natural polymer materials include starch, chitosan, alginate, alginate, chondroitin sulfate, hyaluronic acid, etc. [1]. It is a hybrid technology that connects materials science and biology. In some cases, and most of them, biocompatible and prepacking polymers are used for analysis to stimulate the growth of surrounding tissues or to act as the temporary aging of cultured cells for binding and growth, maintaining different jobs [2].

The same words refer to a polymer. They are different materials that consist of many molecules and parts that lead to long chains. These big particles are usually referred to as macromolecules. Polymers have unique physical properties, treatment methods, and their versatility to their molecular structure. There are many implementations [3].

The increasing population and the associated economic growth at the global level are increasing the demand for consumer materials such as polymer-based goods (e.g., elastomeric sand plastics). Many environmental sources can be released into their life cycle from the basic polymers once they reach the environment, some polymer materials lose some mechanical and chemical properties. The change in the polymer structure leads to its breakdown. [4].

1.2.1 Poly- lactic Acid

Lactic acid is a major complex that plays an important part in many biological processes. For example, lactate is shaped continuously. Lactic acid was obtained as a productive measure meanwhile the finish of concentrated on using it industries mainly in eating products for work. For instance, as an acidity regulator, and medicine. In addition, it is a one-sided introduction to the Chinese People's Liberation Army. It can be obtained by common chemical synthesis or by fermentation of carbohydrates. It is the simplest acid, also known as the hydroxyl "lactic acid" with an unequal carbon particle and two visually lived shapes, specifically [5]**.**

Poly lactic acid (PLA) due to its mechanical properties is considered one of the most promising degradable polymers profile properties, thermoplastic process ability and biological properties, such as biodegradability and biocompatibility [6]. PLA is derived from renewable sources, for example, sucrose, sugarcane, and cornstarch, and it is an aliphatic polyester. It is a polymer produced by fermentation of various carbohydrates (Fig. 1.1), called lactic acid: Maltose, glucose and dextrose from potato or cornstarch; lactose from whey cheese, sucrose from beets or cane sugar. [7].

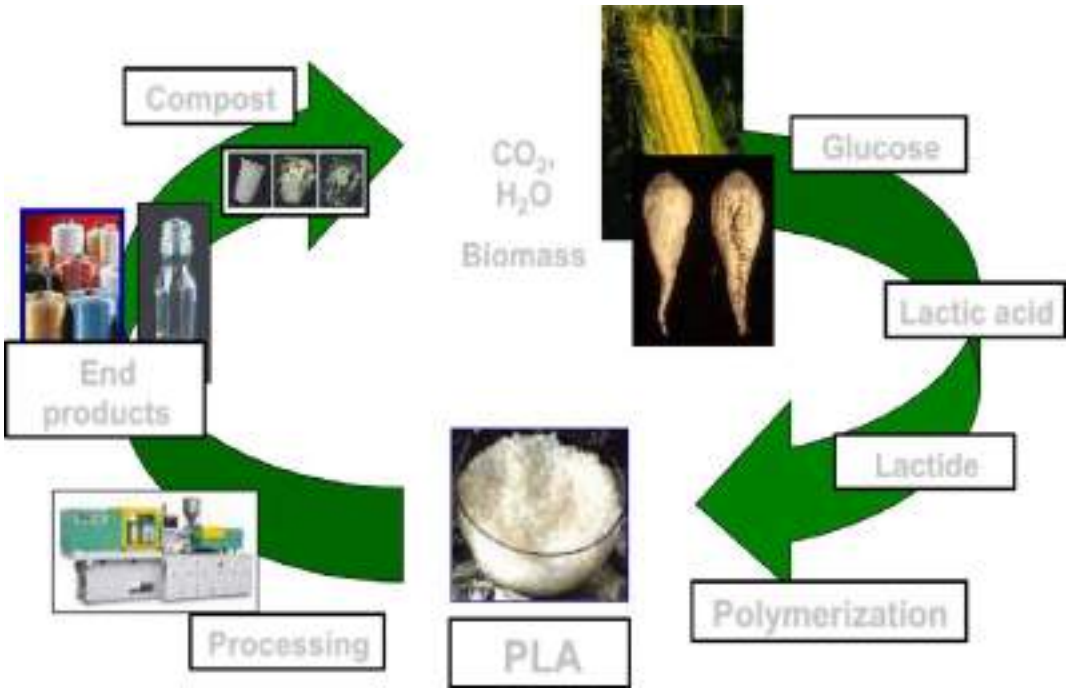

Figure (1.1) The process of manufacturing poly lactic acid [8].

PLA is used in solid containers, some automotive interior parts, and blueness moulded one-use package (for example, nourishment ampules and plates), puffed flasks and flasks, sutures, absorbable tissue fibers and sutures, and biomedical uses (drug delivery capsules, material / biodegradable fibers, and internal osteoporosis implants). It stands the polymerization of the possibility of betony degradation in the human body due to the biocompatibility of a uniform use in the medical field. PLA-based resins may be adapted to adapt to many requests, from disposable nourishment-service items to piece extrusion, and covering for paper [9]. In general, polyolefin has special mechanical properties rather higher than. PLA is a solid, the same hardness as acrylic (such as methyl methacrylate). Due to its toughness property, some cracking occurs along the edges, resulting in some of its products which cannot be used. To avoid these limitations, PLA ought to be added with the other hardness control materials [10].

1.3 Impact Materials

In general, the damage caused by influence does not pose a threat to metal framework because the nature of the material is ductile and the energy absorbed by it is large. On harvest stress, the material may move

into very large rings with a constant rate before work hardening. Sometimes, some composite materials that have a variety of patterns and contain the effect damage visible to the naked sense can nosedive, harshly plummeting the structural strength of the component. The compound materials are mostly brittle with flexible deformations and thus can only absorb energy through the wear mechanisms, not through plastic distortion. [11]. Through the test device, it is possible to determine the mechanical properties resulting from the shock, except for the energy absorbed or the damage in the material. Threshold hole energy, peak impact strength, and recovery coefficients, tests are used to study the effects that occur in changing the test specifications, some such as sample geometry, arrangement, conditions and limitations, material properties, mass and drop height and nose collider dimensions. [12].

Impact creates an impact within the composite material structures and damages that cannot be visually inspected. Interior damage can cause a sharp drop in strength and can grow lower than load. Therefore, the effects of foreign object impacts on the composite structures must be studied, and proper measures should be taken in the design process to account for these expected events. Concerns about the effect of impacts on the performance of composite structures have been a factor in limiting the use of composite materials [13].

1.3.1 The general categorization of impact

1. Low-velocity impact (LVI) is caused by conditions arising from the fall of the tool, usually at speeds below 10 m /s.
2. Intermediate velocity impact occurs between the 10 to 50 m/s range.
3. High /ballistic velocity impact is generally a result of small weaponry fire or fulminatory warhead fragments and usually occurs at the range (50 m/s - 1000 m/s).
4. Hypervelocity ≥2-5 km/s, the projectile is moving at very high velocity and the target material behaved like fluid [14].

1.4 Energy Absorption

Ideal materials need to absorb the energy and drain the kinetic energy of the effect, to remain the same force exerted on them less than a certain limit, which reduces the risk to passengers. Some tests and considerations were made, such as the shape of the protective model, which transfers the

load within the ability to absorb elastic energy, shocks and control deflections. [15]. When designing cars, energy-absorbing materials are used to protect the occupants inside the car if it is exposed to shock. Each unit of the result absorbed from the chassis is less likely to be carried out on the passenger. The ability of exoskeletons to absorb energy and deform under the influence cellular structures can also reduce the plastic deformation on the interior of a vehicle. The fulfilment of energy- soaking up competences and developments of a lattice construction is extremely desired. To efficiently and accurately improve the energy absorption of these structures, the disappointment devices must be well recognized to design [16].

1.5 Failure Mechanisms

The failure mechanisms of the polymer structure will be analyzed in this thesis. Failure mechanisms are the underlying cause for plastic deformation in a specimen, such as bending, buckling, fracture, corrosion, creep, etc. During an impact from a random projection angle, they underwent pressure, tension, bending and twisting loads. Depending on the direction of the element, these loads can lead to normal shear stress and shear stress. These stresses produce different types of failure, depending on the ductility of the material [16].

1.6 Poly Lactic Acid Applications

It is one of the environmentally friendly materials that use a poly-lactic acid polymer that is widely sold in the medical and industrial field because it has good mechanical properties. In other areas, it is applied to connect human bones and form lactic acid applications shown in figure (1.2).

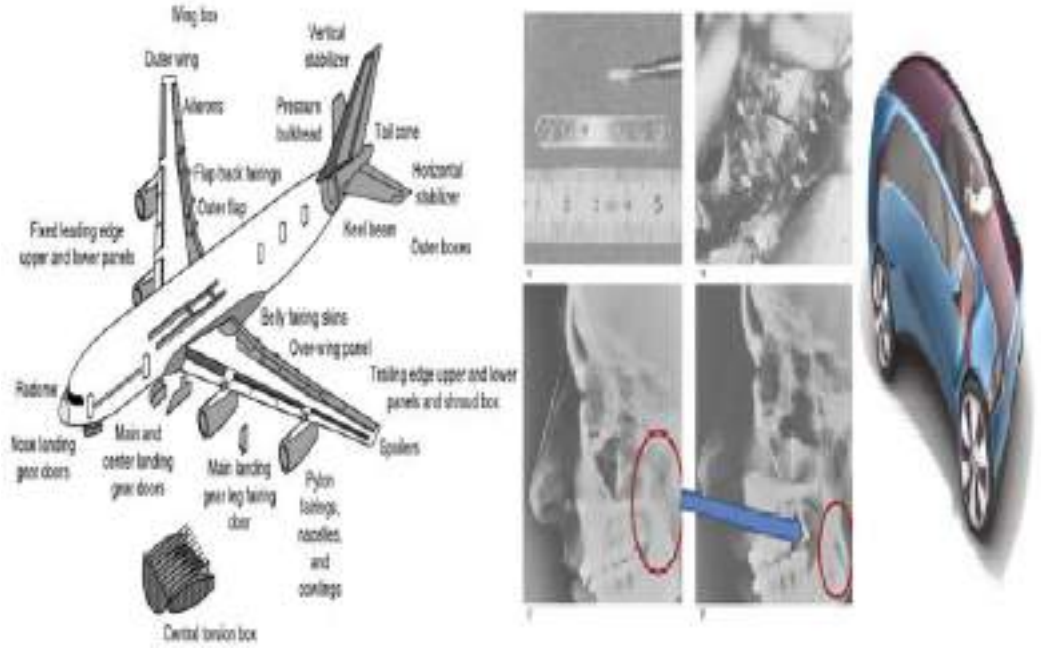

Figure (1.2) Polymer (Poly-Lactic acid) applications [17].

1.7 Aims of Study

The research aim is to study the influence of the low impact on the absorbed energy and on the damage of PLA (poly-lactic acid) under low-speed effect 3D damage model with a solid element was developed to predict the description and scope of the damage. The research sought to follow the following steps:

1. The test samples were designed and made by a 3D printer of poly-lactic acid (PLA) according to the ASTMD7136 standard with different thicknesses.
2. Low-velocity impact experiments on PLA (poly-lactic acid) with different thicknesses, velocity and height impactor of have been conducted in different amplitudes of energy.
3. The harm model was applied in the FE code (ABAQUS/ Explicit) by an employer-defined material subroutine.
4. A comparison between the numerical results and experimentally obtained result was presented.

5. Studying of the effect of different thicknesses, velocity impactor, effect of impactor height on the failure modes and damage level of polymer.

ChapterTow
Literature

Review

Chapter Two

Literature Review

2.1 Introduction

In this chapter we will address previous research on the effect of low velocity (L.V.I), both experimental and numerical in nature.The aim of this literature review is to understand previous research conducted on topics related to this thesis, such as low velocity impact testing, and energy absorption. Lactic acid plate manufacturing processes are discussed. Similar low-speed impact tests are being sought. the first part includes the study of the low speed impact and mechanical properties on 3D printed polymer materials for polylactic acid (PLA).

2.2. Previous Studies of the Impact Study of 3D Printing

H. Louche, et al 2009 [18], Experimental studied and modeling of the thermomechanical behavior of the ABS (Acrylonitrile Butadiene Styrene) polymer During an impact test. The structural component was the heel of a woman's shoe Made of ABS polymer material strengthened or not by pin. Kinematics and measurement of the full thermal field The techniques were used to monitor structural materials and components during the initial experiment .Tensile and impact tests. With the kinetic fields it was possible to determine the stress - the stress response, which takes into account the localization of the neck. The positive differences were in size, too it was observed during these tensile tests, which were associated with the insane damage mechanisms in this polymer type. The thermal fields measured during these tests showed high temperature changes.

Roberson, et al (2015) [19], studied a 3D printed ABS (Acrylonitrile Butadiene Styrene) test in the ISO test and in the ASTM standard D256-10. The results were statistically similar when comparing the pressure samples at the printing and automatic center. Injection at a 45-degree angle by calculating the impact and break strength and energy has the greatest impact resistance. It showed that the printed material at the center of the X-axis, Y was better than the three-dimensional printed material in the three axes of the shock, and less

force was observed due to impact resistant. The results were close through the specifications for the effect in both cases and were statistically equal for the center of the cut and printed pressure **.**

Lanzotti, et al (2015) [20], mentioned three methods:rapid prototyping, additive manufacturing, and 3D printing. ABS polymer materials were used, and the mechanical tests were studied by three parameters of layer thickness, orientation, and absorption and shock on the 3D printed ABS parts. The experimental test (polymer) was performed in this study. A tensile test was used, and the results showed that the polymer was brittle. The attendance of failure was in the least cross-unit .

To determine the impact absoribtion capacity of polylactic acid (PLA), a 3D-printed fabricated technique using fused deposition modelling was employed by **Tsouknidas, et al (2016) [21],** the effects of parameters, such as infill patterns, density and layer altitudes on the energy absorption of the printed PLA cylinders were evaluated and examined. The test results appeared that the apparent density has a significant influence on the impact dissipation capacity of composite. On the other hand, the effects of both filling patterns and layer height were negligible.

Shubham, et al (2016) [22], investigated the preparation of standard samples with different thicknesses and layers using 3D printing technology, which worked according to the standard of the fused deposition modeling (FDM) process. The 3D printed ABS polymer examples were examined to understand the effect of the layer thickness on the numerous mechanical properties of the constituent. And, it was compared with a sample from the standard injection molding method. The results showed that the tensile strength (36 MPa), shock resistance (103.6 J / m), and hardness (R107) were the highest for the samples made by injection molding method among the 3D printed samples, and the features were better with smaller layer thicknesses. As the thickness of the layer increases, there is a negative effect on the mechanical features as the tensile strength, impact strength and stiffness decrease.

On the other hand, **Yarwindran, et al (2018) [23]** examined the percentages and their effect on the sample filling pattern, which affect the stiffness, tensile strength, bending strength, and orientation of the sample. FDM (fused

deposition modeling) 3D printing technology was used. In addition, it is possible to know the mechanical properties of the footbed on the printed frame. It is filled in various proportions using 3D printing. Mechanical tests were performed, and the results were obtained for specimen that was well packed with good bending resistance, tensile strength, and shocks.

Ryan, et al (2017) [24] 3D printing, officially known as Additional Manufacturing (AM), for rapid prototypes and fast manufacturing, is already approved soon. AM technologies are the most used polymers. Ideals commonly used for the ASTM and ISO mechanical testing, which have been used by various research groups to examine the strength of the 3D printed parts, have been studied. The mechanical properties of the 3D printed parts are affected, in particular, the properties under different types of loading such as tensile and bending, pressure, fatigue, impact, etc.

Sarvestani, et al (2018) [25] used a lightweight printed sandwich plate , a specific semi-analytical part was applied, the effective tests were performed to evaluate the performance, and the specific elements method was used to accurately predict the mechanical properties.Also, the Ansys program was used to analyze the behavior on the sandwich panels under the influence of low speed, and the samples were prepared through the three-dimensional printing of a substance (The polymer of the polylactic acid) . A low-speed test was done to find the absorbed energy through the X-ray tomography to study the microscopic features before and after the effect. The results showed that the sandwich panels are suitable for the energy absorption applications of strength, to print three-dimensional panels.

Patterson, et al 2018 [26], fully demonstrated the impact strength of the polymer materials used has been in different directions and angles by smelting. They were ten different materials used, seven in various angles, three prints, seven pure materials, three compounds, and three printing directions were used. Seven different pure substances plus three compounds were tested. These were ABS, Normal PLA, High-Temperature Aluminum PLA ,PLA, Nylon, PETG, HIPS , Polycarbonate, , Wooden PLA, and Carbon Fiber PLA. ASTM and Izod E type tests with 2.7J were used with the pendulum. The results showed that the direction of the crust and the point angle are the main drivers for determining the impact properties along the slit.

Abbas Tahssen, et al 2018 [27], discussed the studied Layer on the mechanical properties of multi-building samples Acid. Izod impact test was performed on samples.In accordance with ISO standards, test samples are performed for Various layer thicknesses (0.1, 0.15, 0.2, 0.25 and 0.3Mm) using PLA 3D printing System tested, impact strength and more Parameters include printing speed, coating thickness, filling density, And the steering part. Layer thickness increased from 0.1Mm to 0.3 had a more positive effect on mechanical While it will be time to print the sample Decreases with layer thickness.

D.W.Abbot, et al 2019 [28], Pressure test was used for different materials of PLA, ABS, HIPS polymers. The samples were designed with different density ratios by 3D printer and the shape used was a cube with dimensions of 25 mm * 25 mm * 25 mm. The finite element method was used, the external force was applied to the materials, and the stability was measured by means of a strain gauge.

Haitham Hadidi, et al 2019 [29], The studied investigated the effect of low velocity on polymer (ABS) that is processed by fused filament fabric. Two different print directions on the effect of low strain rate impact behavior were examined after evaluating material fabrication. A charpy impact test was used to reveal the effect of printing orientation on energy absorption and fracture resistance.

Bandar Abdullah Aloyaydi, et al 2019 [30], Investigated of the effect of filler density (ID) on the microstructure and bending behavior of 3D-printed parts with a three-point test (3PBT) procedure. The bending behavior of the 3D printed parts mainly depends on the identifier that is applied during printing. Polylactic acid (PLA) thermoplastics were chosen as a material that could be better suited for synthetic tissue / bone engineering applications. Moreover, most bone / synthetic tissue fails due to bending loads. Therefore, the effect of ID on the bending strength of PLA (biodegradable) material is important; Which was covered in this research work. Here, the PLA was printed using fusion deposition modeling (FDM) with variable ID (40, 60, 80, and 100%). The 3D printed cylindrical specimen with a diameter of 15 mm and a span of 30 mm was used. Flexural responses were investigated and reported in terms of

bending stress and deflection of bending strength at each ID. Moreover, fracture bending stress, fracture bending stress, bending modulus, and hardness of the printed sample were measured and correlated with ID. The result indicated that the 80% identity was the optimum ratio possessing great strength and stiffness. Besides, the sample surface and fracture shape.

2.3 Summary

The literature review in this chapter examines several aspects of the effects of the impact on the polymer materials. However, a very little work has been found to deal with the effect on the polylactic acid whose samples are designed by the 3D printer instead of the traditional method. In this field, the main interest of researchers is concentrated on the experimental and theoretical investigations of the energy requirements for shells or the plain composite plates As a result, it was decided to investigate the state of influence on the polymer plates used in various fields (medicine, transportation, sports, etc.). This includes studying the energy requirements of the panels installed at both ends. Also, new materials, such as polymers, citric acid, collision weights and different velocities will be used in this work.

Chapter Three
Theoretical and Numerical Analysis

Chapter Three

Theoretical and Numerical Analysis

3.1 General

The mechanical behavior of the poly-lactic acid (PLA) material depends on the type of density at which the samples were manufactured. Some calculations are made including energy absorption, total energy, force and acceleration. Also, the specified element method is used in the Abaqus / Explicit Dynamic program, and the total energy and impact are calculated through the program.

3.2 3D Printing Technology

Three-dimensional printing technology is one of the advanced technologies that promise to change the future of industries in the world. It has entered strongly in many fields, its amazing applications have varied, and the medical field has benefited from it like other fields, especially in the human organs industry [31].3D printing technology has the potential to revolutionize industries and change the production line. The adoption of 3D printing technology will increase the production speed while reducing costs. At the same time, the demand of the consumer will have more influence over production. Consumers have greater input in the final product and can request to have it produced to fit their specifications. At the meantime, the facilities of 3D printing technology will be located closer to the consumer, allowing for a more flexible and responsive manufacturing process, as well as greater quality control. Furthermore, when using 3D printing technology, the need for global transportation is significantly decreased. This is because, when manufacturing sites located nearer to the end destination, all distribution could be done with fleet tracking technology that saves energy and time. Lastly, the adoption of 3D printing technology can change the logistics of the company. The logistics of the companies can manage the entire process, offer more comprehensive and start-to-finish services [32]. There are three types of 3D printers [33]

1. Thermoplastic printer
2. 3D laser printers
3. Optical printers

3.3 Materials in 3D Printing

The materials used in the three-dimensional printing technology are considered functional materials for general purposes of the production of prototypes and final use, the materials used in the 3D printing technology are highly performance and therefore are used in the medical and space fields. The most common types of these materials are thermoplastics, which use fused deposition modeling (FDM) technology, and have important mechanical properties, such as good properties of flexural strength and depict a high impact and tensile strength [34]. In general polymers can be split into two categories: thermoplastics and thermosets. Thermoplastics are polymers that, after forming, can be melted and formed again (e.g polyethylene). Thermosets are polymers that once formed cannot be melted and reformed [35].

3.4 Determination of Both Total and Absorbed Energy

Absorbed energy can be evaluated as a quadratic dependence of the difference between the incident and transmitted pulses. This evaluation is derived from an analogy in the assessment of the absorbed energy from the difference between the impact and the residual kinetic energies of impactor at impact; however, the force-displacement response is not assessed [46].
The impact event is divided into two stages, the first is the impact stage which starts with impact velocity (Vo) and ends with the velocity and time at the maximum deflection (v_1 and t_1), and the second is the rebound stage which starts with (v_1) and ends with the final velocity and time after rebound ($V_2$and t_2). In the first stage, the kinetic energy of the impactor decreases to zero by losing its momentum, and then the kinetic energy increases in the second stage by gain of rebound momentum into the final value of kinetic energy after the impactor leaves the surface of the specimen with (v_2).
The value of (v_2) can be calculated by equation (3.1), since the rebound momentum is equal to the area under the (force-time) curve of the rebound stage represented by the integral in this equation [36].
The change in momentum (rebound momentum) of the impactor ball is

$$m(V_2 - V_1) = \int_{t_2}^{t_1} p\, dt \quad \text{..... (3-1)}$$

Where, (V_1=0)
Then, the absorbed energy is:

$E_{ab} = \frac{1}{2} m(v_0^2 - V_2^2)$……(3-2) [36].

The total impact energy is determined from the following equation: -

$E_t = 0.5 * M * v_2$ …… (3-3) [13].

M: the mass of impactor (ball)

3.5 Acceleration calculation

Acceleration of the falling objects is under the influence of gravity. On the ground, for example, if you let an object falls freely from a height, then its velocity of the moment you left it is equal to zero, but it reaches the ground at a speed exceeding zero. The more time that passes during the fall of the object, its speed increases, by neglecting air resistance [37].

Acceleration is calculated based on the different speeds, which is the initial velocity and the final velocity divided by time. The equation (3-4) shows that [37].

$$a = \frac{dv}{dt}$$

$$a = -\frac{v_f - v_i}{t} \quad \text{……(3-4)}$$

3.6 Force Calculation

Assume that something falls into the atmosphere close by sea level. Express a differential equation that depict the movement. We start by inserting character to represent different amounts of potential benefit in this trouble. Movement occurs over a certain period of time, so let's use t to evidence of time. The speed of the fall of the body. The velocity will Possible change with time, so we reason of v as a function of t; in other words, t is the separate changing and v is the reliant on variable. The selection of units of measurement is somewhat arbitrary, and there is naught in the declaration of the trouble to recommend suitable units, so we are free to make any option that appear sensible. Specifically, let's calculates the time t in seconds and the velocity v in meters / second. We'll assume the velocity is positive towards the downs orientation, that is, when the body is subsidence. The law that governs the motion of bodies is Newton's second law, which is expressed by multiplying the mass of a topic by an acceleration equal to the total strength of the object. It is expressed through Equation (3-5). [38]

Newton's second law states that if a force affects an object, it gains acceleration, proportional to its force and inversely to its mass.

F= ma …….... (3-5)

3.7 Numerical Considerations

One of the well-established and convenient techniques for the computer answer of complex problems is the finite element method (FEM) that used in various fields of engineering: mechanical engineering and civil engineering. FEM can be used as a tool for the approximate solution of difference reckonings characterizing various physical processes [39].
FEM is now extensively used in various fields in manufacturing and discipline. FEM has been used with interest in the rapid development of digital computers with big memory interplanetary as well as rapid calculation. It is believed that this method is unevenly known as the best robust geometric method, and the reason for this is due to its competences, as it has nonlinear properties and multifaceted limits for the material. In this effort, FEM was used with the help of Abaqus 2016 Method Analysis Software as a numerical tool to get the result of the pollen on the possessions. The determination of using Abaqus / Explicit is to verify investigational results in this work.

The Abaqus / Explicit cypher was secondhand to run the numerical FE model where the proposed disappointment starts and break criteria remained applied composed with the shear harm material model described in the earlier sections. Suitable geometrical models were constructed, and the kinematic and filling boundary conditions were defined to characterize the investigational set awake [40].

3.7.1 Geometrical modelling

The model is designed according to the data used in the experimental work in the laboratory, and according to the criteria of shock test, one begins to design the required form ABAQUS / Explicit through the following steps of designing the form. The model is drawn through this part of the program.

The sample is drawn in dimensions of 150 mm * 100 mm and a thickness of 3.5 mm, 4 mm, or 4.5 mm. A hemisphere is drawn with a diameter of 16 mm and a weight of 1 kg. The mechanical properties are introduced into the designed model and also the impactor properties of the model are introduced as shown in Figure (3.1).

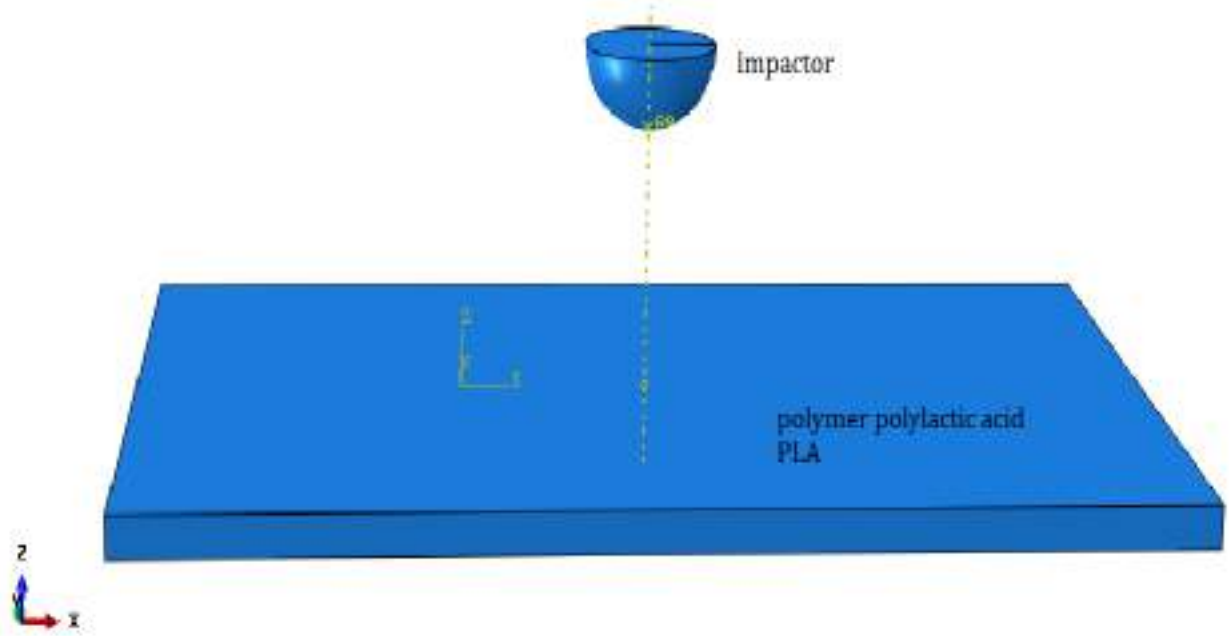

Figure (3.1) Abaqus Model Used for Impact Analysis.

3.7.2 Definition

All kinds of elements request the physical properties of the physical.
Contingent on requests, the obligatory possessions are:

1. Mechanical properties
2. Static and Dynamic Explicit
3. Anisotropic, orthotropic or isotropic.

Through property, the mechanical properties are inserted; mass density, Poisson's ratio, modulus of elasticity, the strength of yielding and ultimate tensile strength from a tensile test. Then, one chooses the type of movement, it is dynamic or static, through the step option. Then, the time is period entered.

3.7.3 Boundary and initial Conditions

Figure (3.2) depicts the boundary conditions for the second part of the model. The edges of the two edges of the polymer plate are fixed by making the displacement on it (U1, U2, U3, UR1, UR2, UR3) zero. The initial condition of the impactor has a velocity in Z-axis (U3) in the reference point of the impactor, and then the impactor moves as a projectile to impactor on the surface of the polymer. See Fig (3.2).

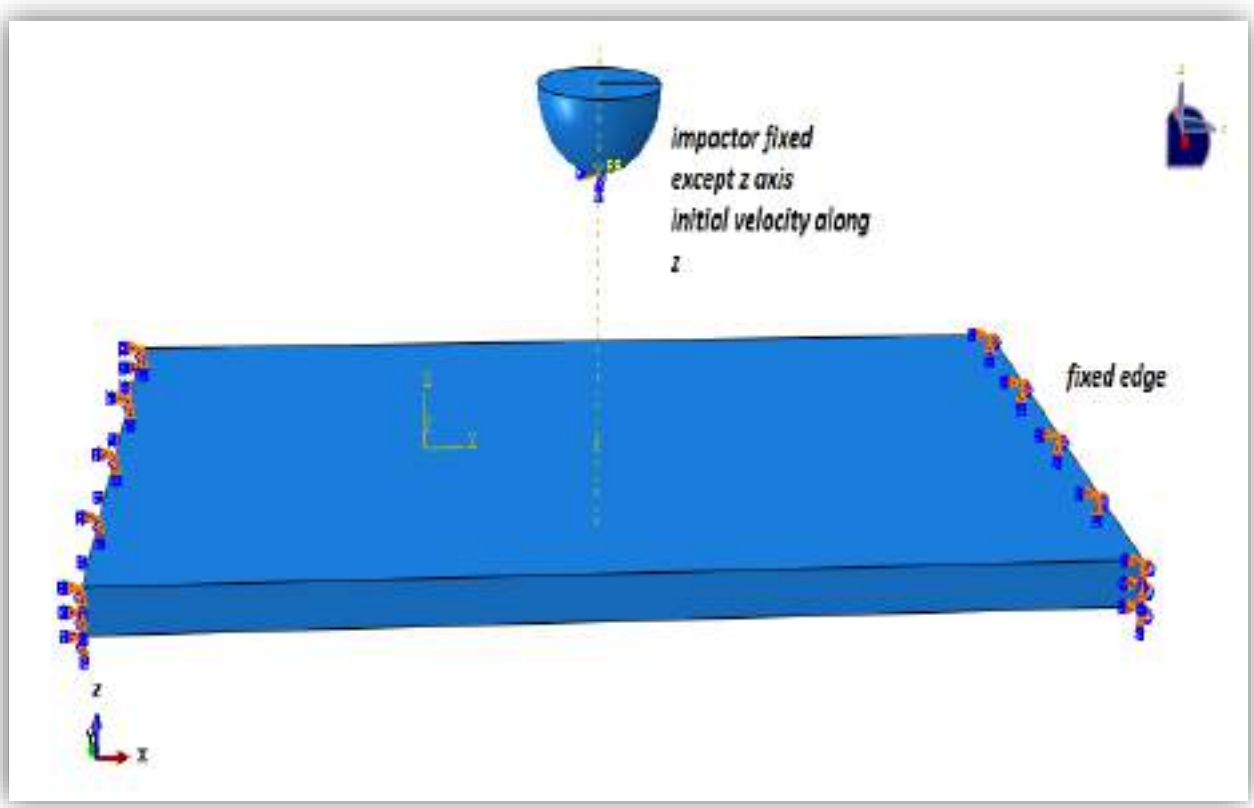

Figure (3.2) Boundary conditions of the model

3.7.4 Types of finite element used and mesh density

All calculations were performed with the ABAQUS / Explicit 16.9.1 commercial program using the User Materials (VUMAT) subroutine. The model consists of two parts shown in Fig. 3.3, impact material and polymer, the collider diameter is of 16 mm. The polymer plate comprises eight three-dimensional solid nodes, and the reduced integration elements (Abaqus element type: C3D8R). A hexagonal grid was used, and the number of elements was 8300. The contact state between the first part (collider) and the second part (polymer) was determined during the time period of 0.005 second. All the mechanical properties of the poly-lactic acid (PLA) were used in the simulation. The stress-strain curve of PLA was assumed elastic-perfectly plastic model for FEM analysis. Geometric nonlinearity was also considered for the examination to reflect the large distortion that occurred during the speed impact test of 3D printed plate.

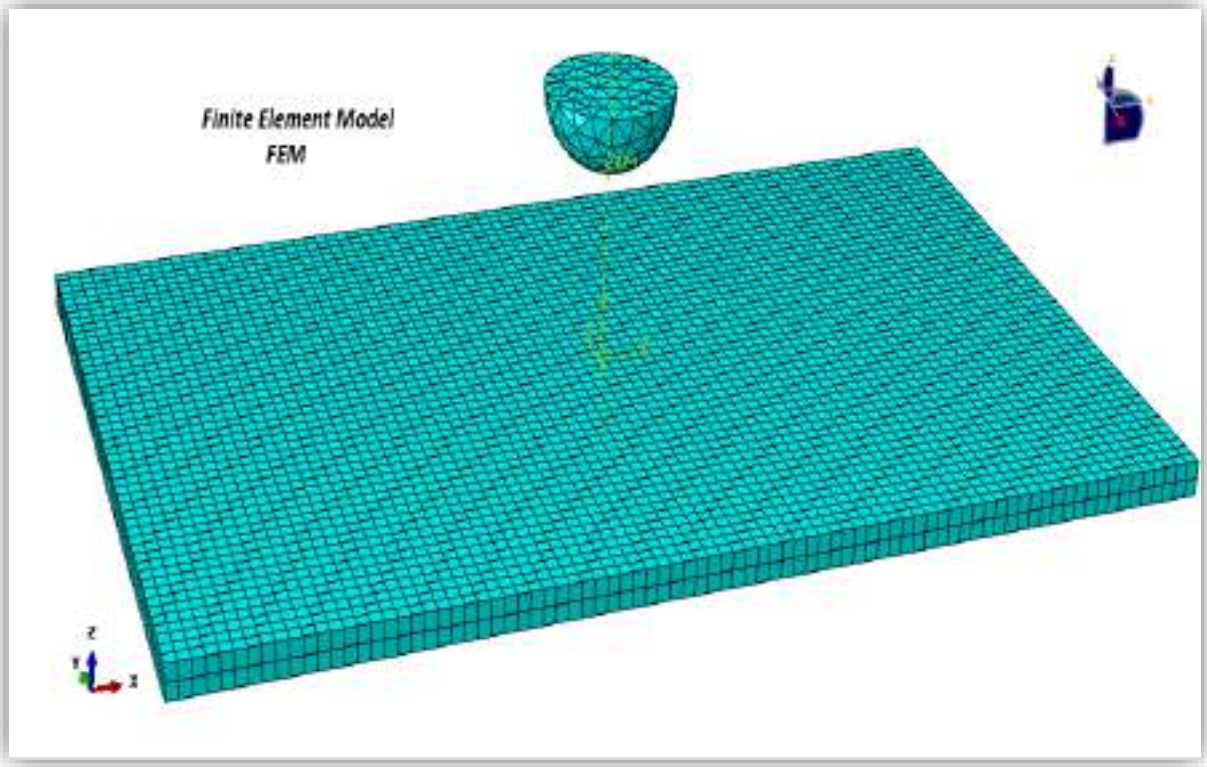

Figure (3.3): Finite element model of PLA under impact loading

3.7.5 Analysis and solutions

This section describes the steps required to build a finite element model. At this stage, the focus is shifted for running the model using Abaqus / Explicit Dynamic as an analyzer, and the results are studied with the post-resolution tool, and the simulation results were compared to the experimental results. As the total energy in this work obtained from this program as it gives the amount of energy through which it can be knowing the impact, damage and stress on polymer materials can be known. This will be mentioned in Chapter Five.

Chapter Four

Experimental work

Chapter four

Experimental Work

4.1 General

The chapter includes designing and manufacturing samples of different sizes; the material used is polymer (PLA). Also, the impact test device is designed, a three-dimensional printer is used in the design, and a tensile test is performed to know the mechanical properties. Following, the flowchart in figure (4.1) describes the experimental work procedure.

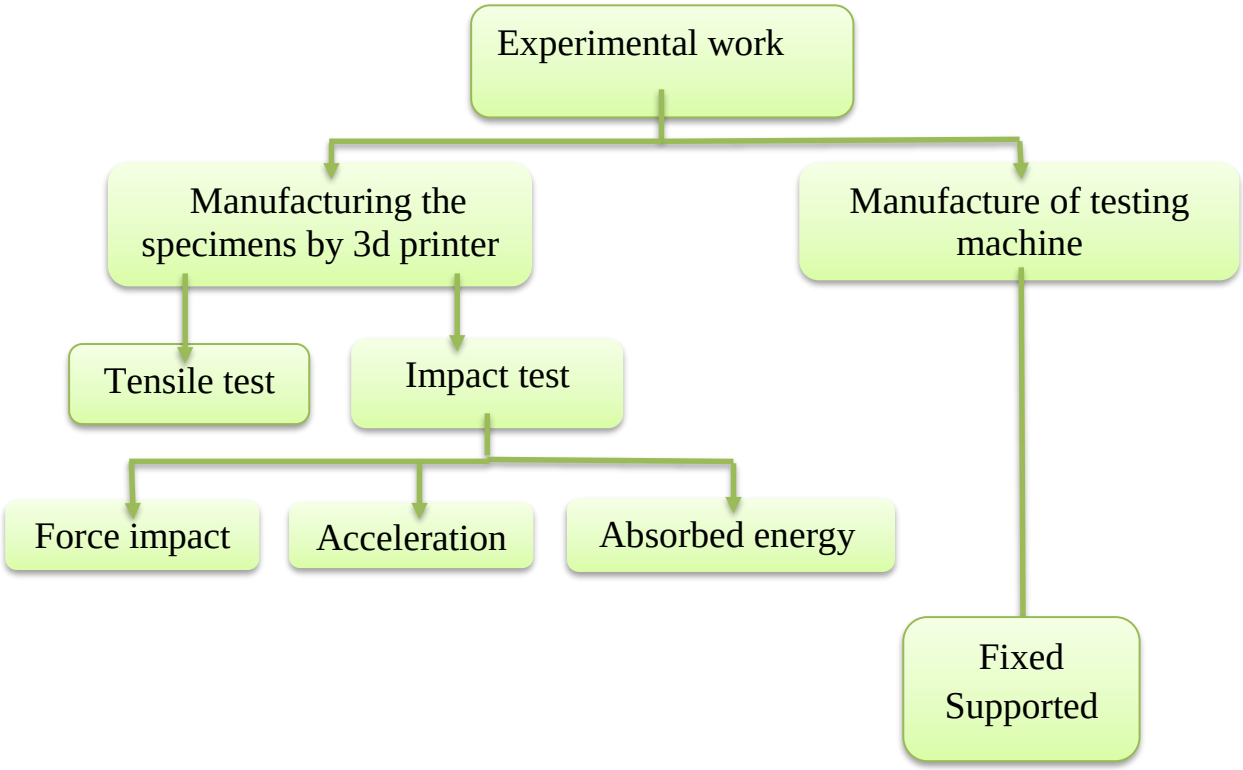

Figure (4.1) Flow chart of the Experimental Work.

4.2.1 Poly lactic acid (PLA) filament

Some PLA types are used in medical implants that decompose into the human body. Over time, no damage is created and replaced with a growing tissue. The most important advantages of PLA used in FDM (fused deposition modeling) printers, they do not emit gases that are toxic during

melting and are able, therefore, for printing without a system of ventilation [41]. It is used in the manufacture of household appliances, different equipment and children's toys, and PLA wires are suitable for use in the case of flexibility is not a prerequisite in the work of printing as they are vulnerable to break when exposed to any pressure. This material is not suitable for the manufacture of heat-dissipating models, where they lose their shape when exposed for some time at temperatures of 60°C and above. PLA wires are not used in the manufacture of models that are exposed to direct sunlight for long periods or those that are involved in the formation of car parts, and are not suitable for building kitchen pieces that are included in dishwashers for instant [42], see figure (4.2).

Figure (4.2) PLA filament

4.2.2 3D printer machine

The 3D printer was used in Tevo Tornado package and was a large size 3D printer that allows you to 3D print anything imaginable with a construction size of 300 * 300 * 400 mm and it was the best printer used on the market, as shown in Figure (4.3).

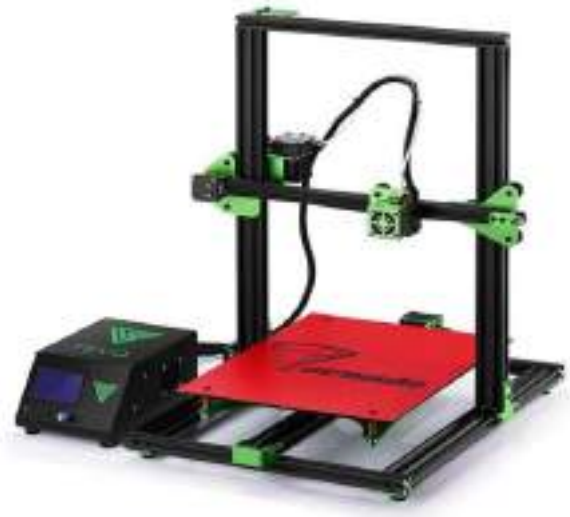

Figure (4.3) 3D printer machine (FDM technique)

Specifications: 3D printer: -

1. Layer Accuracy of 50 microns.
2. Maximum print speed: 150 mm / sec.
3. Case size: 300 x 300 x 400 mm.
4. E3D Bowden long distance extrusion machine is all metal with Titan.
5. Material Type: ABS, PLA, Wood, PVA, PETG.
6. The diameter of the material used is 1.75 mm.
7. Positioning accuracy: Z 0.004mm, XY 0.012 mm.
8. One color for printing.
9. Nozzle diameter: 0.4 mm.
10. Recommended extruder temperature: 210°C.
11. Heating plate temperature: 60-110°C (proper winter warming and summer-appropriate cooling).
12. Best ambient temperature: ≥25°C.
13. Connection: TF card or USB.
14. The file print format: STL, G-Code.
15. Compatibility: Windows, Linux, Mac.
16. CE, FCC specifications: CE, FC, ROHS.
17. Device weight: 14 kg.
18. Equipment size: 560X 600X620 mm.
19. Package size: 660X 560X 310 m.

4.2.3 Specimen preparation

In order to design the samples required in testing, the samples were designed and drawn in Solid Work Edition 2016, and the file was transferred to the STL format that was the format in which the file was transferred. The autopsy program that cuts the body to be printed layer by layer, where the repetier Software program was used, and the file in G-Cod format was converted to a 3D printer and according to the criteria as follows:

1. Tensile test according to ASTM D638, one type of stand [43].
2. Testing the impact according to ASTM D7136 standard [44].

Then, transfer the drawing to the printer by attaching a program on a computer or via an SD card. The 3D printer software STL file opens (repetier Software) and the software checks the files for design errors. Like focal points, modeling programs have several of them, and send the corrected file to the Slicer partition. This program signs the form in a large number of layers and slides, produces a G-Code file and contains many information and commands that aid in efficient printing. The print density was solid at 50% speed, and the nozzle diameter used was 0.4 mm.

The printer was on and the file was chosen to print. The print nozzle was heated at 210 °C and the printer platform was heated to 70 °C, which corresponds to the polymer PLA. When the print nozzle reaches the required degree, the polymer descends and the printer works by creating the pattern as required, as the printer moves in three axes (x, y, z) and after the printer finishes designing the sample, the model was left to cool down. The table below shows the thickness of the samples and the dimensions of the sample.

Table (4.1) The thickness and dimensions of the sample

Material	The number of samples	Dimensions (mm)	Thickness mm
PLA	18	150*100	3.5 ,4, 4.5

PLA	**9**	**165*19 ASTM D638**	**3.5,4,4.5**

Models were designed according to the ASTM D7136 test standard by creating a 3D object using Computer Aided Design (CAD) software, according to the dimensions of 150 mm * 100 mm, as shown in the Figure (4.4).

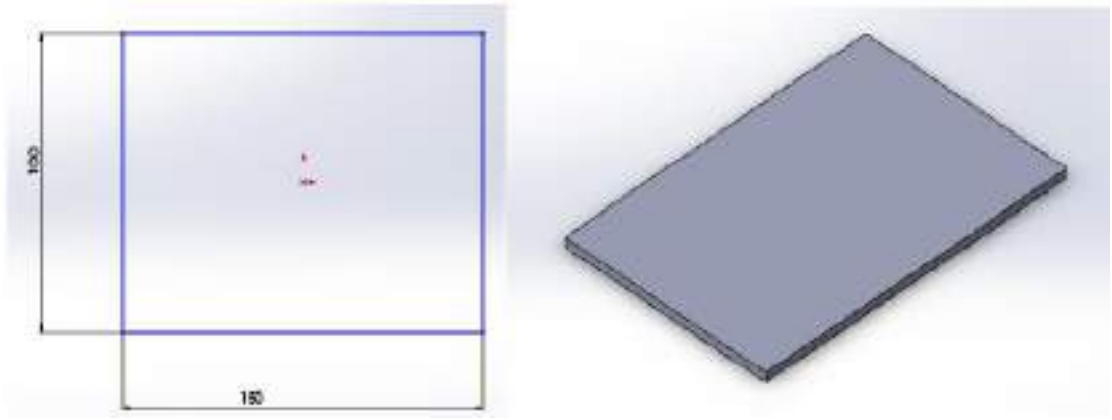

Step 1: Draw the sample in Solid works program for 3D.

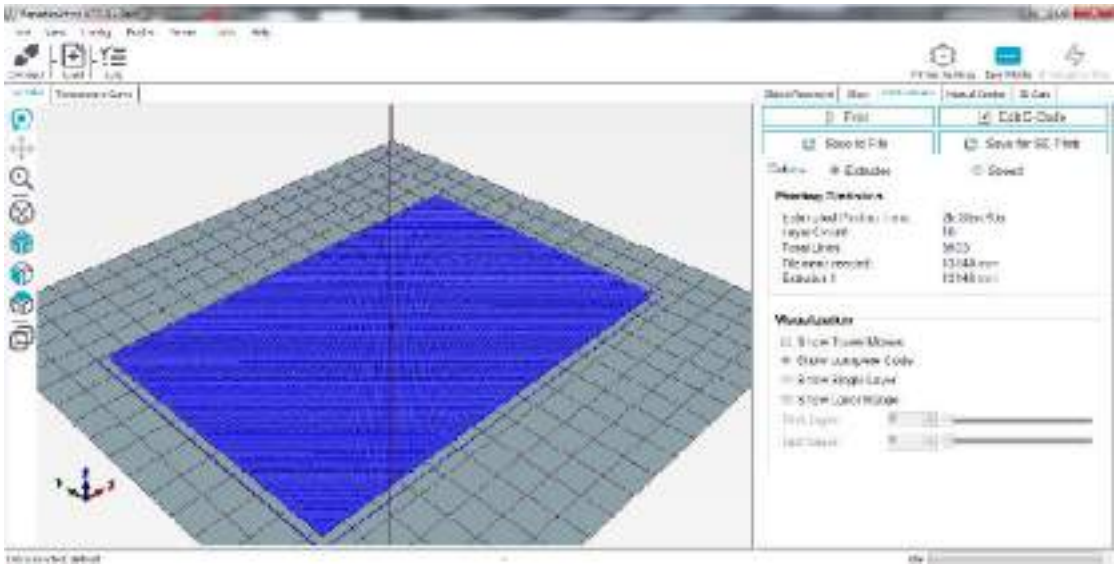

Step 2: Convert to G-code file

Step 3: Adjust the 3D printer start printing

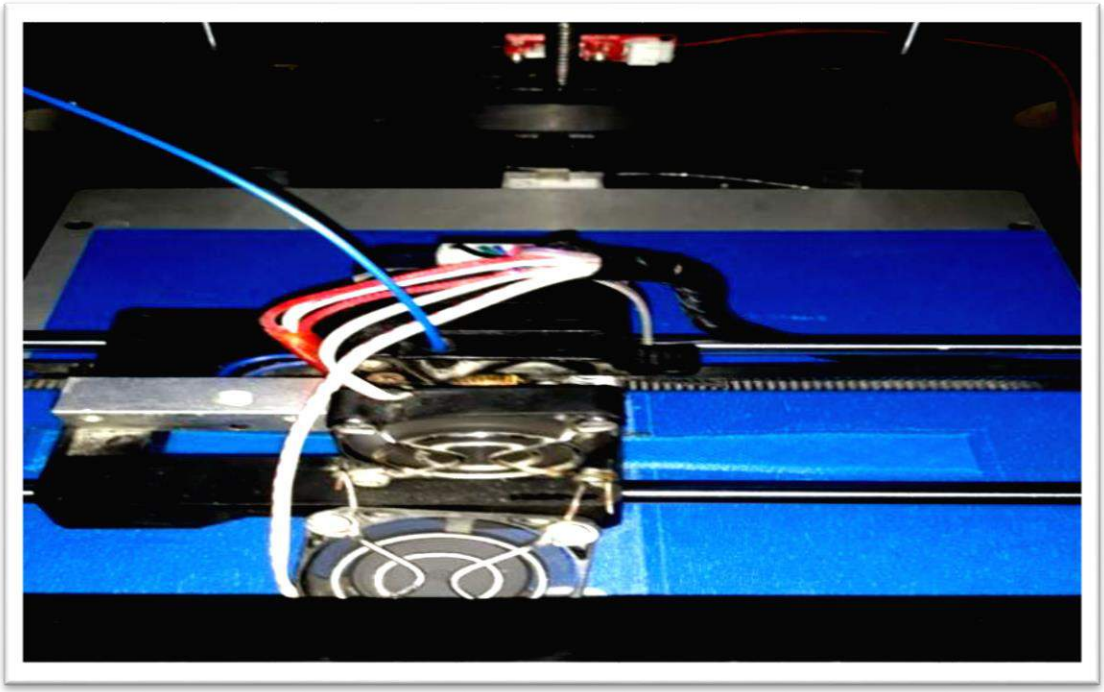

Step 4: During the sample settings before the printing process

Figure (4.4) Manufacturing of the specimens

The samples were printed as one group, and each group contains four samples with different thicknesses. Each sample lasts more than two and a half hour; this time depends on the type of sample filling.

4.3 Low-Velocity Impact Testing

4.3.1 Apparatus design:

The mechanical impact test machine was designed in accordance with the international standard, ASTM D7136 low-velocity impact tester. All materials needed to manufacture the testing machine were produced according to the materials available in the market. The device was designed prior to work in Auto CAD 2016 using Computer-Aided Design (CAD) software to develop a 3D model of the device. CAD software uses modeling to help create a design package that details the complex and individual assemblies. Then, it will finish and take some time. A picture of the design of the device before work and after work is shown schematically in Figure (4.5), appearing in the numbered parts in general layout view

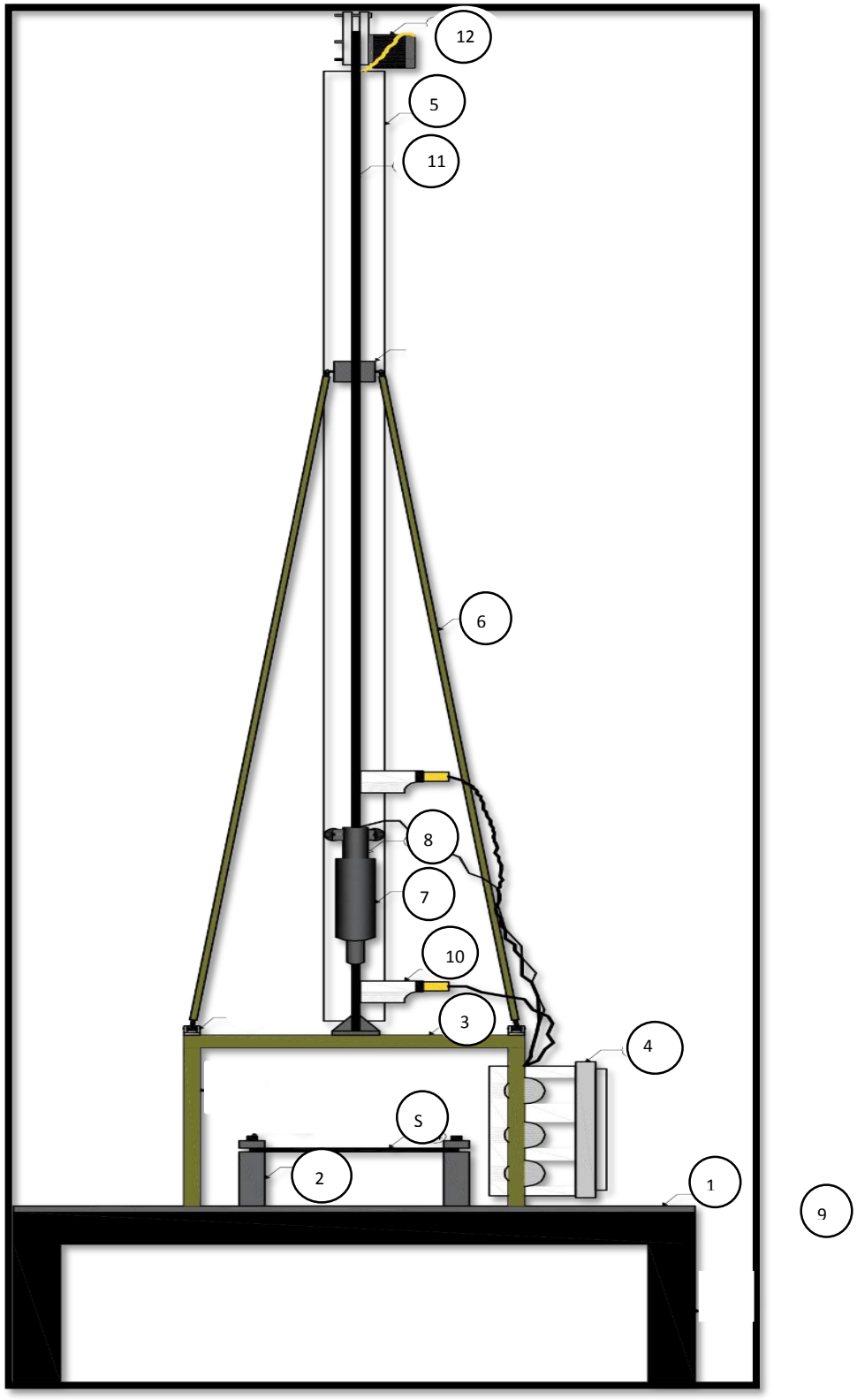

Fig (4.5) AutoCAD schematic Drawing for the Impact Test Device

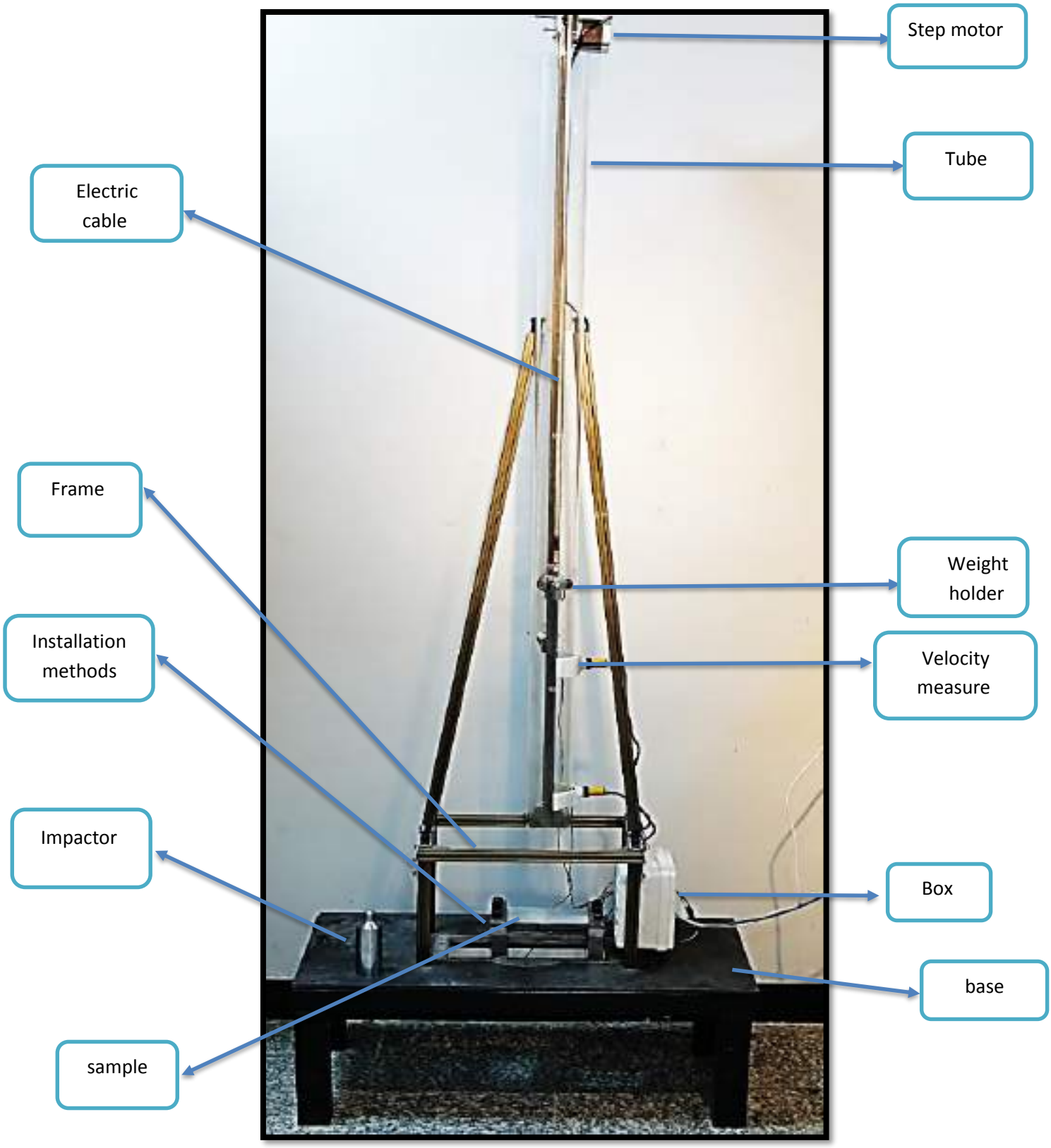

Fig (4.6) The Impact Test Device

The main parts of the low-speed impact apparatus are listed below, with more details:

1. **Base of the device**

The rectangular base was designed with dimensions of 70 cm * 35 cm, engraved in measurements of 25 cm * 8.2 cm from the center of steel as shown in Figure (4.6), and fixed from the bottom with four bumpers in order to absorb the vibrations resulting from the impact. And, make four holes were made on the base to install the structure on which the tube was based.

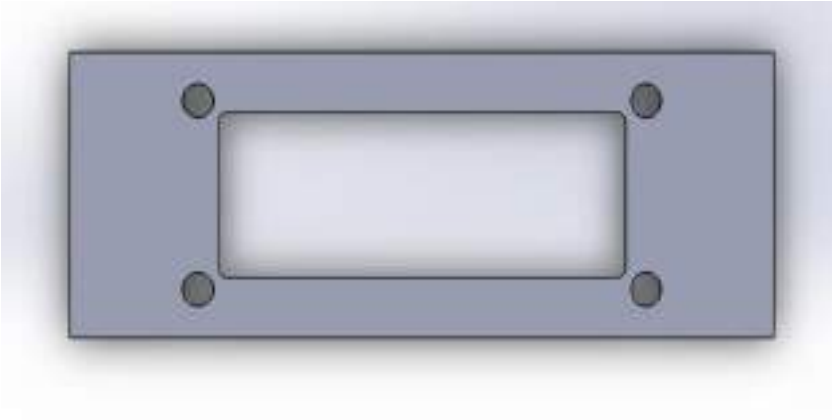

Figure (4.7) The basic base on which the device and the supports are based

2. Installation methods

There are different methods of fixing the samples, which include fixed support and simply support, the device was developed, wherein the previous method, the fixing methods were from all sides. One part of the supports will be fixed on the base and the other on the perforated part, which will act as a slide on the base, as shown in Figure (4.7).

Figure (4.8) The dowels of the samples the device.

3. Structure design over the base

The base of the frame was made using four pieces of equal steel angles connected in a square shape and their dimensions were 35 cm * 20 cm. Four legs were connected by a height of (25 cm) in the corners of the square base. All parts were fixed by gaskets and tightly attached. Chopping was installed on the base as shown in figure (4.8).

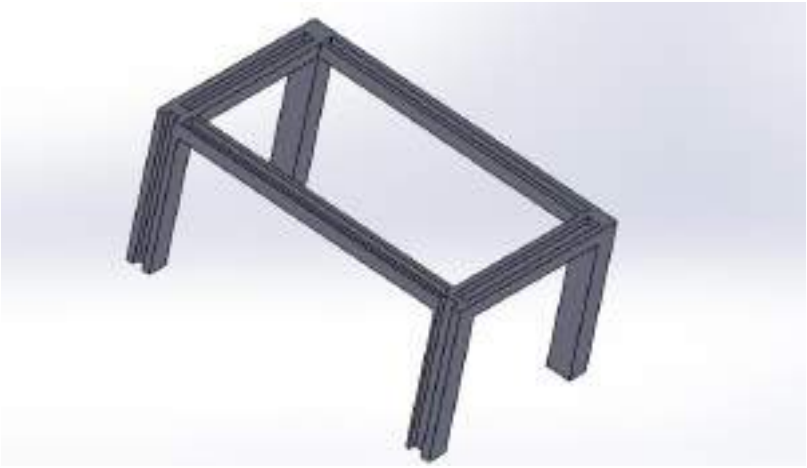

Figure (4.9) The frame design

4. Box of power supply and Arduino

It is a box that holds the Arduino board, the power supply, and some wires that connect with the sensor.

5. The tube

A transparent plastic tube with a diameter of 62 mm and a height of 2000 mm was used.

6. Tube support

Three pieces of aluminum rulers of various lengths were designed to fix the tube, with dimensions of 200 cm along the length of the tube, which support two lengths of 100 cm from the middle and all rulers were fixed to the frames.

7. Impactor

The shock ball was designed of steel with a diameter of 16 mm. The impact ball was 1 kg in weight.

8. Weight holder

It was an electromagnet that carries the weight as the maximum energy to carry 10 kg. The shape of the magnet was circular.

9. Impact program used (ImpLab Ver.1.0)

The laptop computer was used to collect data, connect the Arduino program, and control the program through the computer from the peak of the fall, and give instructions for doubling the sample. Figure (4.9) shows the design of the test interface designed in the Arduino program. And output the test values and control the device. A flow chart shows the way data is entered and output as shown in figure (4.10).

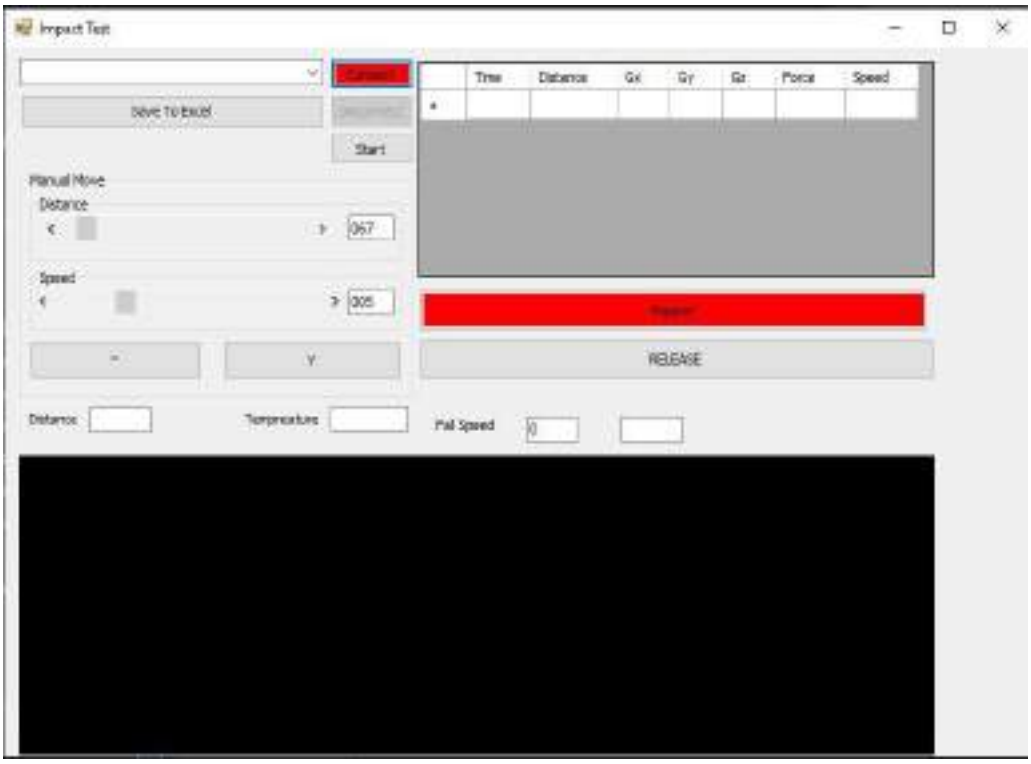

Figure (4.10) The results of the output interface in the computer.

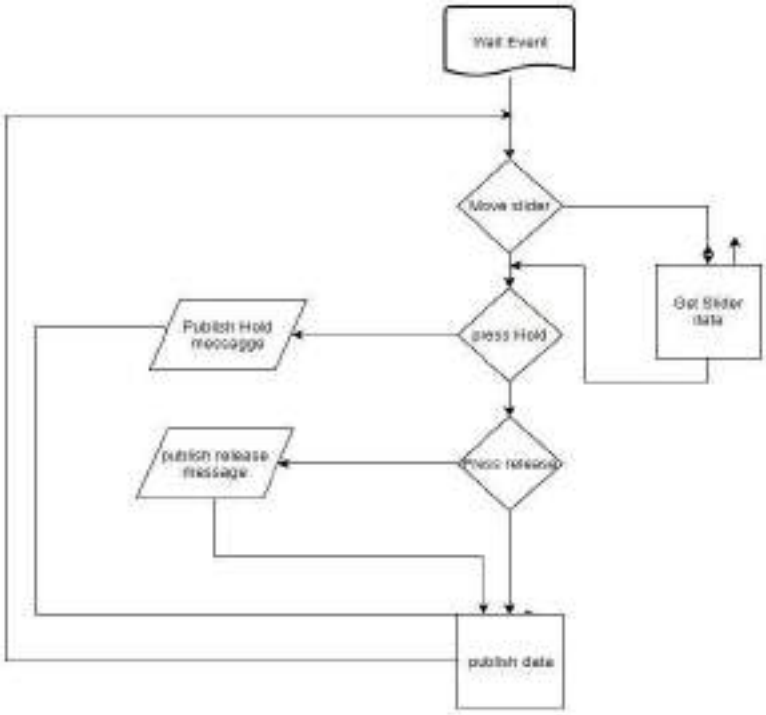

Figure (4.11) Flow chart with output

10. Velocity measurements device

It was one of the types of infrared sensors. It works with infrared ray and the principle of sending and receiving to determine the presence of an object at a certain distance, in the present work, the length is (50) mm and the diameter is (17.75) mm. See Figure (4.11).

Figure (4.12) Velocity device

Impact velocity can be calculated using the equation (4-1) of simple free fall [47].

$$v = \sqrt{2gh} \qquad (4\text{-}1)$$

Table (4.2) shows the velocity calculated by the sensor and calculated through the equation.

Table (4.2) Values of measured and calculated impact speeds against the height

Height (cm)	Speed measured (m/s)	Calculated speed (m/s)
25	**2.001567**	**2.214723**
50	**2.98466**	**3.13209**
75	**3.19753**	**3.83601**

11. Electric cable

When using the conventional cable, warping problems are arising So, it was replaced by an electrical cable with inner wires. A crane raises the impact weight by several ties with the magnetic weight holder. Where, the

holder was connected via a cable because it contains wires that are connect from the inside

12. Electric rotating alternative step motor

It rotates and raises the shocking weight through the shear connected to it and takes instructions from the program to give the command from the computer. That connects to the Arduino board. See Figure (4.12)

Figure (4.13) Electric rotating alternative step motor

4.4 Arduino Uno R3

It is an open-source electronic board developed by the Arduino Company, and so it is called by that name. The board contains the main element, Micro Control, which is the part responsible for programming and restoring it, and it connects the input and output units. The transformer was the part responsible for delivering energy to the micro-control because it was not used for direct energy. Therefore, it is transferred via the computer. The USB is the part that connects the computer to the Arduino board, which can feed the Arduino with electricity and transfer data to the computer. It contains fuses and voltage regulators. Power collector was a maximum input power of 9 volts, as it is converted through the voltage regulator to 5 volts. It also contains two capacitors, and TVS was a translate voltage suppression that is used to smooth and control the voltage inside the controller. It has a dual amplifier and contains the oscillator of the controller that generates the clock pulses, which the controller needs. There are digital inputs and outputs that are known as digital (PWM), analog input modules known as ANALOG IN, and the feeder foot controller known as POWER. See Figure (4.13)

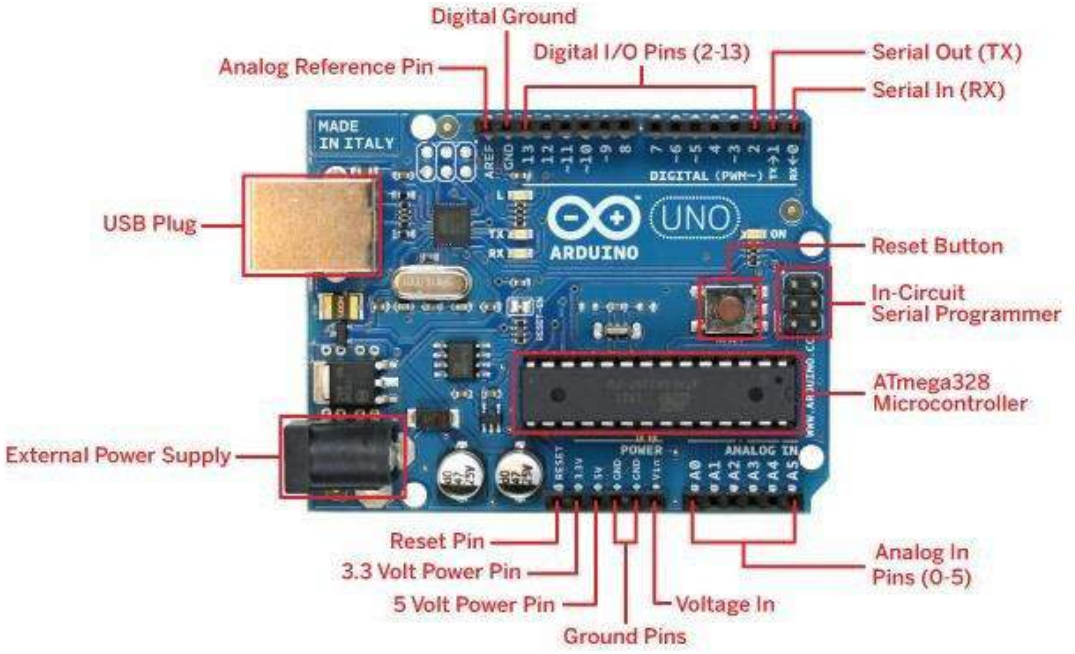

Figure (4.14) The Arduino board and the parts mark on it

4.4.1 Force Sensitive Resistor (F S R) sensor

Force sensor composes of the conductive polymeric materials. After a force is applied to the surface, it changes the resistance in a predictable manner. It has different shapes. The sensor consists of both conductive and non-conductive particles attached to a matrix. Particles are of sub-micrometre sizes. They are formulated to reduce heat dependence, improve possessions and increase surface durability. The force applied to the sensor causes the particles to touch the conductive electrodes, which leads to a change in the resistance of the sensor, as in all resistance-based sensors. Power sensor resistors require a relatively simple interface and can operate satisfactorily in somewhat hostile surroundings. Likened to other force devices, the advantages of FSRs are their size (thickness typically less than 0.5 mm), low price and good tremor confrontation. The disadvantage is their low precision: measurement results may differ 10% and more. Force-sensing capacitors offer larger sensitivity and long term constancy but require more complicated drive electronics. The figure below shows the force sensor used to measure the impact force, figure (4.14)

Figure (4.15) The force sensor used in the calculation

4.4.2 Gyroscope Accelerometer MPU6050

It was one of the sensors that know the movement of the body, that was, it calculates the acceleration in all directions and the rotation of the object. It was used in planes and robots to find the balance of bodies. The accelerometer was a meter that measures the acceleration relative to the free-fall experience of the effect of gravity. The models available were single-axis and multi-axis, which detect the magnitude and the direction of the acceleration as a vector force of quantity, and can be used for intended steering, vibration and impact. See Figure (4.15)

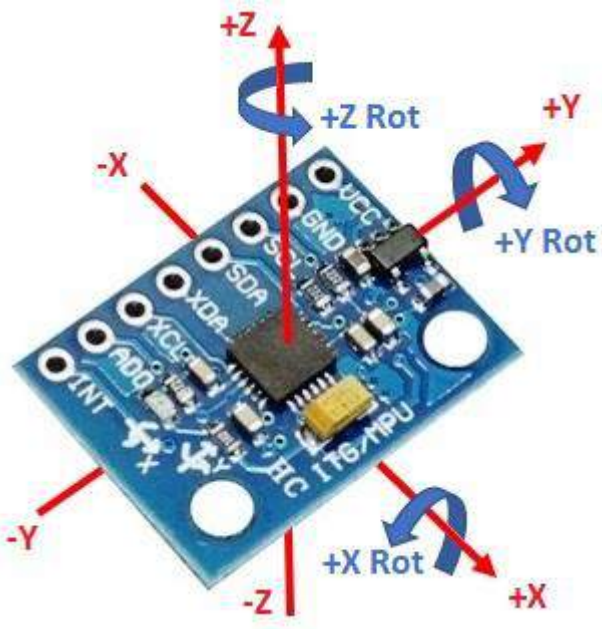

Figure (4.16) The acceleration sensor type MP6050

4.4.3 Calibration

The measured impact force was calibrated according to the static calibration process through a linear relationship to the resistance / conduction force sensor resistors that can be calibrated by applying different weights to the middle of the fixative sample period and measuring the FSR output voltage. The value of the titration constant is found to be (1.11) N / mV [13].

4.5 Testing of Specimens

4.5.1 Tensile Test

In order to determine the mechanical properties of 3D printed materials, it was important to perform a tensile test to study the mechanical properties. This was done in accordance with the standards of ASTM D638, Figure (4. 16) showing the scheme, design of the sample and its dimensions according to the measurement. The Young's modulus (E), yield strength (σy), tensile strength (UTS), were obtained using the (TINIUS OLSEN) machine (University of technology, Material engineering department).
Figure (4.17) reveals specimens of tensile test specimens prior and beyond the test. The modulus of elasticity was obtained by from the stress-strain curve.

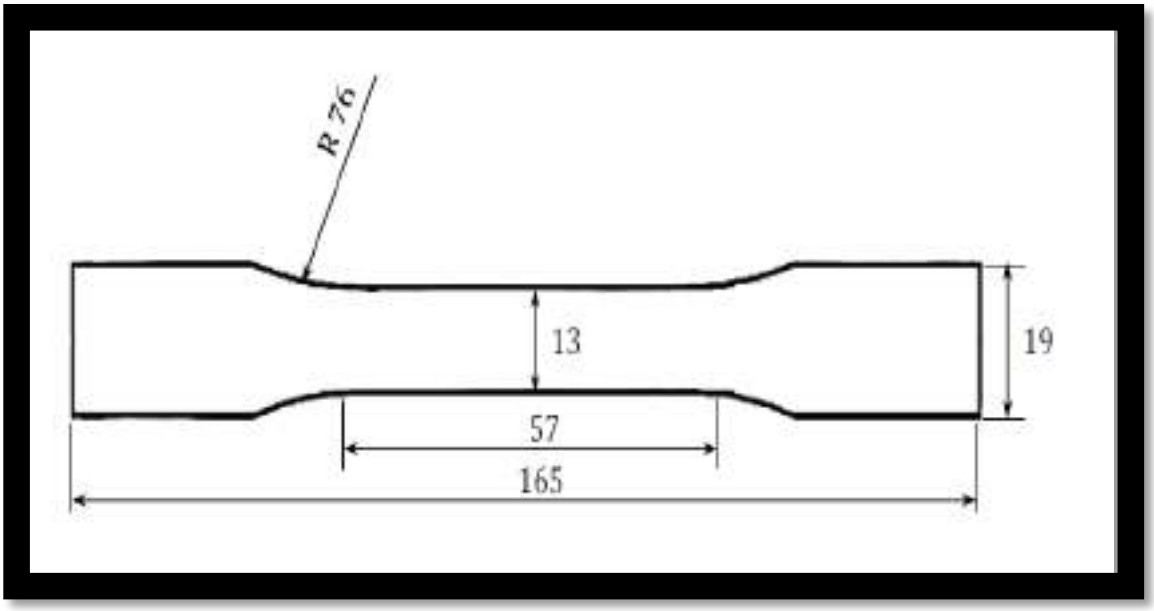

Figure (4.17) The tensile test specimen according to the standard ASTM D-638.

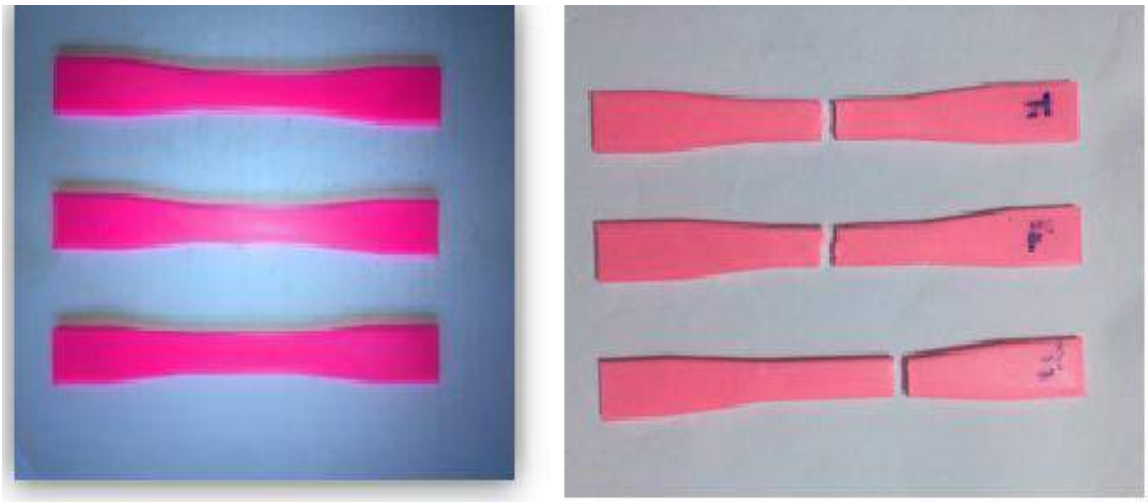

A) Sample before the test B) Sample after the test

Figure (4.18) The tensile specimens for PLA.

4.5.2 Impact Test

Samples were designed according to ASTM D7136 standard shown in Figure (4.18), after designing them in Solid Work, and then transferred to the 3D printer using as card (SDC). After the samples were designed, the test was carried out in a test machine designed according to the required standard.

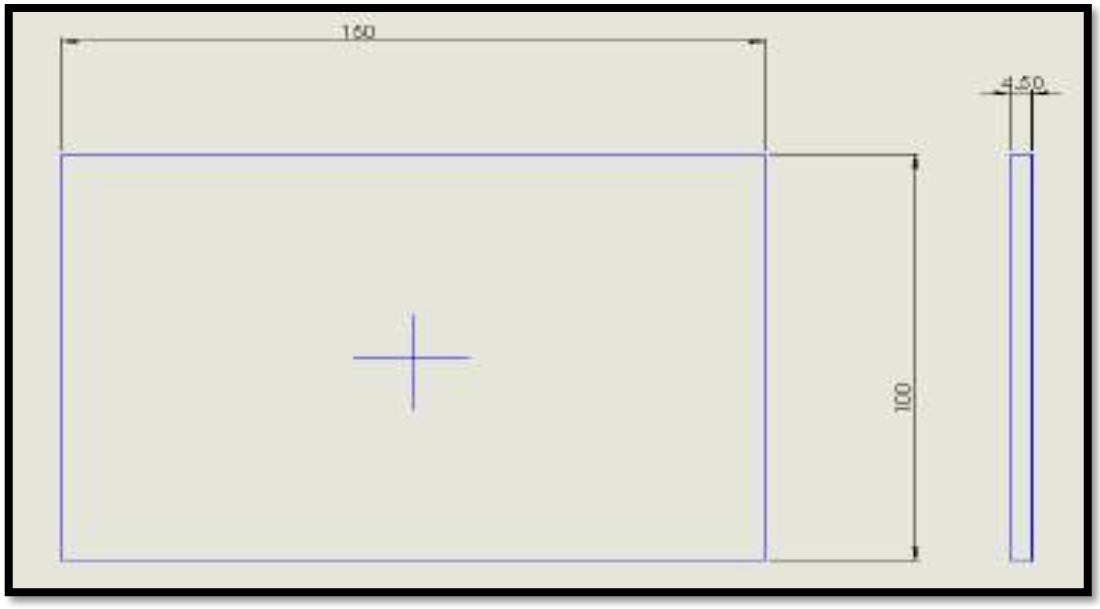

Figure (4.19) The impact test specimen according to the standard ASTM D-7136.

Two methods of the fixation of samples have been adopted, which were simply supported and static methods, as shown in Figure (4.19).

Figure (4. 20) The method of fixing the sample to the stents.

The sensors were fixed so that each of the FSR is in the middle of the sample in the jacket part of the sample. The MPU 6050 was also installed, and the falling height was measured by a metric Alfie tape measure, as shown in the figure (4.20).

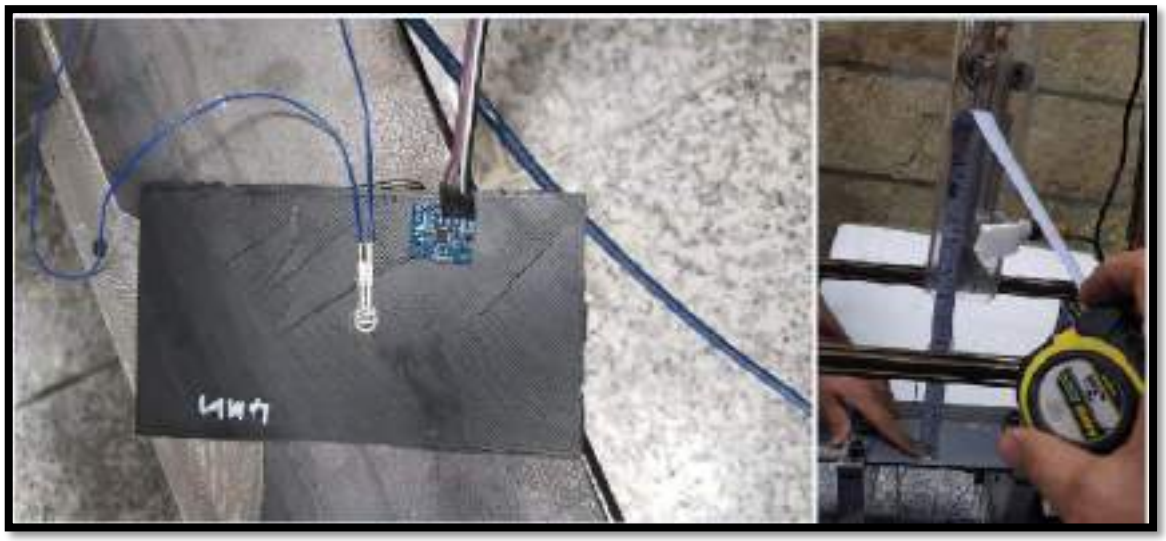

Figure (4.21) The method of fixing the sensors to the sample

Table (4.3) shows the type of fixation, the falling height, and thickness of the sample that was tested in the test machine. Figure (4.21) depicts the impact specimens for PLA.

Table (4.3) The type of fixing, drop height, and specimen thickness

test no	Type of fixing	Impact height (mm)	Thickness (mm)
1	fixed	25	3.5
2	fixed	25	4
3	fixed	25	4.5
4	fixed	50	3.5
5	fixed	50	4
6	fixed	50	4.5
7	fixed	75	3.5
8	fixed	75	4
9	fixed	75	4.5

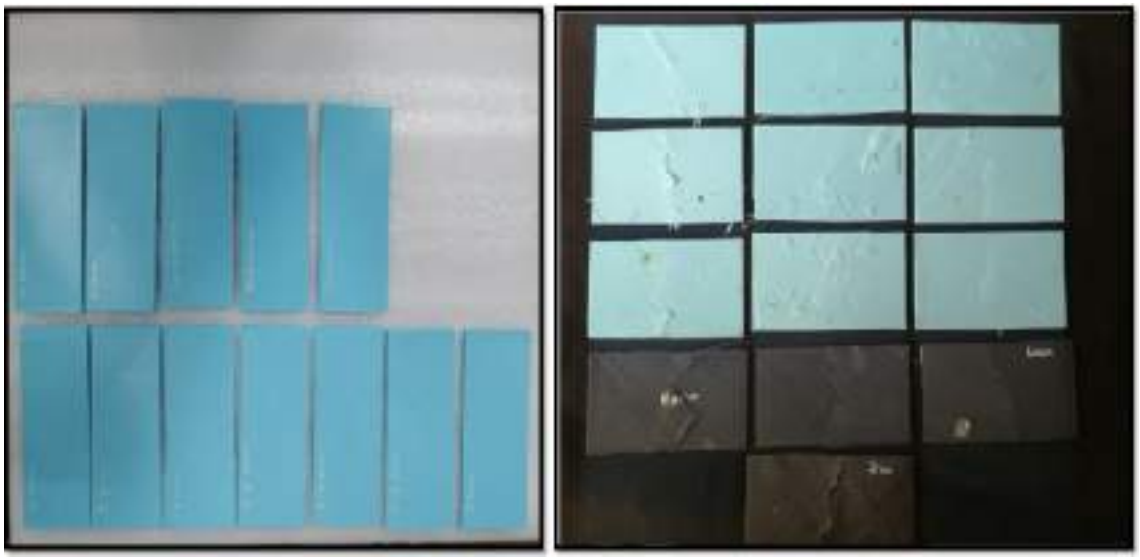

A) before test B) after test

Figure (4.22) The impact specimens for PLA

Chapter Five
Result and Discussion

Chapter Five

Result and Discussion

5.1 Introduction

This chapter discusses the experimental and numerical results, obtained from Abaqus/Explicit simulation program. Mechanical properties are identified by means of the experimental tensile tests. The practical results of impact force, acceleration, and total energy are calculated and discussed. The experimental results are compared with numerical values. The results showed a convergence between them at different energy levels, 2.49 J, 4.9J and 7.3 J.

5.2 Tensile properties

The ultimate tensile stress ,elastic modulus , yield stress and elongation % were obtained using tensile test for all specimens. Table (5.1) gives the mechanical properties (Modulus of Elasticity ,Ultimate Tensile Stress, Yield Stress and Elongation %) of samples of PLA (polylactic acid). As shown in the table, the samples with higher thickness gives better mechanical properties .

Table (5.1) Experimental Mechanical Properties for all Tensile Samples

Samples	Thiknees	Mechanical Properties			
		σ_{ult} (MPa)	E (GPa)	σY (Mpa)	εF elongation %
Sample 1	**3.5mm**	**42**	**1**	**36**	**9.7**
Sample 2	**4mm**	**45**	**1**	**34**	**8.11**
Sample 3	**4.5mm**	**47**	**1.087**	**31**	**7.3**

5.2.1 Stress – strain curves

Tensile test was performed on the specimens to obtain the load– elongation and stress–strain curves. Figures (5.1 to 5.3) illustrate considered materials(PLA) with thicknees (3.5, 4 and 4.5)mm. This figures (5.2 and 5.3) clearly show increase in the ultimate tensile stress by (0.07% and 0.12%) respectively in comparison with figure (5.1). The end result is a higher strength of PLA (poly lactic acid) for samples with a thickness of 4.5 mm because the elongation is lower. The increase in the thickness of the PLA specimens leads to a higher resistance to deformation which results in higher tensile strength. But the presence of pores in the som samples manufactured by the 3D printer leads to a decrease in the tensile properties. In another word, the pressure is likely to be concentrated inside the sample pores, which leads to slipping occurrence inside the material due to the external load. Similar results trend also have been found by Tsouknidas et al. [21], thicker samples demonstrate a significant improvement and a higher resistance to deformation because of higher tensile strength.

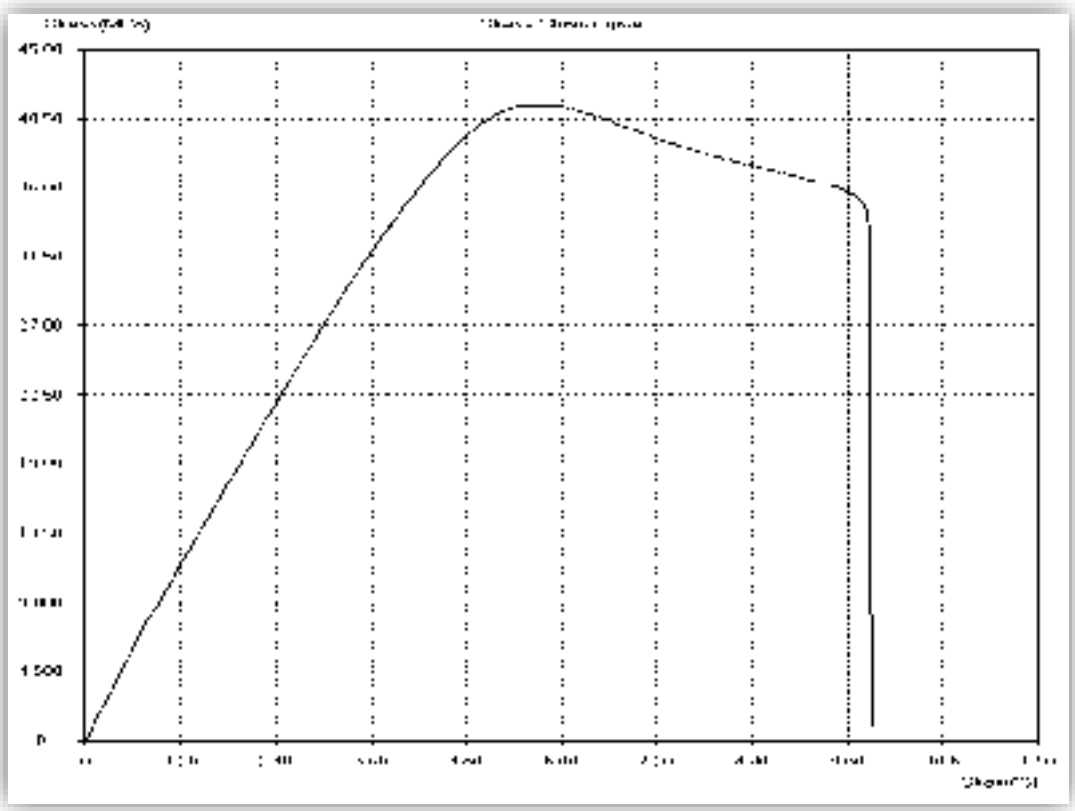

Figure (5.1) Stress – strain curves of PLA sample at 3.5 mm thickness.

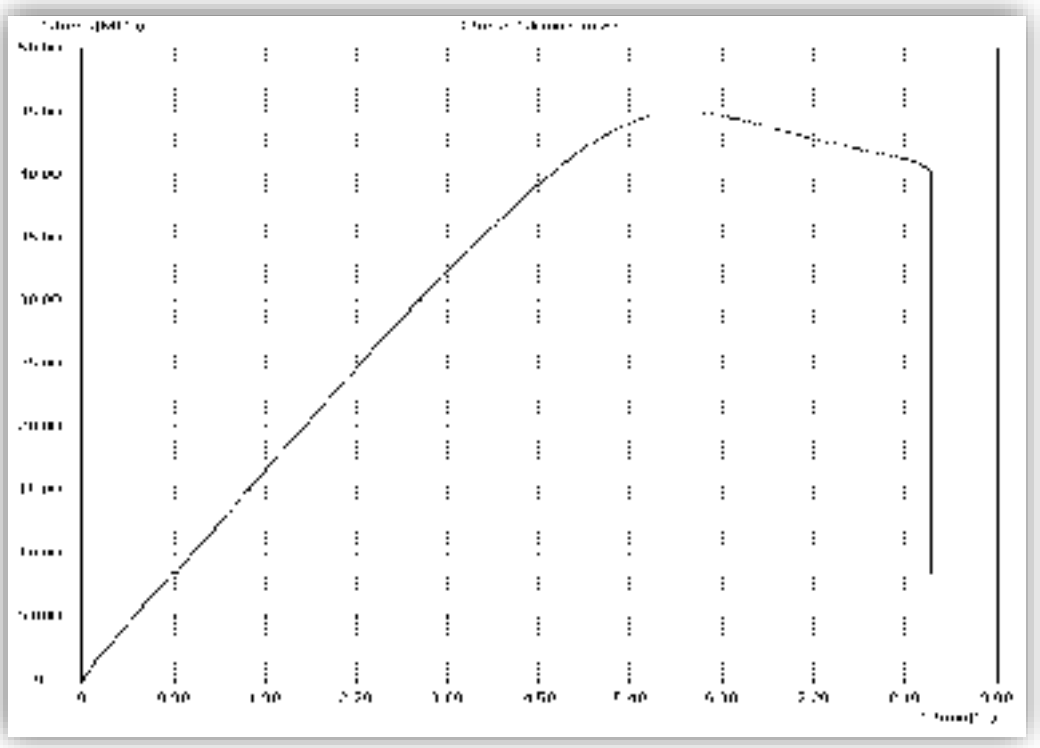

Figure (5.2) Stress – strain curves of PLA sample at 4 mm thickness.

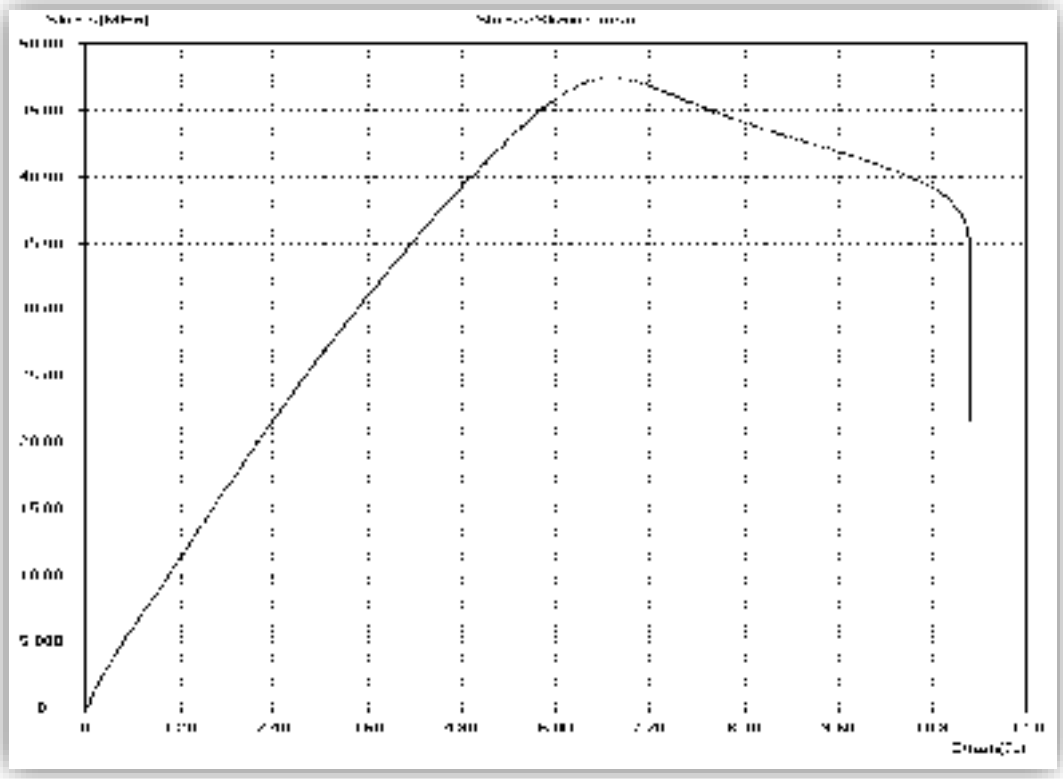

Figure (5.3) Stress – strain curves of PLA sample at 4.5 mm thickness.

5.3 Impact Test Result

The experimental and predicted impact strength curves were simulated versus energy time to assess the validity of the **applied** model in an attempt to estimate the resistance of the materials that were used in the experiment to poly lactic acid.

5.3.1 Impact Force Result

The fluctuations in the curve (f-t) show the possibility of malfunctions in the manufactured material because the material lacks rigidity. The decreased strength indicates that the material has a high strength and toughness, under the influence of low speed. The peak strength on the curve (f-t) is one of the important characteristics of the polymer durability after impact. Before reaching the peak strength value. The curve (f-t) reveals a sudden decrease in strength due to the presence of a crack on the affected part of the material and the dissolution of the sample after reaching the peak strength, and the sample reaches fracture and shattering.

Figures (5.4) to (5.6) depict the typical force date and time curves for samples with variable thicknesses. It was observed in Figures (5.4 to 5.6), similar behavior during the period (starting roughly from 0 to 3.5 ms). The experimental results showed a slight defect in the upper surface of the interface in addition to a defect inside the polymer with an impact energy (2.49 J). This leads to a change in the course of force behavior over the period (2 ms to 3.5). This is evidenced by the shape of the oscillations, which are in agreement with Min Sun, **et al. [45]**, reported similar trends for impact force behaviour. The difference in oscillations is a result of the effect of the sample thickness. The apparent changes in shapes are due to the fluidity of movement and due to the beating that is near the sensor. For the simple correlation, its waves continue to oscillate, and this is due to the movement of the sample at the stroke up and down. the curve is like a sine curve, which means there is little damage in the plate.

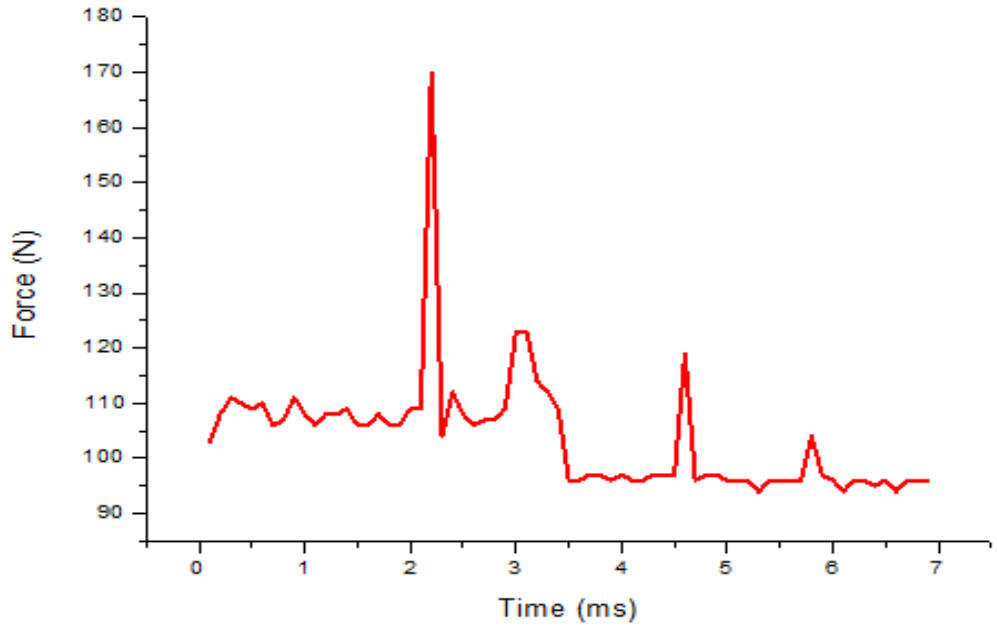

Figure (5.4) The impact force versus time curve of polylactic acid plate at impact energy 2.49J and thickness 3.5mm, high 25 cm.

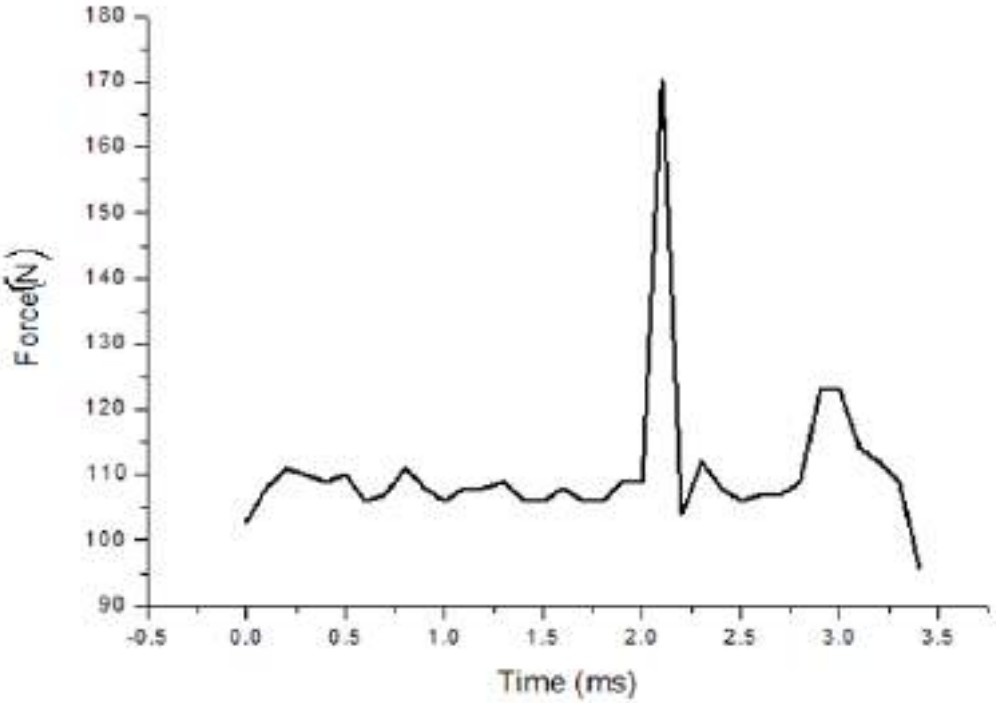

Figure (5.5) The impact force versus time curve of polylactic acid plate at impact energy 2.49J and thickness 4mm, high 25 cm.

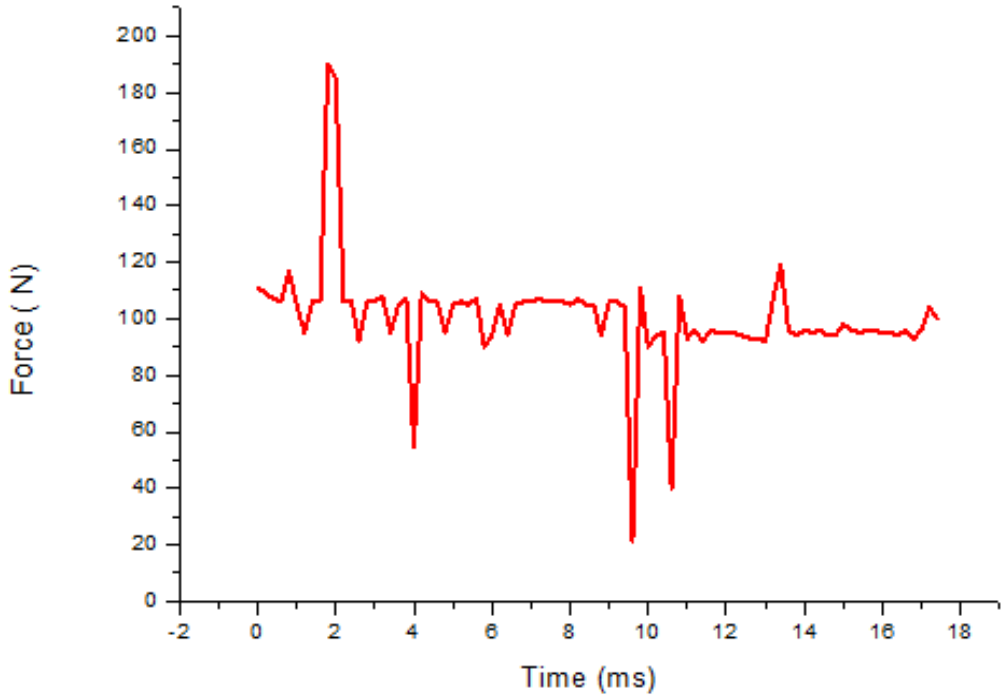

Figure (5.6) The impact force versus time curve of polylactic acid plate at impact energy 2.49J and thickness 4.5mm, high 25 cm.

Figures (5-7 to 5-9) show the value of failure modes similar to the face paper that led to a change in the path of the force behavior (disintegration of some parts of the sample abdomen) with an impact energy of 4.98 J. The samples in the lower parts of the sample during the period (2.5 ms to 3.6 ms) were the different in the level of effect with the stability of the impact weight, as it was observed that the damage caused by the blow increased significantly, which led to disintegration in some parts of the sample. This is with increasing impact energy, the increase in the shape of the oscillations is due to the material's resistance to a blow. The increase in the impact effect results of increasing the speed. This apparent difference in the shapes is due to the elasticity of the material and the resulting vibrations. It can be noticed that as the number of layer increased, the force required to sample fail also increases. This is due to the increase in samples thickness, which is stated by **Zhang, Xiang, et al [46] .**

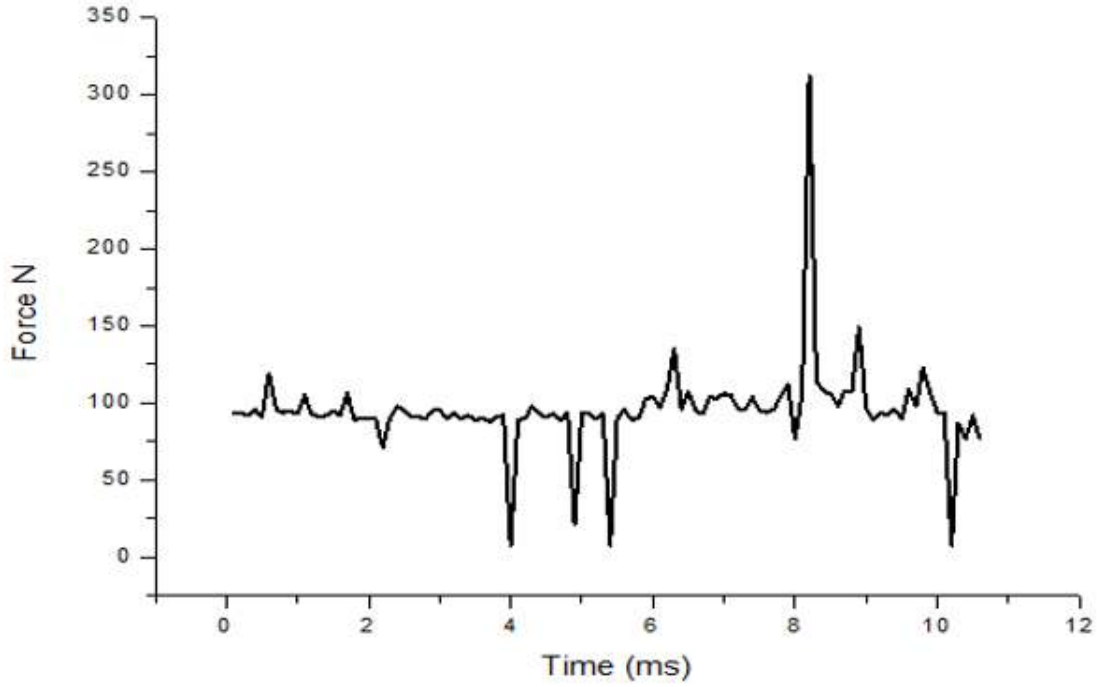

Figure (5. 7) The impact force versus time curve of polylactic acid plate at impact energy 4. 98J and thickness 3.5mm, high 50 cm.

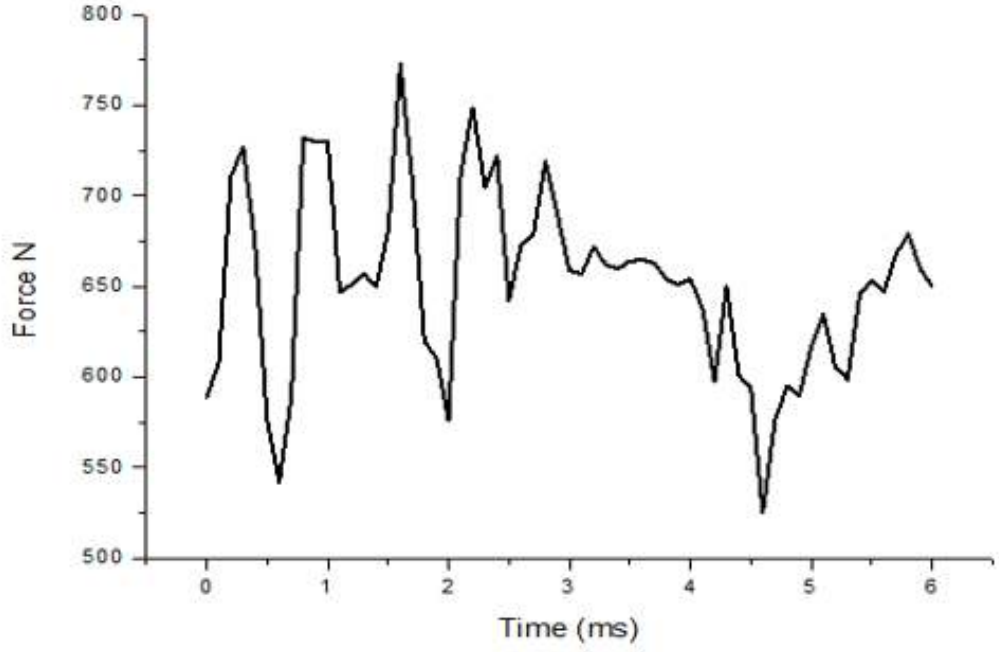

Figure (5.8) The impact force versus time curve of polylactic acid plate at impact energy 4. 98J and thickness 4 mm, high 50 cm.

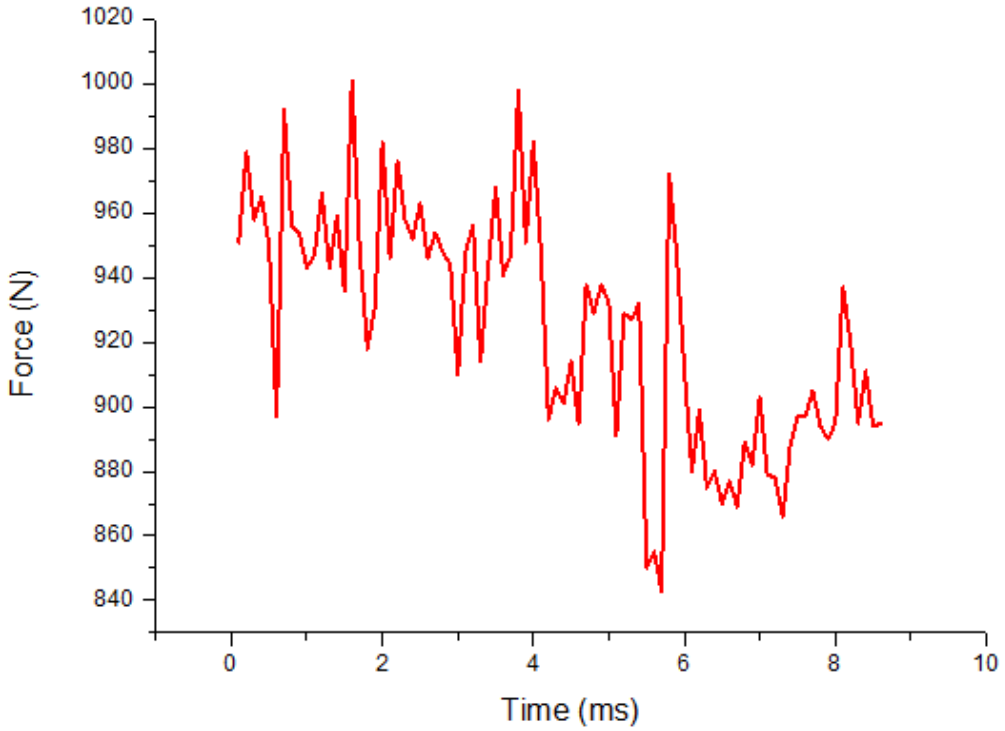

Figure (5.9) The impact force versus time curve of polylactic acid plate at impact energy 4. 98J and thickness 4.5mm, high 50 cm.

Through the test that preceded this test, noted that Figures (5-10) to (5-12) occurred in the failure and breakage of the material and the disintegration of its parts, which led to a change in the force path at the shock energy 7.35 J. This shows the ratios of the increase in strength that would only lead to the collapse of the material, but there are different ratios between each material due to the different thickness of the pattern, on the basis of which the value of the applied force from the period (2 ms to 4 ms) appears, and this is an important factor through which model making can be affected. Impact strength is the ability of a material to absorb the impact load without being broken **[47].** This is an indicator of the hardness of the material. Processed samples have a gradual decrease in impact strength with increasing layer thickness. The failure modes observed in the specimens can be attributed to the brittle nature of the PLA and ABS [48].

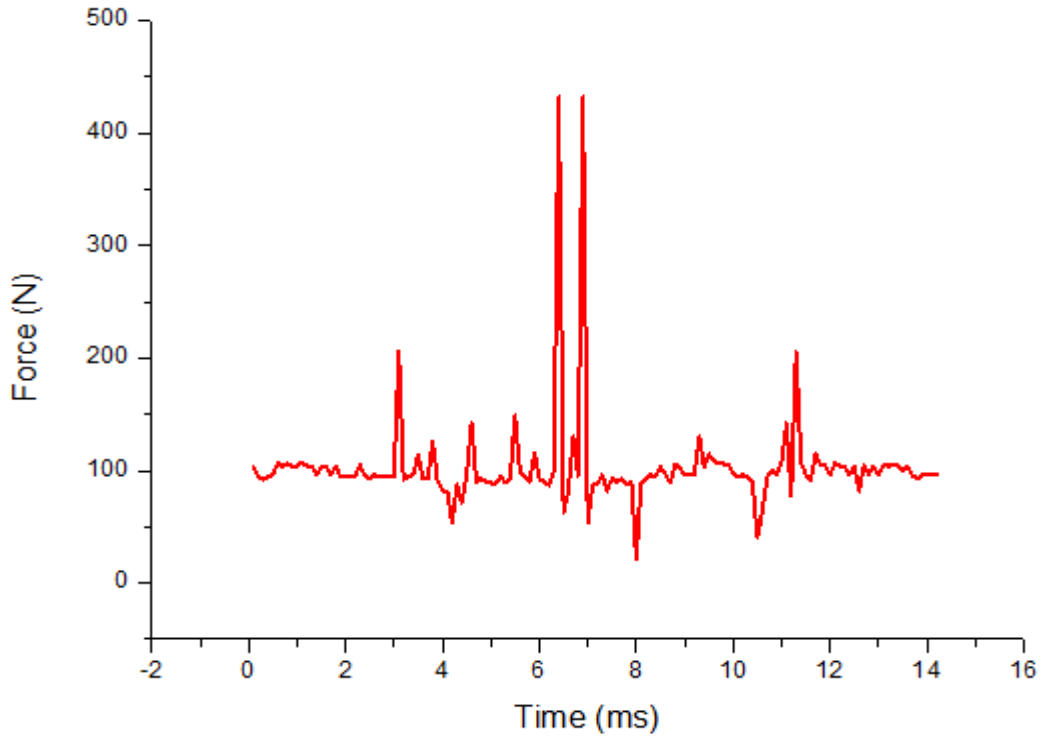

Figure (5.10) The impact force versus time curve of polylactic acid plate at impact energy 7.3J and thickness 3.5mm, high 75 cm.

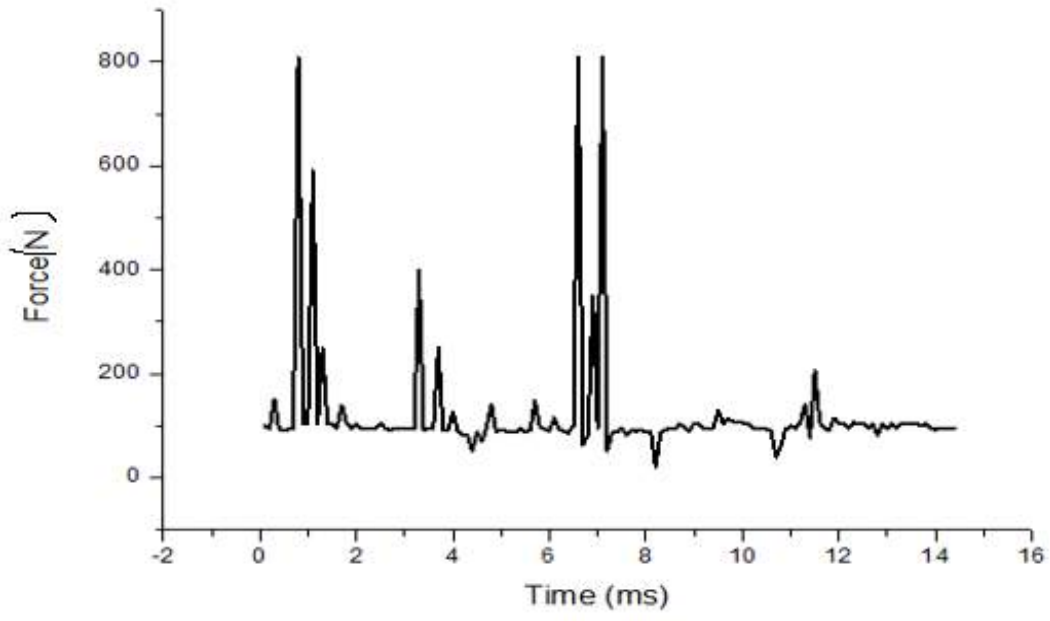

Figure (5.11) The impact force versus time curve of polylactic acid plate at impact energy 7.3J and thickness 4 mm, high 75 cm.

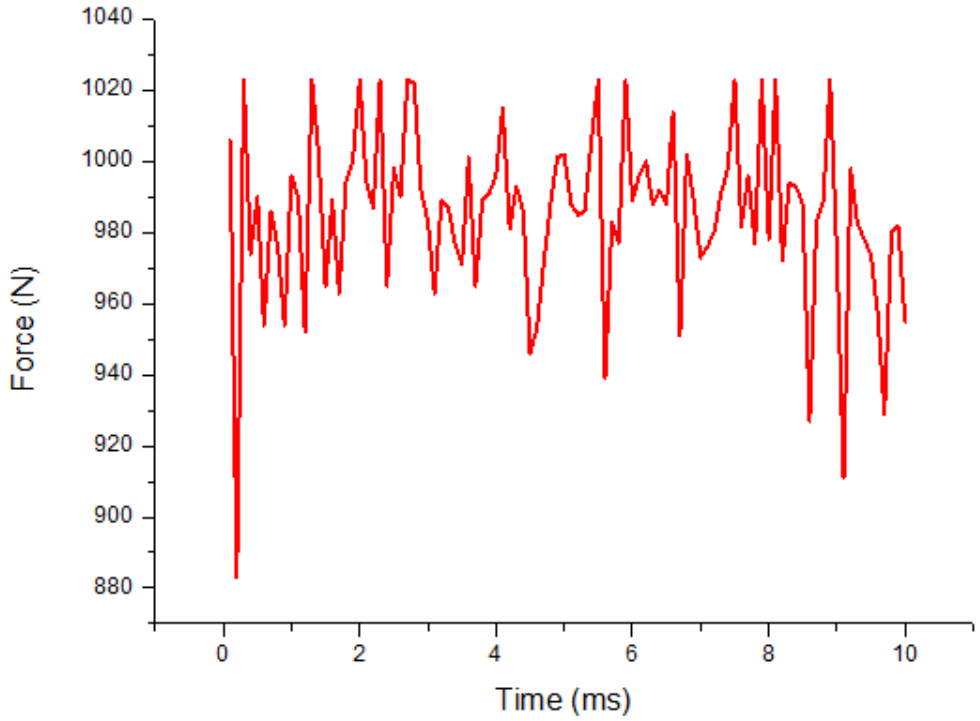

Figure (5.12) The impact force versus time curve of polylactic acid plate at impact energy 7.3J and thickness 4.5mm, high 75 cm.

Looking at the test curves, there was a clear difference between the oscillations or the frequencies. The values of oscillations were increased by the simply supported ophthalmic fixing method, in contrast to the flexible fixed fixation. The results of the effect showed a decrease in the value of the scattering in the supported uniform fixing . This is due to the movement of the sample during the stroke, which leads to its flexibility in movement. This reduces the effect of the acting force. The increased strength in some shapes is due to the increase in the number of layers of the printed sample.

5.3.2 Acceleration impact with fixed supported

Figures (5-13) to (5-15) reveal the effect of time and acceleration, which is very important for measuring the acceleration. Increasing the velocity increases the acceleration, and the sample produces a solid acceleration is inversely proportional to the mass. It can be observed by the oscillations produced by the effect. This will generate a pressure wave. The resulting oscillations can be observed with different sample thicknesses. The figures show the strength of the higher wave, that is due to the increase in the velocity of the strike and the decreatse in the wave downward, which

indicates the decrease in the velocity during the collision. The waveforms depend on the period of time that the wave travels, indicating an increase in speed **[30].**

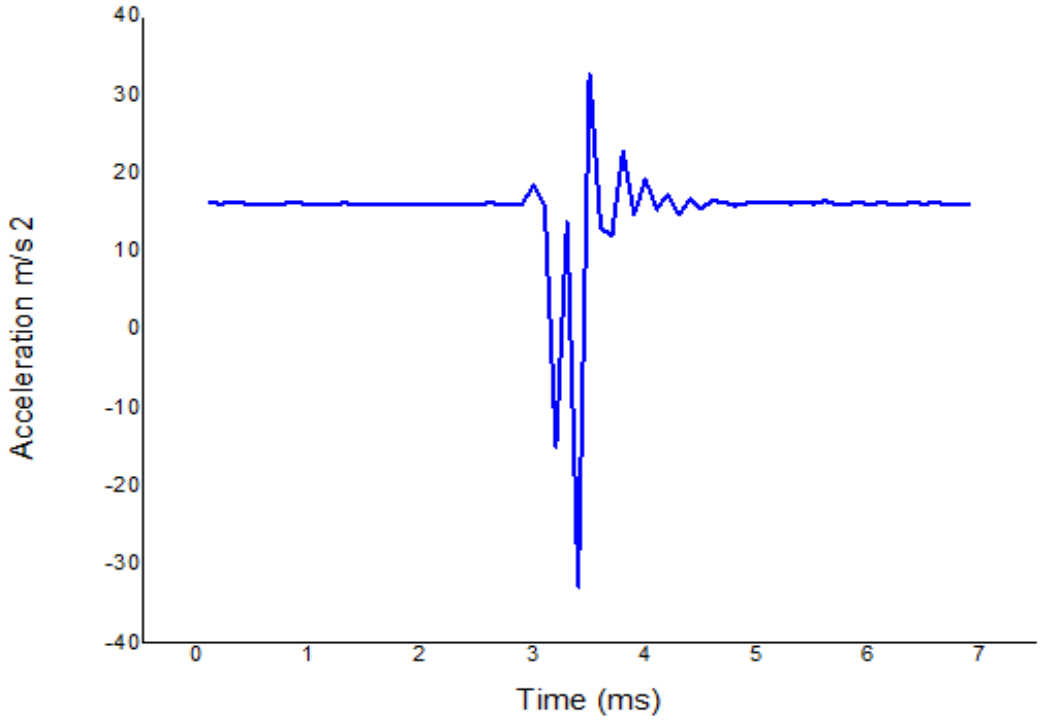

Figure (5.13) acceleration and time history at velocity 2.2m/s ,thickness 3.5 mm , impact energy 2.49J .

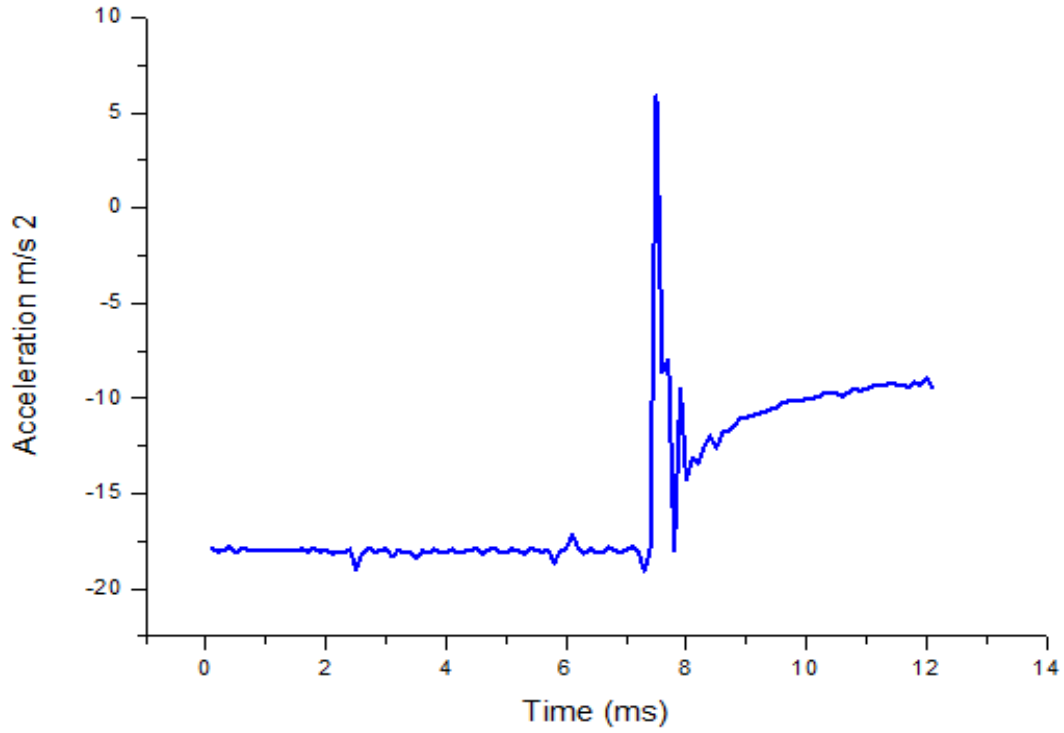

Figure (5.14) acceleration and time history at velocity 2.2m/s ,thickness 4 mm , impact energy 2.49J.

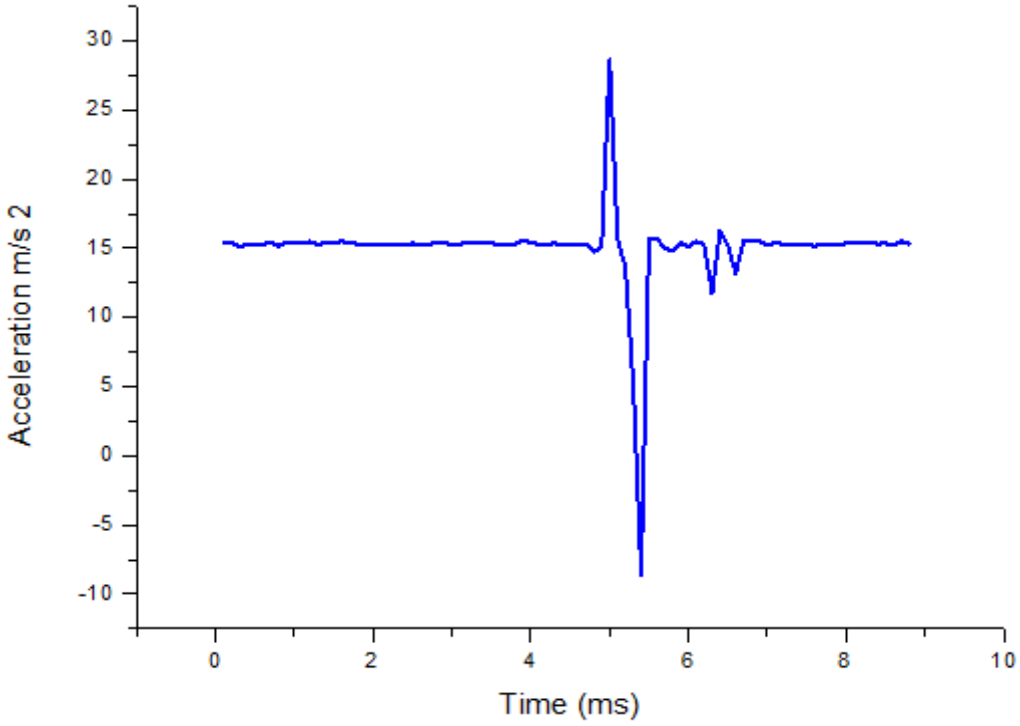

Figure (5.15) acceleration and time history at velocity 2.2m/s ,thickness 4.5 mm , impact energy 2.49J .

From Figs. (5-16) to (5-18), one can see the measured peak value the peak value measured for the hastening of a solid body through its oscillations. But, it is pretentious by collision and resistance and thus reduces the value of the acceleration. The collision procedure amid the collision components and the impact structures is not a whole flexible crash. The waves change due to the velocity of 3.13 m/s during the contact time 0.234 s. The difference in the sampling method has a clear effect from the waves that are based on this simple confirmation of the presence of elasticity in the motion, so sometimes the movement in the direction of acceleration is equal to zero due to the equality of their speed.

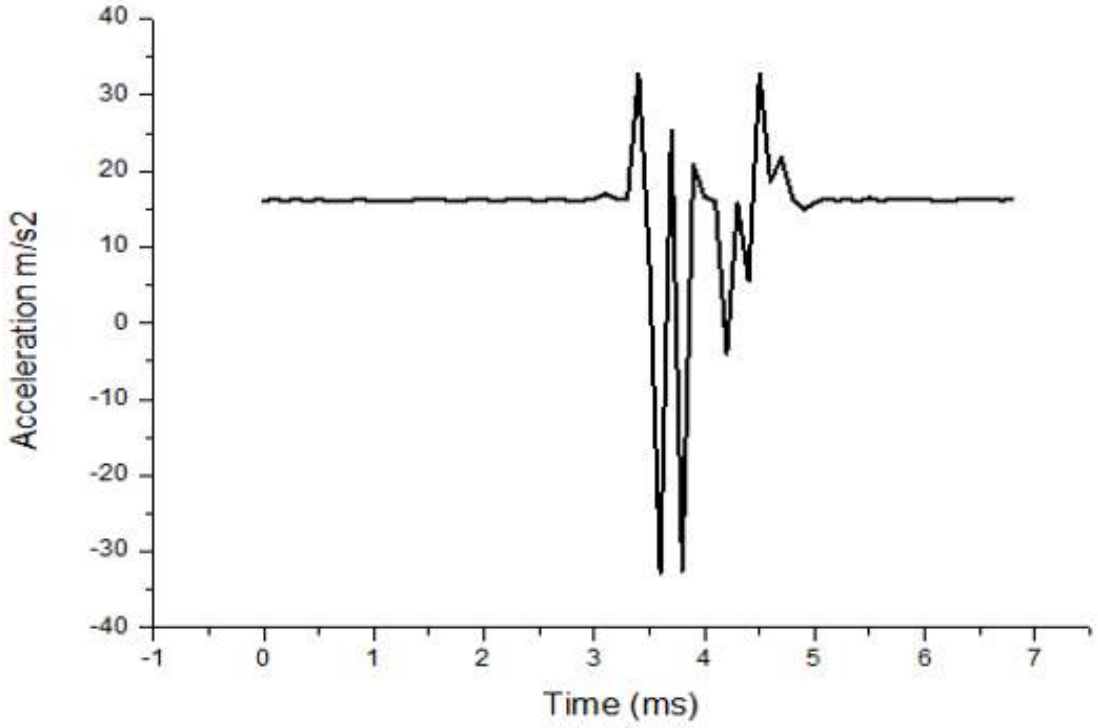

Figure (5.16) acceleration and time history at velocity 3.13m/s ,thickness 3.5 mm , impact energy 4. 98J .

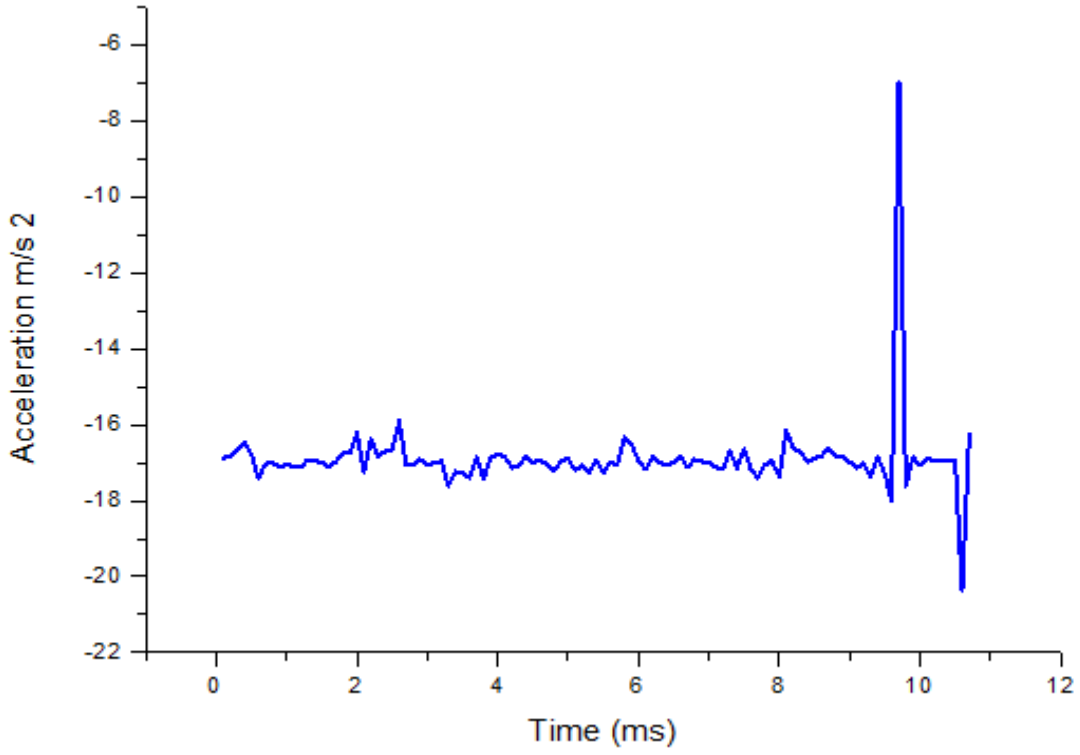

Figure (5.17) acceleration and time history at velocity 3.13m/s ,thickness 4 mm , impact energy 4. 98J .

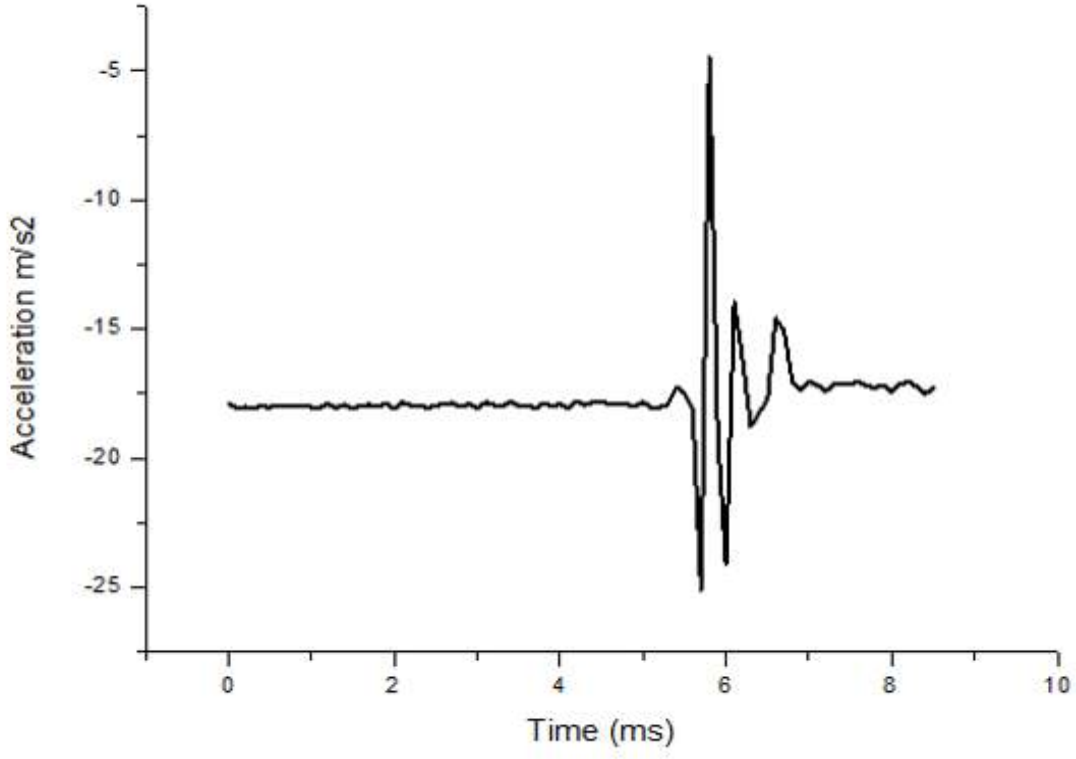

Figure (5. 18) acceleration and time history at velocity 3.13m/s ,thickness 4.5 mm , impact energy 4. 98J .

The Figs. (5-19) to (5-21), with an increase in the velocity of 3.836 m / s during the impact time 0.39 s. This principle is an important increase in the amplitude of the measured acceleration. The unpredictable influence state due to impact and friction transports more results on the acceleration of the stress as well. The sample thickness has an obvious effect through the contact strength.

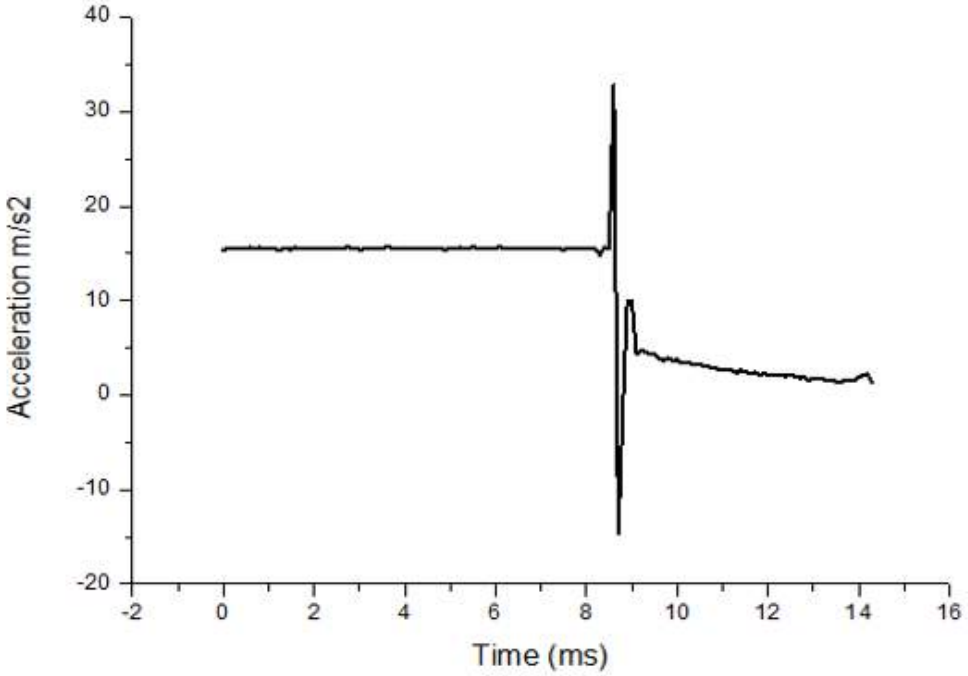

Figure (5.19) acceleration and time history at velocity 3.8m/s ,thickness 3.5 mm , impact energy 7. 3J .

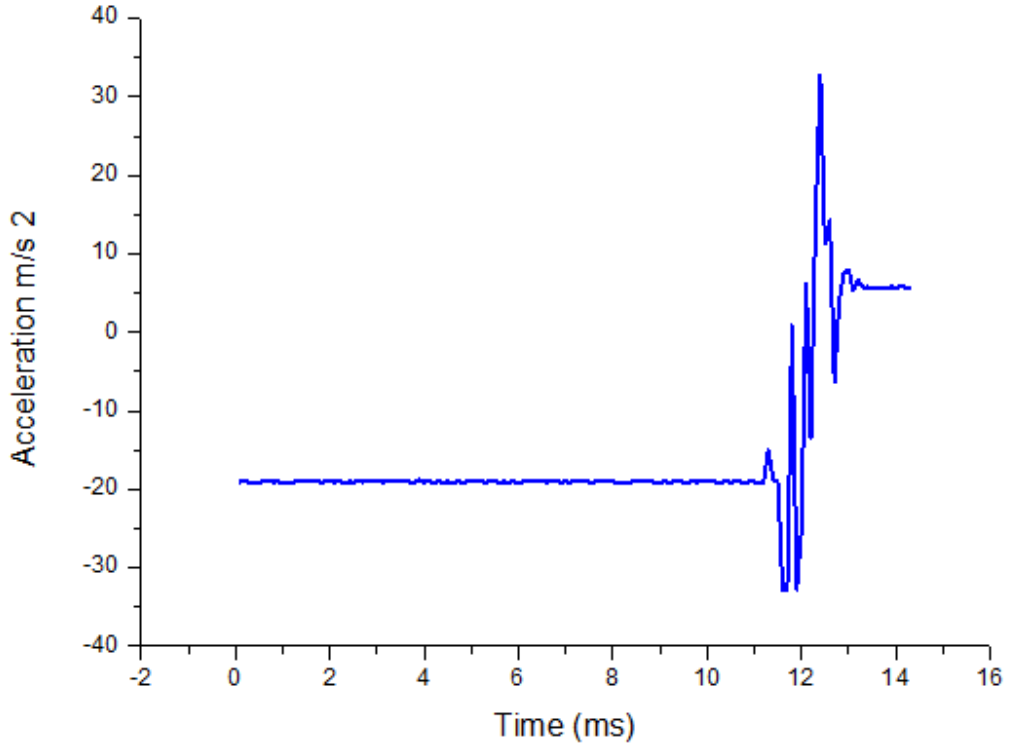

Figure (5.20) acceleration and time history at velocity 3.8m/s ,thickness 4 mm , impact energy 7. 3J .

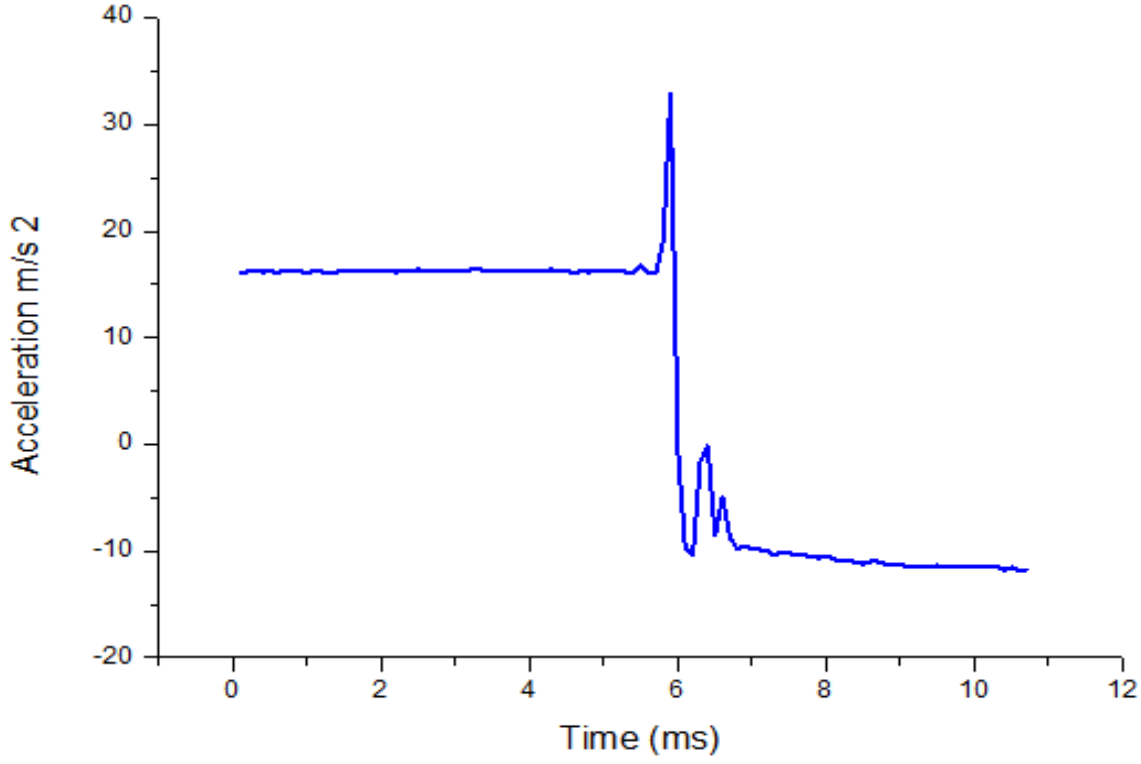

Figure (5.21) acceleration and time history at velocity 3.8m/s ,thickness 4.5 mm , impact energy 7. 3J .

5.3.3 The effect of thickness on energy

To study the effect of thickness on the total energy, the full set of experimental results presented in Table (5.2) were examined. The relationship between the thickness of the samples, the total and absorbed energy is shown in Fig (5.22). The effect of thickness was observed on the tested samples that has a clear effect on the behavior of the material, the contact strength, and the energy absorbed. Samples of 4.5 mm thick have a hardness of 3.5 mm, but lack the ductility factor. Through the tested samples, it was found that the sample with a thickness of 4 mm has good hardness and ductility during the testing process.

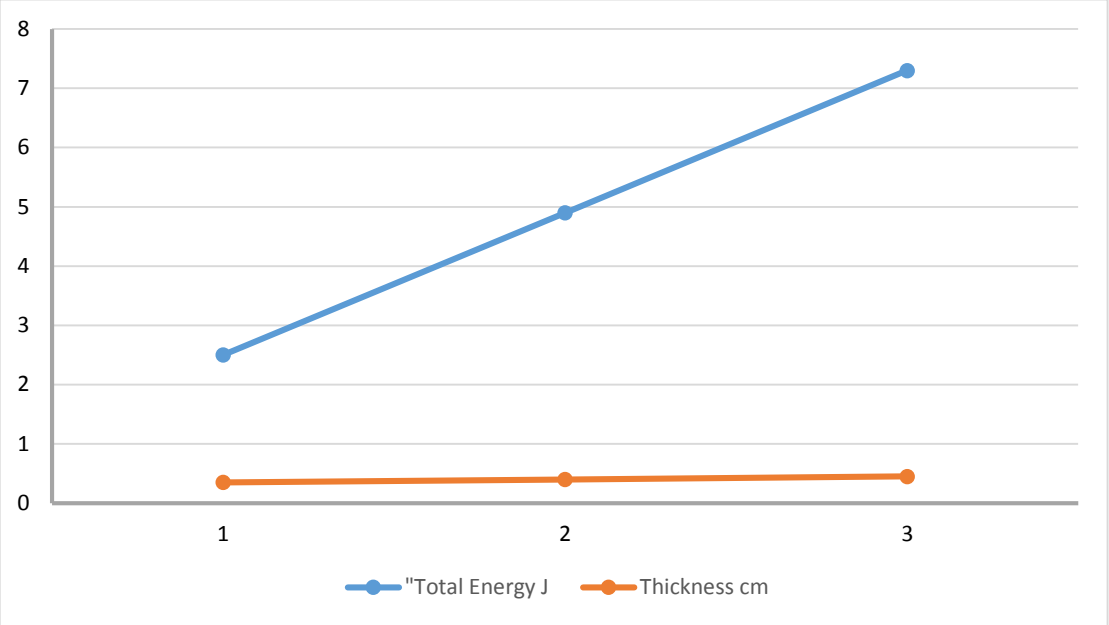

Figure (5.22) Relationship between thickness and total energy.

5.4 Absorbed Energy

As mentioned in section (3.4), the absorbed energy was calculated according to principle of momentum conservation by dependence on the experimental results of impact force for every specimen. The energy absorption in any material under impact loading is mainly through the elastic deformation in the initial stage with some energy absorbed through friction. Once, the energy level is beyond the level required for maximum elastic deformation, the specimen absorbs the excess energy in the form of either plastic deformation in case of ductile materials or through various damage mechanisms in the case of brittle materials. As the polymer materials are inherently brittle in nature, this excess energy is spent in the creation of damages.

The energy required to fail the samples in all cases was reduced with the thickness of the samples, which led to the resistance and hardness of the sample to failure. Through the results obtained from experimental tests, Table (5.2) shows the amount of energy absorbed depending on the speed of the recoil and the impact strength of the collider, where the value of the absorbed energy was at the thicknesses of 3.5, 4, 4.5 mm, respectively fixed supported (1.14J,4.63J,6.75J) , (1.15J, 2.42J, 7.18J) ,(2.25J, 3.20J, 12.8J) and the ratio between them is (0.83% ,o.31%), (0.84%, 0.66%) ,(0.81%,0.75%) . This difference in the energy value is due to an increase in the thickness of the samples, evidence of the material's resistance to impact. Which increases the absorbed energy value, which depends on the impact time from start to finish, indicating the speed of the collider penetrating samples.

Table (5.2) Maximum Force, Total Energy, and Absorbed Energy.

Thickness (mm)	High (cm)	Max. Force (N)	Total Energy (J)	Absorbed energy (J)
3.5	**25**	**170**	**2.49**	**1.14**
4	**25**	**170**	**2.49**	**1.15**
4.5	**25**	**135**	2.49	**2.25**
3.5	**50**	**312**	4.9	**2.337**
4	**50**	**750**	4.9	**2.42**
4.5	**50**	**1003**	4.9	**3.203**
3.5	**75**	**206**	7.3	**6.756**
4	**75**	**800**	7.3	**7.180**
4.5	**75**	**1020**	7.3	**8.81**

Figures (5.23) to (5.25) shows the value of the energy absorbed by the polylactic acid at the action energy for three different levels (2.49J, 4.49, 7.3J) for a samples thicknesses of 3.5 mm, 4 mm, and 4.5 mm, respectivly. It shows the amount of energy absorbed by the polymer and its ability to withstand the impact energy**.** The lower part of the column shows the amount of energy absorbed. The amount of increase in the energy value is observed due to the amount of impact energy and the force acting on the polylactic acid plate.

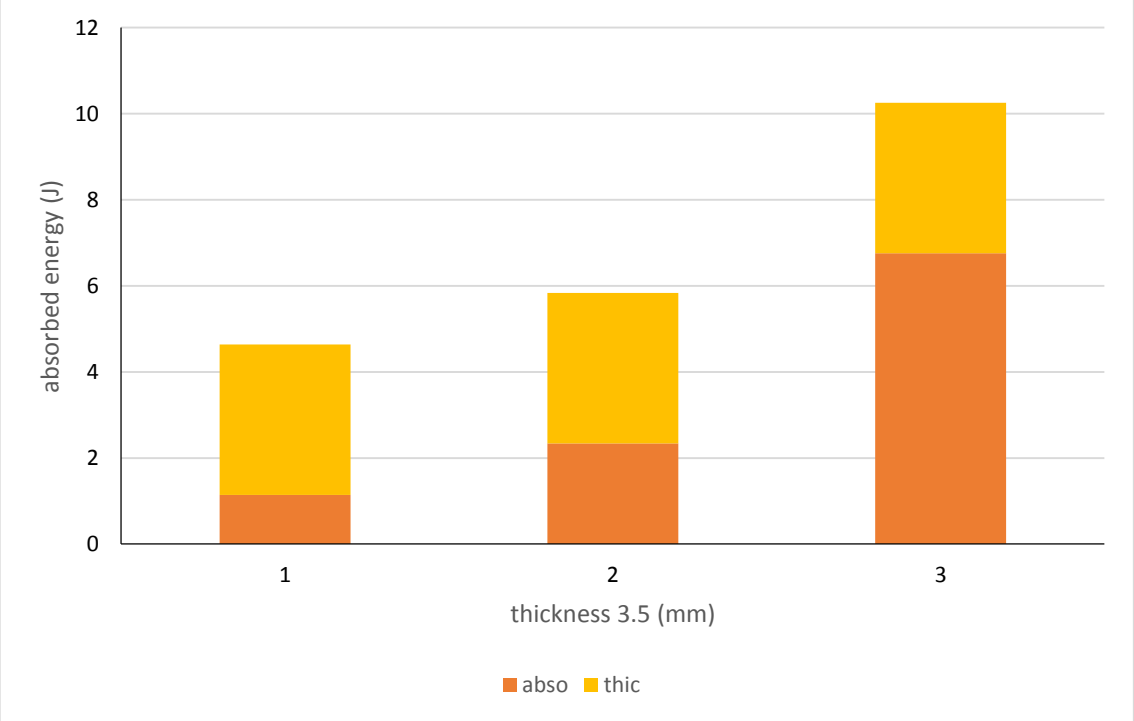

Figure (5.23) Energy absorption at impact energy of (2.49 J, 4.98 J, 7.3 J), thickness of 3.5 mm.

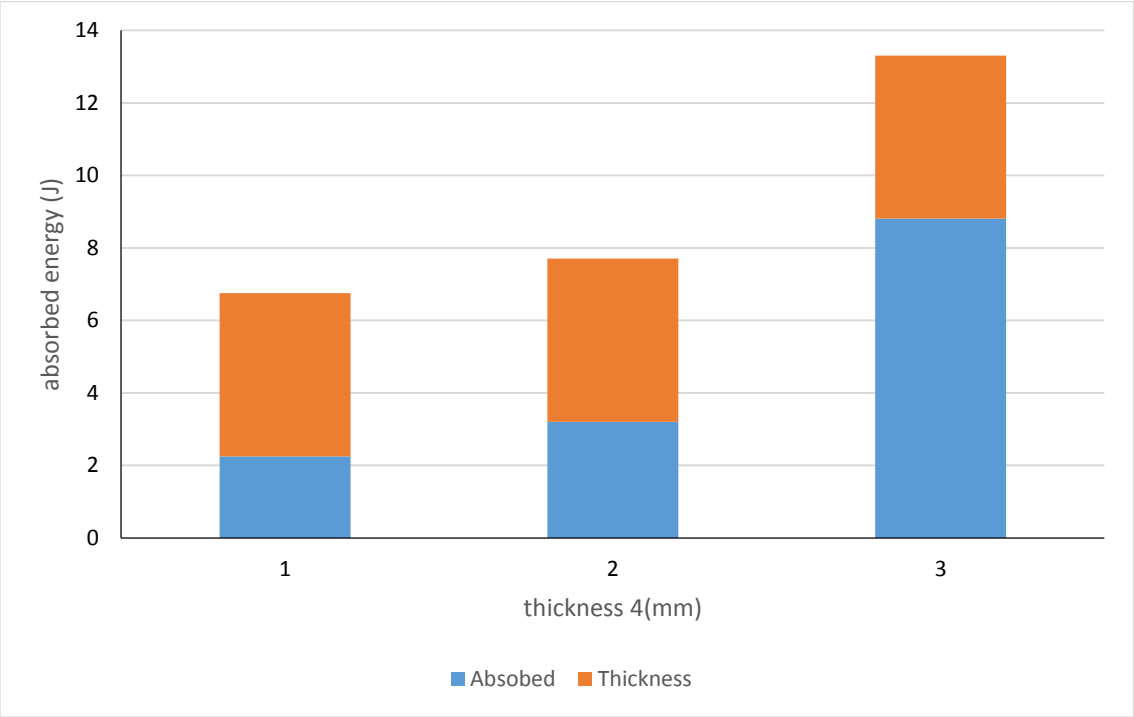

Figure (5.24) Energy absorption at impact energy of (2.49 J, 4.98 J, 7.3 J), thickness of 4 mm.

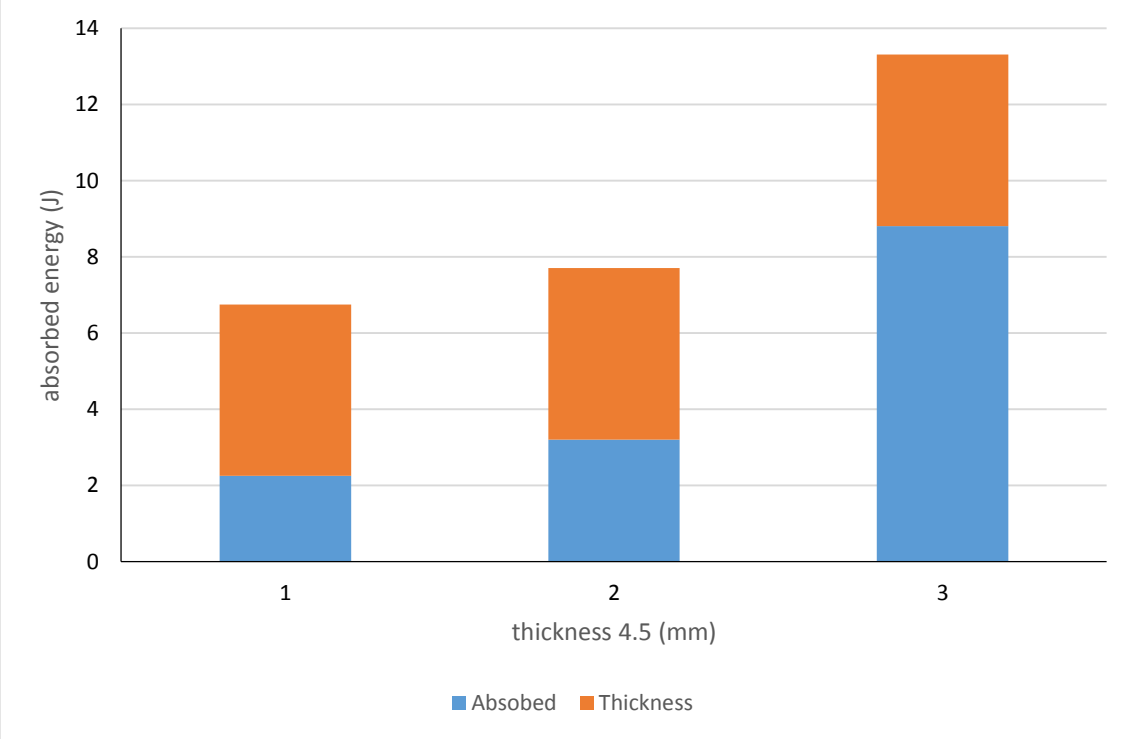

Figure(5.25) Energy absorption at impact energy of (2.49 J, 4.98 J, 7.3 J), thickness of 4.5 mm.

5.5 Numerical ABAQUS Results

The chief aim of the (ABAQUS) program is to compare the kinetic energy with the experimental work and the total energy, to know the entry energy absorbed by the samples, as well as the deformations occurring in the samples through stresses.

5.5.1 Results of the stress distribution

Through the information entered in Abaqus, the stress – strain curve for all groups, the pressure applied (von Mises stress) to the orthosis was obtained, and the same pressure was for all groups. Figures demonstrates the stress applied to the model.

Figures (5.26) to (5.28) shows the deformation obtained at the impact energy(2.49J, 4.98J, 7.3J) and the amount of maximum stress (8.216e+00 ,7.946e+00 ,9.610e+00) which shows the resistance of the sample, and the areas of distortion that are affected by the impact process. The difference in the value of the applied stress depends on the amount of the impact energy, the greater the impact energy, the greater the deformation value. An increase in the stress value during the numerical testing process depends mainly on the thickness of the sample, as the amount of stress was observed to increase with a thickness of 4.5 mm. It can be said that the sample with the larger thickness has a higher fatigue resistance.

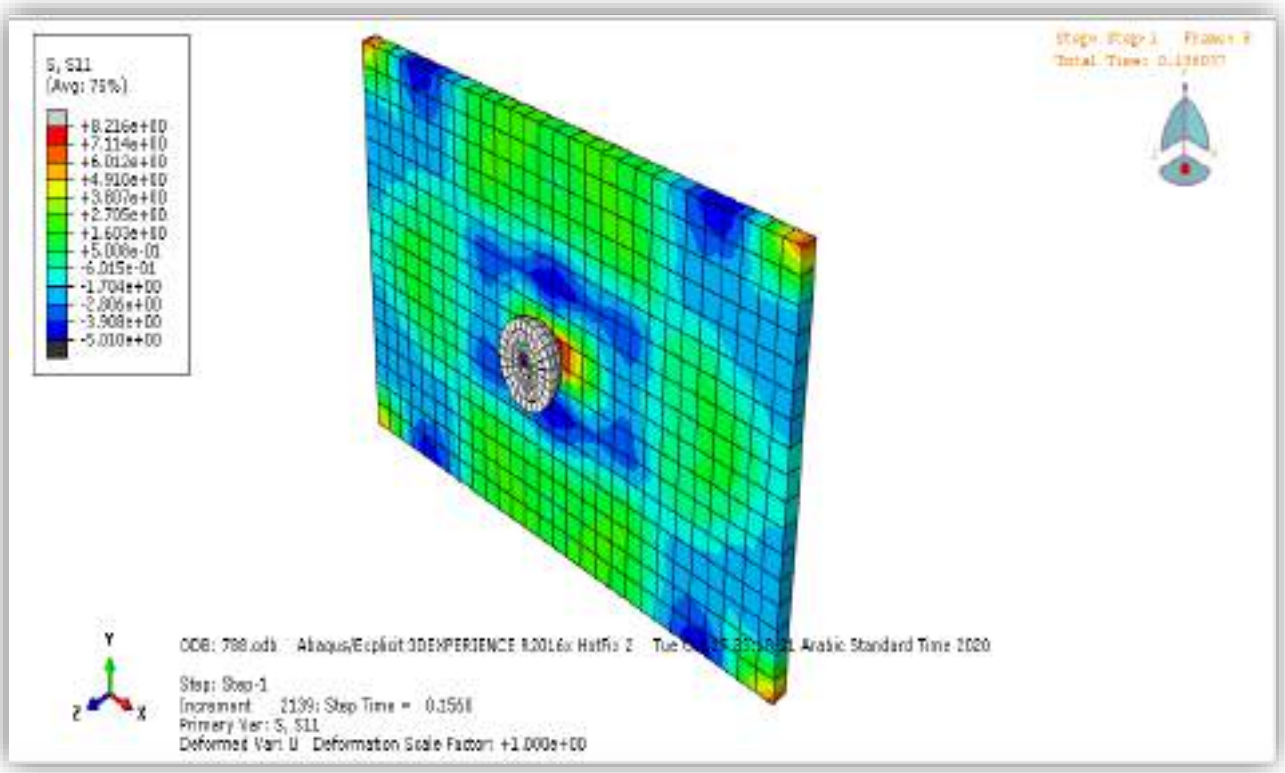

Figure (5.26) Deformation PLA at impact energy 2.49J .

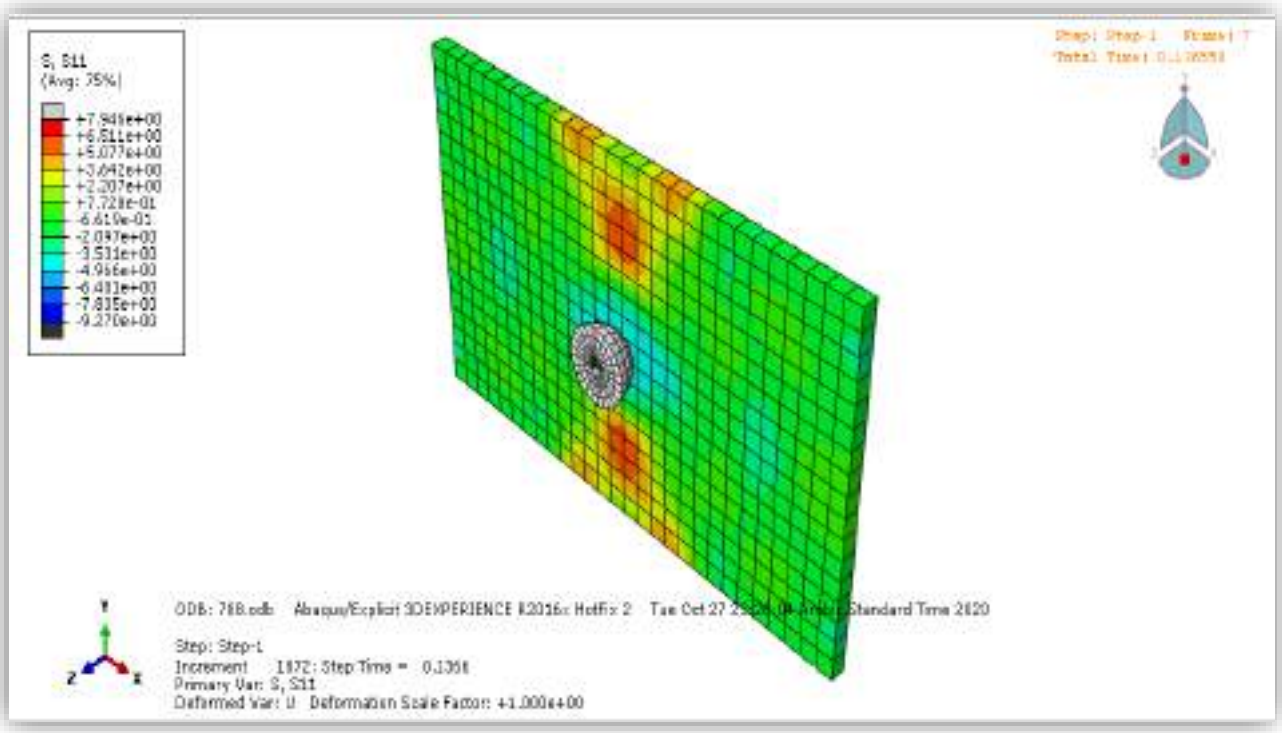

Figure (5.27) Deformation PLA at impact energy 4. 98J.

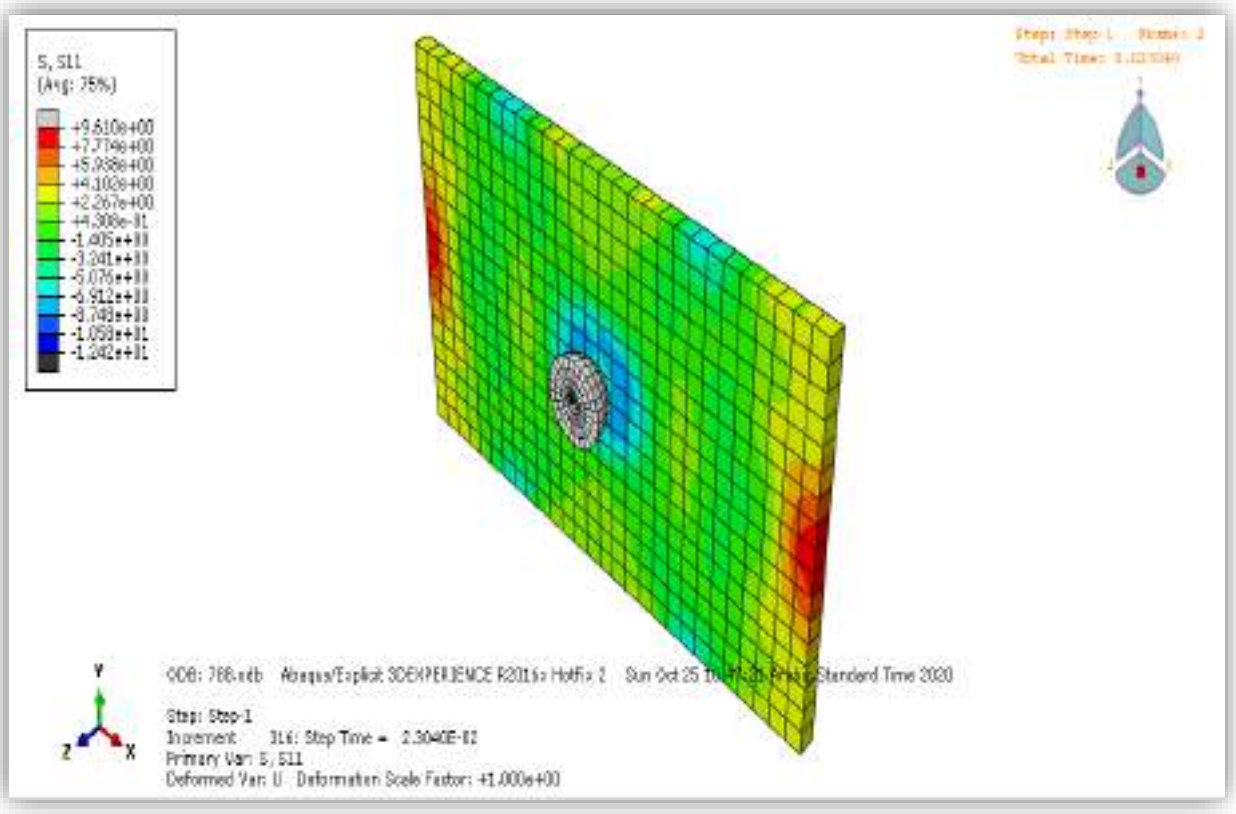

Figure (5.28) Deformation PLA at impact energy 7.3J .

5.5.2 Total energy varies by speed

Figures (5.29 to 5.31) show the effect of the velocity of the effect on the dynamic response of the polylactic acid (PLA). Energy appears as a function of time for three different speeds. Because velocity is the only variable and its effect on dynamic response is shown. The contact force and the impact energy will increase with the increase in speed. This can be seen from the figures (A, B, C). The difference in the impact energy and the height of the frequencies depends on the speed used, so when the figures (A, B, C) the velocity value was 2.2 m / s, 1.3 m / s, and 3.8 m / s. The increase in the deformation value depends mainly on the impact energy value.

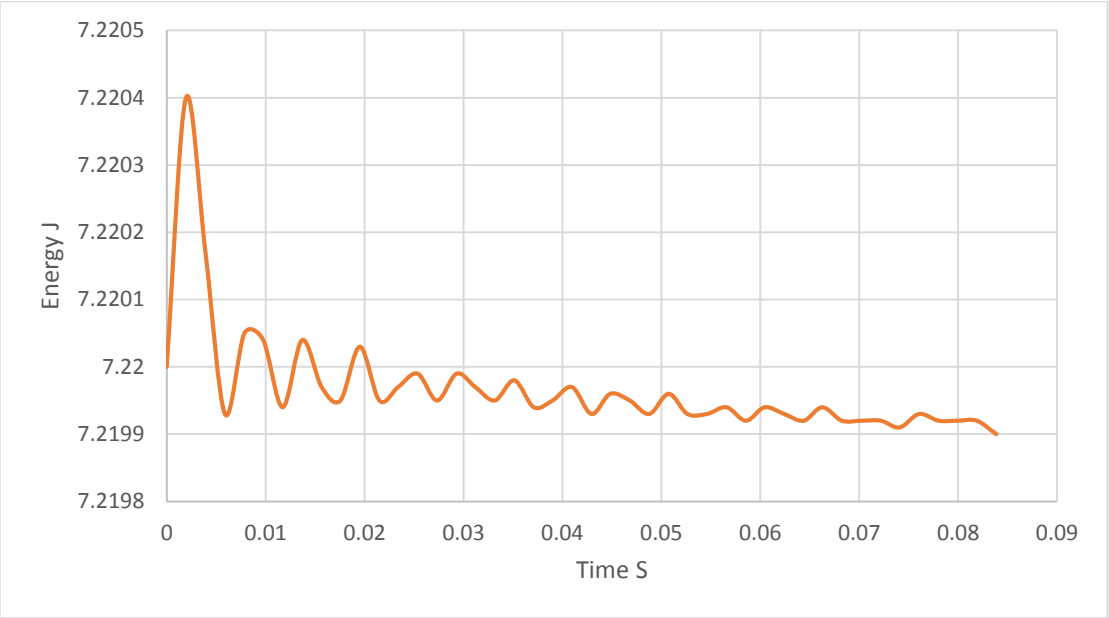

Figure (5.29) The total energy and time curves of polylactic acid (PLA) at velocity 2.2 m/s.

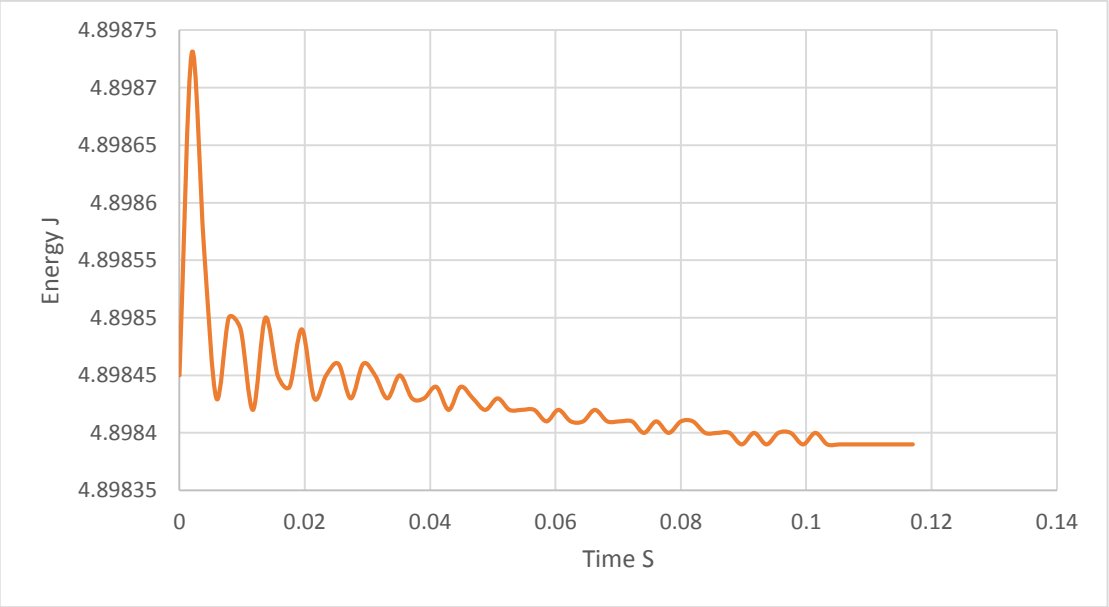

Figure (5.30) The total energy and time curves of polylactic acid (PLA) at velocity 3.13 m/s.

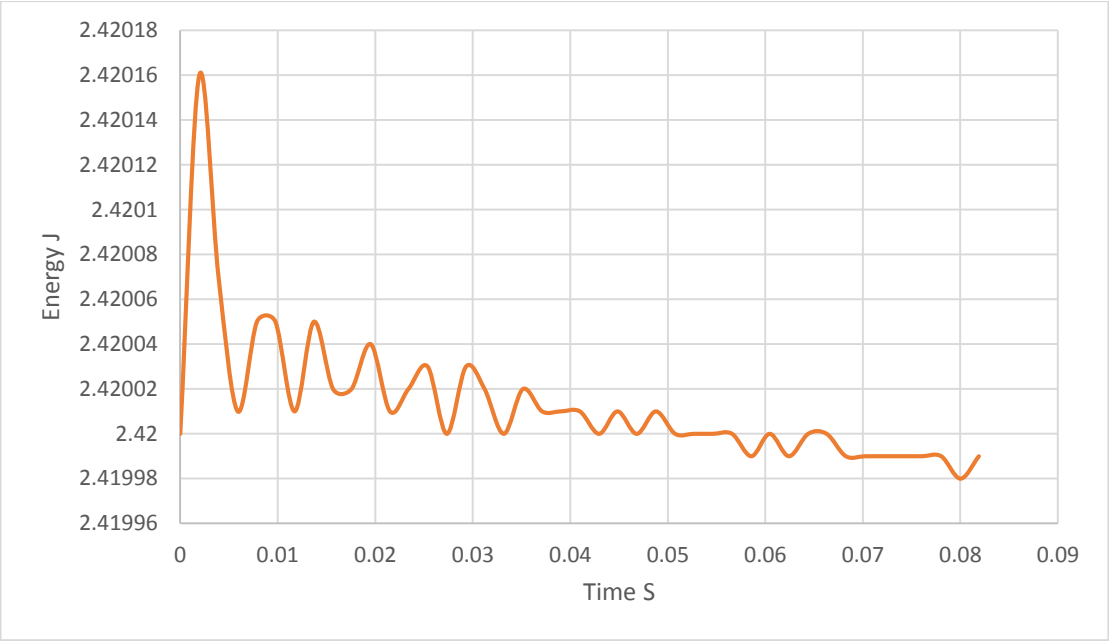

Figure (5.31) The total energy and time curves of polylactic acid (PLA) at velocity 3.8 m/s.

Table (5-3) reveals the amount of impact energy that was measured experimentally and numerically, and the results showed a convergence between them, depending on the speed and mass of the body.

Table (5.3) The total experimental and numerical energy

Test	High cm	Velocity Impactor m/s	EXP Energy J	NUM Energy J	Error %
1	25	2.2	2.42	2.4016	0.7603
2	50	3.13	4.8459	4.8987	1.089
3	75	3.9	7.3575	7.2204	1.863

5.5.3 Impact trace

There are two types of impact damages in polymer laminates: intra-ply damage and inter-ply damage. The intra-ply damage includes , crack, polymer, debonding, and breakage, and the inter-ply damage includes delamination **.**

Figure (5.32) to (5.34) demonstrates the damage comparison chart for dissimilar slices of the experiment. It is the numerical results for the 2.49J state of impact energy. As it can be seen in Fig. (5.16), showing the damage, the graphs of all compound slices were acquired by numerical simulation competition healthy with those acquired by experiments. Also, in footings of the damage morphology, the little thickness was affected by 2.49J, which distorted the material particles**.** The damage was observed visually after the effect process, where the dissolution of the formed lactic acid (PLA) layers was observed through the 3D printer sample manufacturing process. Likewise, the deformation of the upper part of the sample is less than the diameter of the impactor. The damage caused by the impact process in the first level shows the material,s resistance to impacts due to the fact that the material is ductile. There is a clear difference in the damage in the samples revealing that the sample of thickness 3.5mm is more harmful than the sample 4.5mm due to the increase in the thickness of the sample, which has better impact resistance.

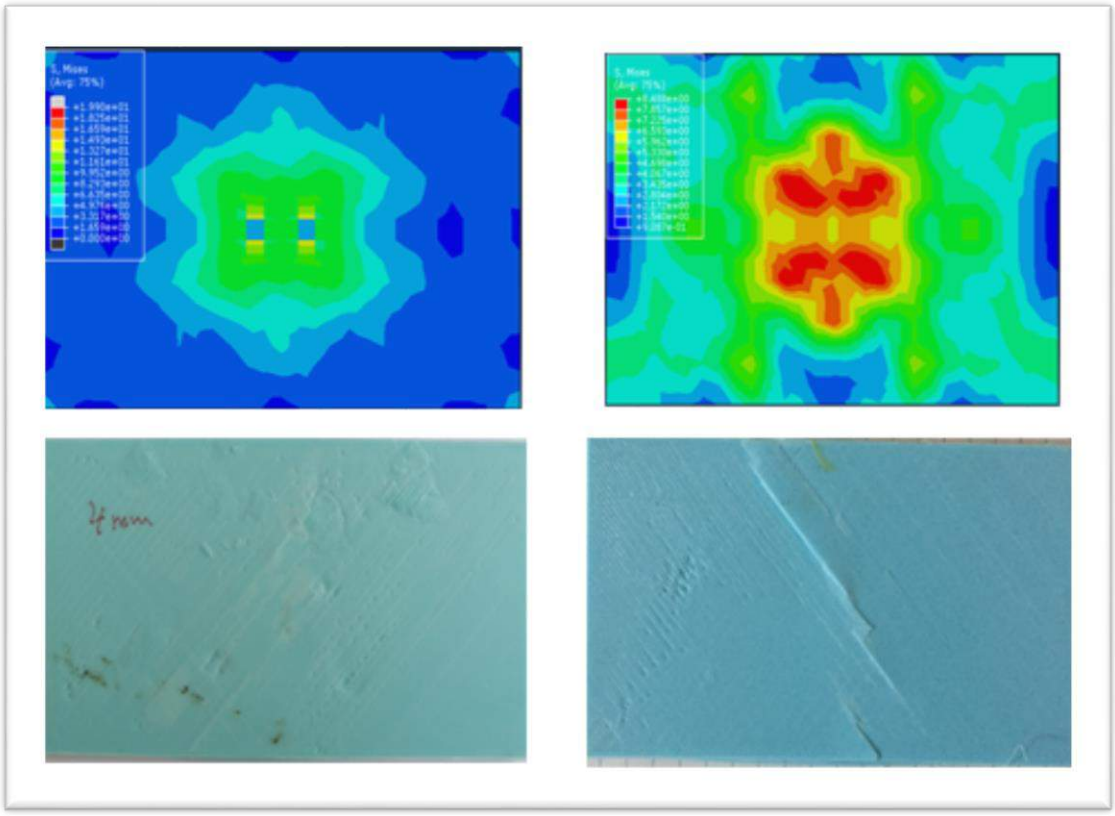

Figure (5.32) The damage of impact with an energy of 2.49 J, 4mm thicknesses and hight 25cm.

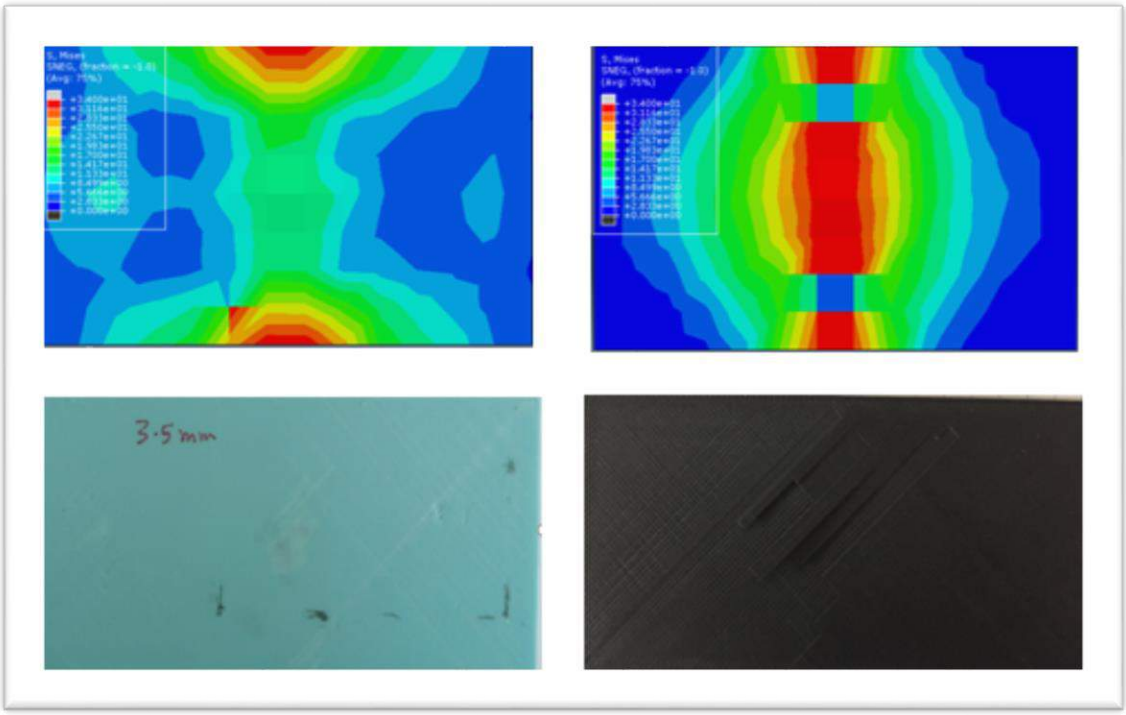

Figure (5.33) The damage of impact with an energy of 2.49 J, 3.5mm thicknesses and hight 25cm.

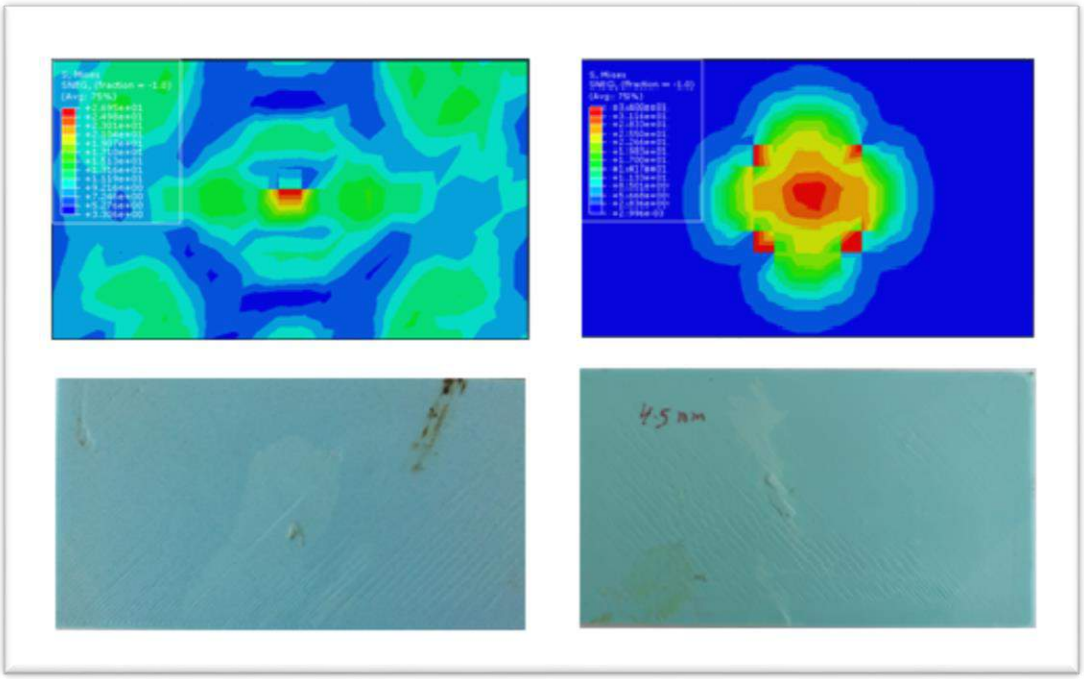

Figure (5.34) The damage of impact with an energy of 2.49 J, 4.5mm thicknesses and hight 25cm**.**

Figures (5.35) to (5.37) demonstrate the damage caused by the hit in the practical part compared to the numerical part at a collision energy of 4.9J. It was observed that there is a difference in the damage from the first case, a change in the material particles and a disintegration in a part of the layers. The important step in studying the impact behavior of polymer materials is to characterize the type and extension of the damage induced in the impacted specimens.Spread of damage over a wide area in a sample of 3.5 mm thickness. Only shear (crash and cracks) appeared in this specimens as indicated in .(A, B, C), because the combination of normal and shear stresses in several elements of the resulted a maximum shear stress reaches the critical shear stress. And this is the same reason for all other types.

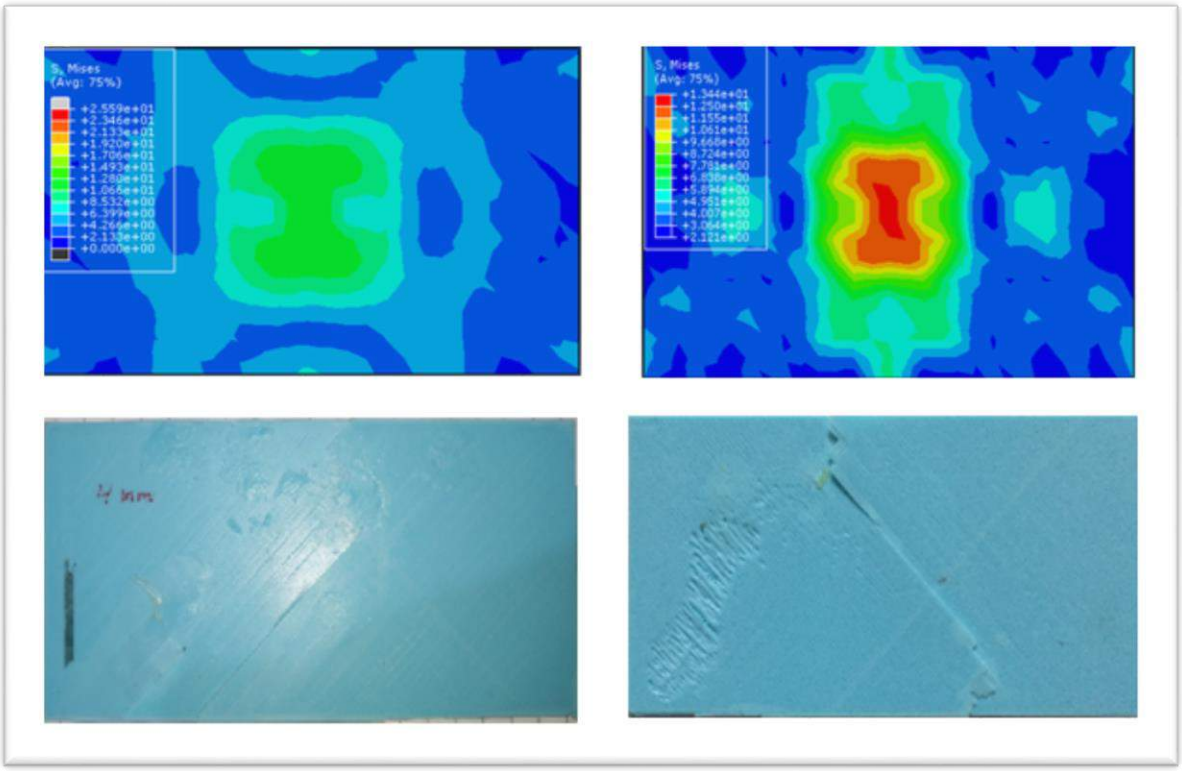

Figure (5.35) The damage of impact with an energy of 4.9 J, 4mm thickness and hight 50cm.

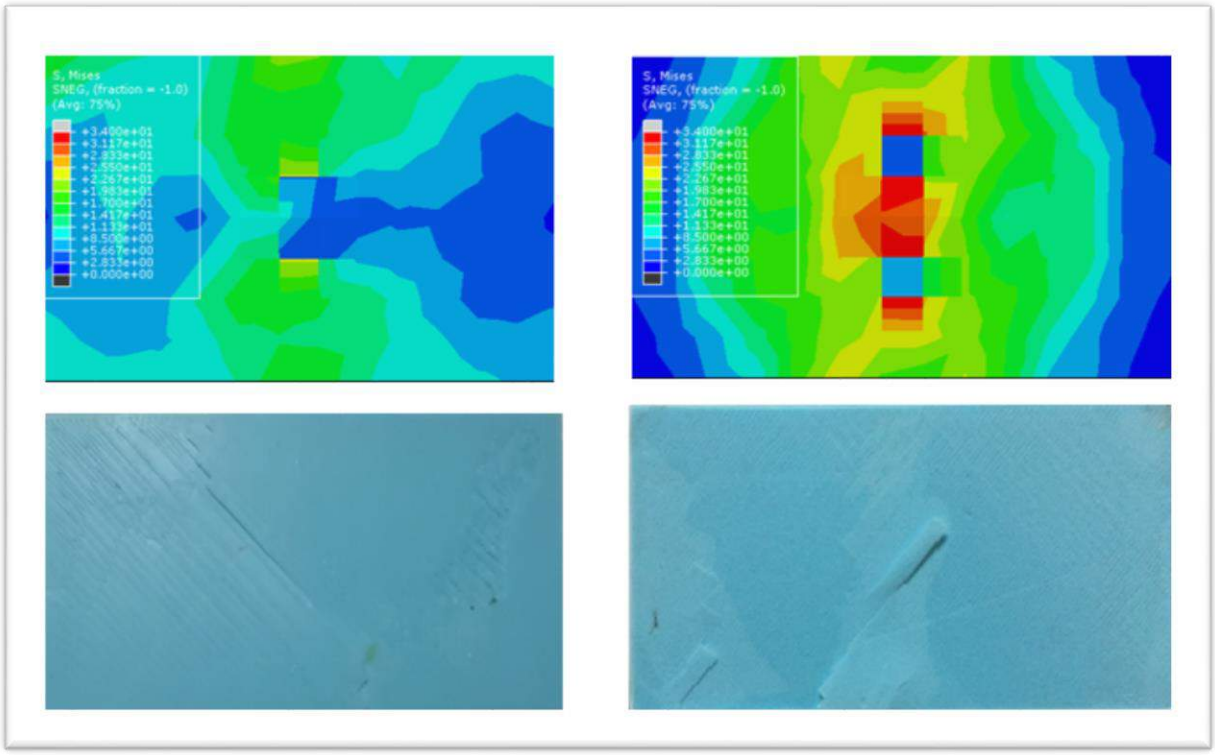

Figure (5.36) The damage of impact with an energy of 4.98 J, 3.5mm thickness and hight 50cm.

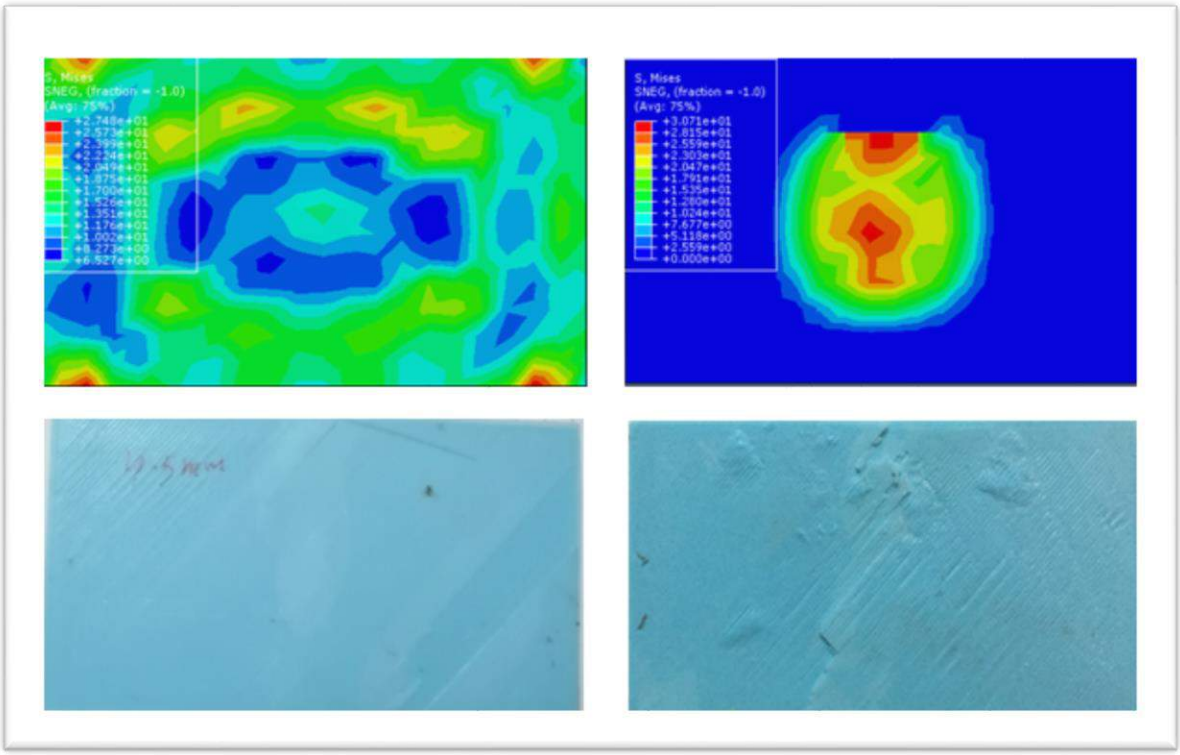

Figure (5.37) The damage of impact with an energy of 4.9 J, 4.5mm thickness and hight 50cm.

Figures (5. 38) to (5.40) views the damage caused by the impact at an energy of 7.3 J. During the time period 0.3.9, by looking at the samples, the highest deformation in the particles of the internal material and the dissolution of the sample at the impact were noticed. As well, as the program shows the damage in the areas that are subject to beating. Through visual inspection and numerical simulation program, it was found that the most damage samples have an impact energy of 7.3 Joules. The sample with thickness of 4.5 mm is the least effective in all tests, this is due to an increase in thickness.

The plastic deformation of the layer material that occurred due to the higher applied impact energy strength of the layer. In addition to that there are signs of delamination between the layers. The applied load was shear on the layers' interface and leaded to the failure of the adhesion bonding of them. addition to the fact that all specimens were plastically deformed before their fracture. Upper face yielding (fracture), core shear (crash and cracks), and lower face

yielding (fracture and cracks) appeared in this specimens as indicated in fig.(5.32).

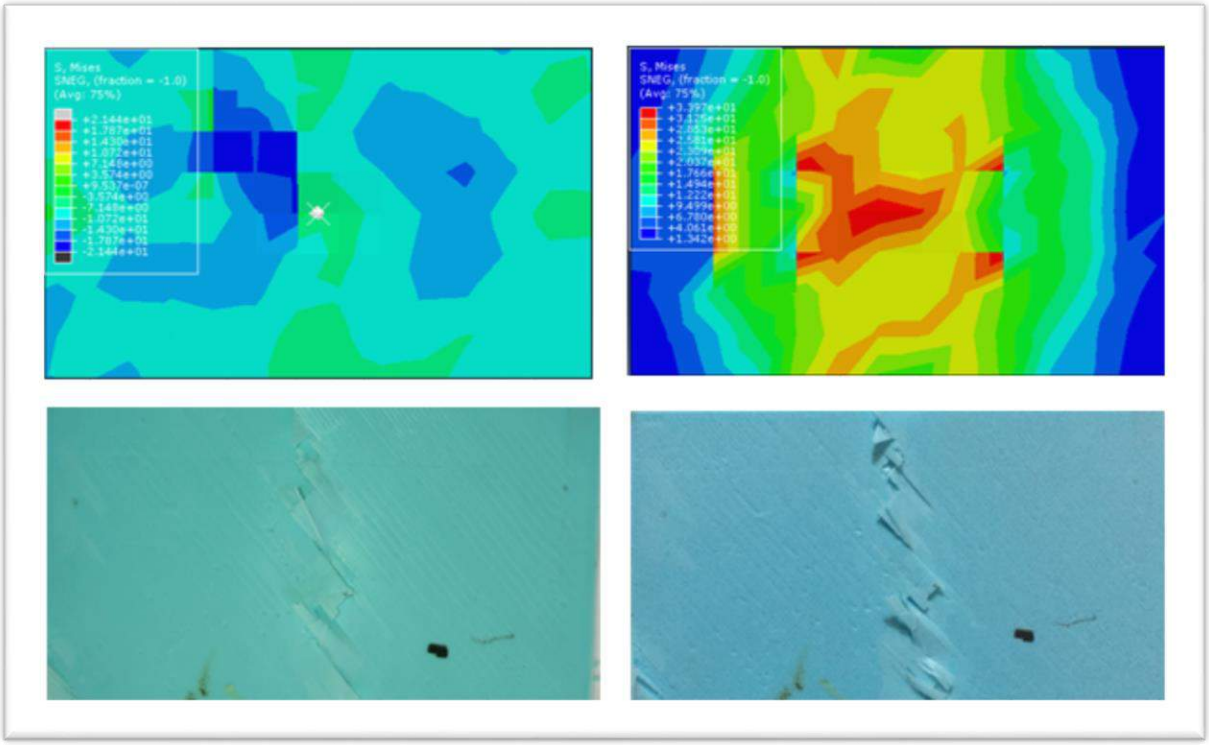

Figure (5.38) The damage from impact with an energy of 7.3 ,3.5mm thicknesses and hight 75 cm.

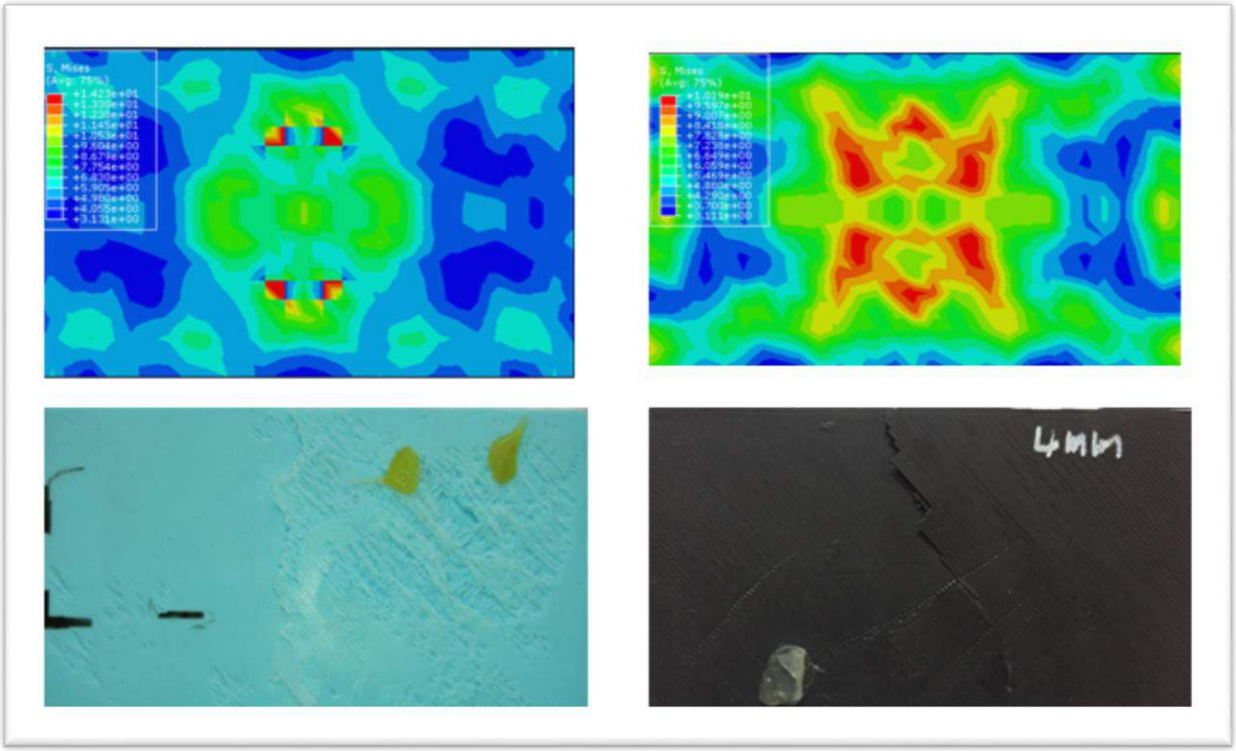

Figure (5.39) The damage from impact with an energy of 7.3 ,4mm thicknesses and hight 75 cm.

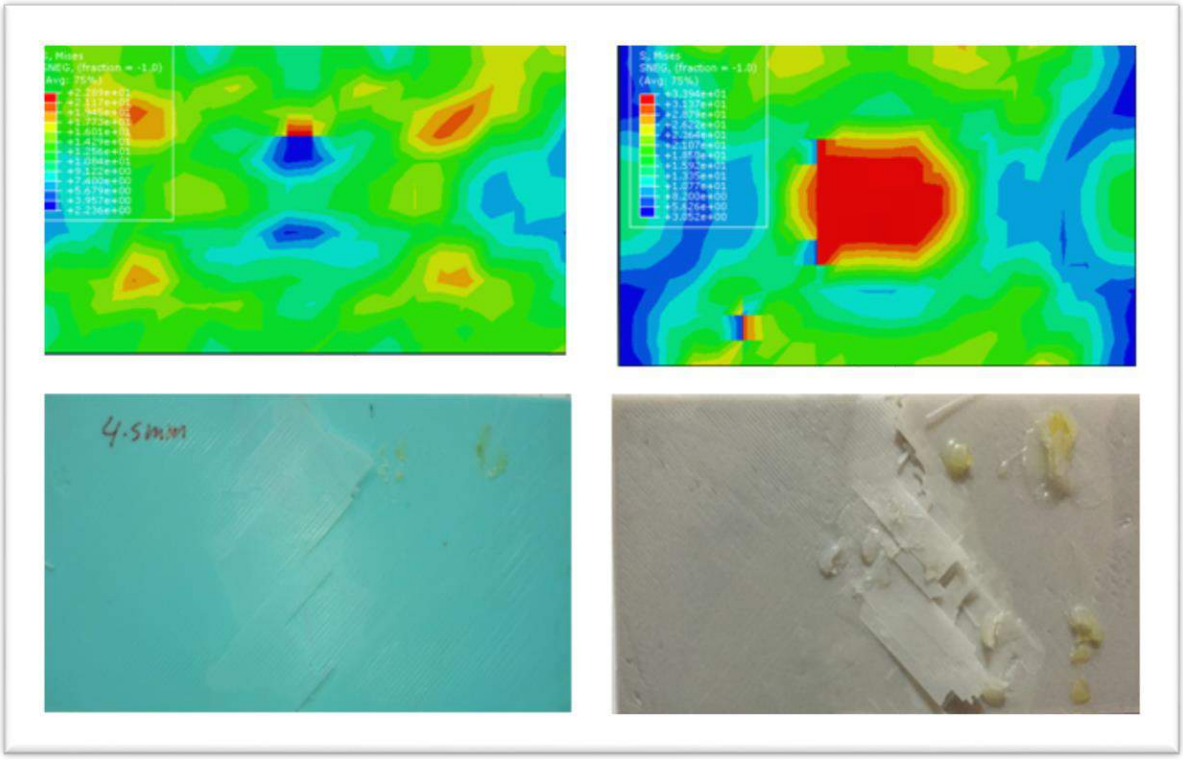

Figure (5.40) The damage from impact with an energy of 7.3 ,4.5mm thicknesses and hight 75 cm.

In this research, the impact response and the damaging effect of the type of poly-lactic panels were studies. An experimental and numerical study was performed under three different impact energy levels. An effect-based failure criterion was used. During the damage spread in the model, the results and the observations of peak strength, displacement and energy were positively compared. In numerical simulations,the damage was accurately captured. The physical behavior was less accurate, and the model predicted less expected energy absorbed by the permanent deformation strike during the impact of 7.3 joules. This decrease is likely due to the variation in the thickness and the quality of the printed sample.

Chapter Six

Conclusions and Recommendations

Chapter Six
Conclusions and Recommendations

6.1. Conclusions

From the whole structure of this study, the following conclusions can be derived:

1. The variation in the tested polymer samples showed a significant difference in the behaviors of the impact force and the energy absorbed according to the applied impact energies.

2. Both the impact force and the impact energy will increase as the sample thickness increases at the same speed as the impact.

3. The increase in impact force and energy is required to fail the samples with the increase in the thickness at all tested velocities.

4. Failure modes increase in number and intensity with the increasing of impact energy for most specimen types. The specimen types that experienced the least failure modes are the specimen types (1) and (2).

5. The absorbed energy increases as the impact energy increases for all types of samples.

6. The results of the total energy and impact strength of the numerical model manifested its acceptance compatibility with the experimental results.

*6.*2 Recommendations for Future Work

The following recommendations can be advised to enter the study consideration for the future works:

1. Selecting composite materials with other PLA to examine mechanical shock impact and mechanical properties.

2. Study the effect of creep and it's in influence on the 3D printed materials.

3. Developing the test device by adding additional sensors to measure the vibration and sample dimensions

4. Investigating the effect of bending and torsion on the 3D printed materials.

5. Studying the influence of impact on the 3D printed materials such, as ABS and PLC.

REFERENCES

References

1. Han, J., Zhao, D., Li, D., Wang, X., Jin, Z., & Zhao, K. "**Polymer-based nanomaterials and applications for vaccines and drugs**" Polymers 10.1, 31. ,2018.

2. Gomes, M. E., Ribeiro, A. S., Malafaya, P. B., Reis, R. L., & Cunha, A. M. "**A new approach based on injection moulding to produce biodegradable starch-based polymeric scaffolds: morphology, mechanical and degradation behavior**" Biomaterials 22.9: 883-889, 2001.

3. Grover, Mikell P., and Mikell P. Groover. " **Fundame ntals of modern manufacturing** " (1996).

4. Lambert, Scott, Chris Sinclair, and Alistair Boxall. **"Occurrence, degradation, and effect of polymer-based materials in the environment."** Reviews of Environmental Contamination and Toxicology, Volume 227. Springer, Cham, 1-53,2014.

5. Avérous, Luc. "**Polylactic acid: synthesis, properties and applications.**" Monomers, polymers and composites from renewable resources. Elsevier, 433-450,2008.

6. Aliofkhazraei, Mahmood, ed. **Advances in Graphene Science**. BoD–Books on Demand, 2013.

7. Savioli Lopes, M., A. L. Jardini, and R. Maciel Filho. "**Poly (lactic acid) production for tissue engineering applications.**" Procedia Eng 42: 1402-1413,2012.

8. Raquez, J. M., Habibi, Y., Murariu, M., & Dubois, P. "**Polylactide (PLA)-based nanocomposites**." Progress in Polymer Science 38.10-11: 1504-1542, 2013.

9. Sarker, Dipak Kumar. Packaging Technology and Engineering: Pharmaceutical, **Medical and Food Applications**. John Wiley & Sons, 2020.

10. Murariu, Marius, and Philippe Dubois. "**PLA composites: From production to properties.**" Advanced drug delivery reviews 107: 17-46, 2016.

11. Agrawal, Sandeep, Kalyan Kumar Singh, and P. K. Sarkar. "**Impact damage on fiber-reinforced polymer matrix composite–a review.**" Journal of Composite Materials 48.3 : 317-332, 2014.

12. Nawres Jabar Nasser Al-Rammahi " **Study of the Effect of Impact on Curved Composite Plates** " M.Sc. Thesis, Mechanical Engineering Department, Mustansiriyah University, 2011.

13. Sinan Zuhair Sabri **'' IMPROVEMENT OF POLYMER MATRIX COMPOSITE MATERIAL BEHAVIOR USING OPTIMUM ADDITIVES PERCENTAGE OF GRAPHITE AND ALUMINUM UNDER LOW VELOCITY IMPACT''** M.Sc. Thesis, Materials Engineering Department, Mustansiriyah University, 2013.

14. Shengqing Zhu, and Gin Boay Chai." **Low-velocity impact response of fibre–metal laminates – Experimental and finite element analysis**" Elsevier Composites Science and Technology 2012.

15. Avalle, Massimiliano, Giovanni Belingardi, and R. Montanini. **"Characterization of polymeric structural foams under compressive impact loading by means of energy-absorption diagram."** International Journal of Impact Engineering 25.5: 455-472,2001.

16. Turner, Andrew Joseph. **Low-velocity impact behavior of sandwich panels with 3D printed polymer core structures.** Diss. Wright State University, 2017

17. Farah, Shady, Daniel G. Anderson, and Robert Langer. **"Physical and mechanical properties of PLA, and their functions in widespread applications—A comprehensive review."** Advanced drug delivery reviews 107: 367-392,2016.

18. Louche, H., Piette-Coudol, F., Arrieux, R., & Issartel, J **"An experimental and modeling study of the thermomechanical behavior of an ABS polymer structural component during an impact test."** International Journal of Impact Engineering 36.6: 847-861,2009.

19. Roberson, D. A., Perez, A. R. T., Shemelya, C. M., Rivera, A., MacDonald, E., & Wicker, R. **"Comparison of stress concentrator fabrication for 3D printed polymeric izod impact test specimens."** Additive Manufacturing 7: 1-11,(2015).

20. Pei, E., Lanzotti, A., Grasso, M., Staiano, G., & Martorelli, M. **"The impact of process parameters on mechanical properties of parts fabricated in PLA with an open-source 3-D printer."** Rapid Prototyping Journal (2015).

21. Tsouknidas, A., Pantazopoulos, M., Katsoulis, I., Fasnakis, D., Maropoulos, S., & Michailidis, N. **"Impact absorption capacity of 3D-printed components fabricated by fused deposition modelling."** Materials & Design 102: 41-44,2016.

22. Shubham, Pritish, Arnab Sikidar, and Teg Chand. **"The influence of layer thickness on mechanical properties of the 3D printed ABS polymer by fused deposition modeling."** Key Engineering Materials. Vol. 706. Trans Tech Publications Ltd, 2016.

23. Dizon, J. R. C., Espera Jr, A. H., Chen, Q., & Advincula, R. C. **"Mechanical characterization of 3D-printed polymers."** Additive Manufacturing 20: 44-67,2018.

24. Chepelev, L., Wake, N., Ryan, J., Althobaity, W., Gupta, A., Arribas, E., ... & Sheikh, A. **"Radiological Society of North America (RSNA) 3D printing Special Interest Group (SIG): guidelines for medical 3D printing and appropriateness for clinical scenarios**." 3D printing in medicine 4.1: 1-38,2018.

25. Sarvestani, H. Y., Akbarzadeh, A. H., Niknam, H., & Hermenean, K. **"3D printed architected polymeric sandwich panels: Energy absorption and structural performance."** Composite Structures 200: 886-909, 2018.

26. Patterson, A. E., Pereira, T. R., Allison, J. T., & Messimer, S. L. **"IZOD impact properties of full-density FDM polymer materials with respect to raster angle and print orientation**." Journal of Mechanical Engineering Science XX (X) 1: 13,2018.

27. Abbas, Tahseen Fadhil, Farhad Mohammad Othman, and Hind Basil Ali. **"Influence of layer thickness on impact property of 3D-printed PLA."** Int. Res. J. Eng. Technol.(Irjet) 5: 1-4, (2018).

28. Abbot, D. W., Kallon, D. V. V., Anghel, C., & Dube, P. **"Finite element analysis of 3D printed model via compression tests."** Procedia Manufacturing 35: 164-173, (2019).

29. Hadidi, H., Mailand, B., Sundermann, T., Johnson, E., Madireddy, G., Negahban, M., ... & Sealy, M**."Low velocity impact of ABS after shot**

peening predefined layers during additive manufacturing." Procedia Manufacturing 34: 594-602, (2019).

30. Aloyaydi, Bandar Abdullah, Subbarayan Sivasankaran, and Hany Rizk Ammar. **"Influence of infill density on microstructure and flexural behavior of 3D printed PLA thermoplastic parts processed by fusion deposition modeling."** Aims Mater. Sci 6: 1033-1048, (2019).

31. Heechang Kim, Eunju Park, Suhyun Kim, Bumsoo Park, Namhun Kim, and Seungchul Lee, **" Experimental Study on Mechanical Properties of Single- and Dual-Material3D Printed Products "** Procedia Manufacturing 10 ,887 – 897, (2017).

32. Shahrubudin, Nurhalida, Te Chuan Lee, and Rhaizan Ramlan. **"An overview on 3D printing technology: technological, materials, and applications."** Procedia Manufacturing 35 (2019): 1286-1296.

33. Kruth, J. P., Leu, M. C. and Nakagawa, T. **"Progress in additive manufacturing and rapid prototyping "**, CIRP Annals –Manufacturing Technology, Vol 47, pp. 525-540, 1998 .

34**.** Olaf Diegel , Sarat Singamneni , Ben Huang, and Ian Gibson , **"Curved Layer Fused Deposition Modeling in Conductive Polymer Additive Manufacturing "** , 2 nd International Conference on Manufacturing Science and Engineering April 9- 11, 2011, Guilin, China .

35- Bates-Green, K., and T. Howie. **"Materials for 3D printing by fused deposition."** Technical education in additive manufacturing and materials : 1-21, (2017).

36. Husam Jawad Abdulsamad Alasady. "**Experimental and Theoretical Study of Low Velocity Impact on Composite Sandwich Beams**". M.Sc. thesis Mustansiriya University 2013.

37. Lee, Se-Han, and Jae-Bok Song. "**Acceleration estimator for low-velocity and low-acceleration regions based on encoder position data**." IEEE/ASME transactions on mechatronics 6.1 , 58-64,2001.

38. Boyce, William E., and Richard C. DiPrima. **Elementary differential equations and boundary value problems.** John Wiley & Sons, Inc. All rights reserved., 2012.

39. Evgeny K. Yalamanchili,**" Introduction to the finite element method "** Institute of materials and Structures , Faculty of Civil Engineering ,Riga Technical university, Riga , 2010

40. Shi, Y., T. Swait, and C. Soutis. **"Modelling damage evolution in composite laminates subjected to low velocity impact."** Composite Structures 94.9 (2012): 2902-2913.

41. Bellini A, Güçeri S. **Mechanical characterization of parts fabricated using fused deposition modeling.** Rapid Prototyping ,Journal 2003 Vol 9(4), Pages 252–264 .

42. Turner NB, Strong R, Gold SA **"A review of melt extrusion additive manufacturing processes: I. Process design and modeling."** Rapid Prototyp J 20(3):192–204, (2014).

43. **Standard Test Method for Tensile Properties of Plastics D638** , This standard has been approved for use by agencies of the U.S. Department of Defense.

44. ASTM D7136/D7136M-12. **"Standard test method for measuring the damage resistance of a fiber-reinforced polymer matrix composite to a drop-weight impact event."** (2015).

45. Sun, M., Chang, M., Wang, Z., Li, H., & Sun, X. "**Experimental and simulation study of low-velocity impact on glass fiber composite laminates with reinforcing shape memory alloys at different layer positions.**" Applied Sciences 8.12: 2405, (2018).

46. Zhang, Xiang, L. Hounslow, and Marcello Grassi. "**Improvement of low-velocity impact and compression-after-impact performance by z-fibre pinning."** Composites Science and Technology 66.15: 2785-2794,(2006).

47. Sagias, V. D., K. I. Giannakopoulos, and C. Stergiou. **"Mechanical properties of 3D printed polymer specimens."** Procedia Structural Integrity 10: 85-90, (2018).

48. Rodríguez-Panes, Adrián, Juan Claver, and Ana María Camacho. "**The influence of manufacturing parameters on the mechanical behaviour of PLA and ABS pieces manufactured by FDM: A comparative analysis.**" Materials 11.8: 1333, (2018).

الخلاصة

تم استخدام دراسة استقصائية على 18 عينة ذات تأثير منخفض السرعة. عند استخدام ثلاثة أنواع من السماكات ، تم إصلاح أبعاد العينة. لوحظ السلوك الديناميكي للمادة بسبب الضربة. تهدف هذه الدراسة إلى التحقق من الصدمة الميكانيكية من خلال قياس قوة الصدمة والتسارع وتأثيرها على المواد المصنعة. تم استخدام حمض بولي لاكتيك لقياس طاقة التأثير من خلال ثلاثة مستويات وتم الحصول على ثلاث طاقات مختلفة وهي 2.4 جول و 4.9 جول و 7.3 ج. تم نمذجة العينات في برنامج أعمال Solidwork ، ثم نقلها بتنسيق G-Code والعينات باستخدام طابعة ثلاثية الأبعاد وكانت كثافة الطباعة 100%. تم استخدام عينات مختلفة السماكات وفقًا لمعايير .ASTMD7136 اختبار الشد وفقًا لمعيار .ASTMD638تم تصنيع جهاز الاختبار وفقًا لمعيار .AISTMD7136 تم تصميم الجهاز في برنامج AutoCAD وتم توفير المستشعرات القوة FSR والتسارع MPU 6050 والمواد المستخدمة. كان قطر الكرة 16 مم وارتفاع الأنبوب الساقط 200 سم. تم حساب الطاقة الممتصة للمادة ، حيث أظهرت النتائج أن حمض اللاكتيك لديه القدرة على امتصاص الطاقة من ضربة منخفضة السرعة. وتم استخدام تقنية العناصر المحدودة (ABAQUS / Explicit Dynamic 16)للتحليل بملاحظة الحد الأقصى من تشوه الضغط الكلي . وأظهرت النتائج أن معامل المرونة وقوة الشد القصوى وضغط الخضوع قد تمت مقارنتها بالمجموعة. وتمت مقارنة نتائج الطاقة الكلية والضرر الناتج من الضربة وكان هناك تقارب بينهما.